Supplementary Figures – First-order continuous- and discontinuous-Galerkin moment models for a linear kinetic equation: model derivation and realizability theory

Florian Schneider, Tobias Leibner

This supplementary contains plots of ansatz functions for all investigated models and prescribed distributions.

S1. Gauss distribution in slab geometry

Ansatz functions for the Gauss distribution on the interval $[-1, 1]$

$$\psi_{\text{Gauss}}(\mu) = \frac{1}{\sqrt{2\pi\sigma^2}} \exp\left(\frac{(\mu-\bar{\mu})^2}{-2\sigma^2}\right) \text{ where } \sigma = 0.5, \bar{\mu} = 0,$$

for all tested models can be found in S1.1-S1.5. Higher-order approximations for all models have been omitted as they are close to the reference solution. M_N models are not shown as M_1 is equivalent to PMM_2 and higher-order M_N models are exact. Errors and observed orders of convergence are listed in Tables 1 and 2.

	HFM_n				PMM_n				M_N			
n	E_h^1	ν	E_h^∞	ν	E_h^1	ν	E_h^∞	ν	E_h^1	ν	E_h^∞	ν
2	4.111e-01	—	3.693e-01	—	4.111e-01	—	3.693e-01	—	4.110e-01	—	3.693e-01	—
4	5.369e-02	2.9	9.541e-02	2.0	1.074e-01	1.9	2.115e-01	0.8	1.371e-15	48.1	1.110e-15	48.2
6	1.959e-02	2.5	3.976e-02	2.2	5.151e-02	1.8	1.036e-01	1.8	5.765e-16	2.1	6.661e-16	1.3
8	9.999e-03	2.3	2.094e-02	2.2	2.967e-02	1.9	6.310e-02	1.7	5.613e-16	0.1	5.551e-16	0.6
10	6.048e-03	2.3	1.286e-02	2.2	1.920e-02	1.9	4.057e-02	2.0	7.779e-16	-1.5	7.772e-16	-1.5
12	4.048e-03	2.2	8.666e-03	2.2	1.342e-02	2.0	2.889e-02	1.9	7.572e-16	0.1	7.772e-16	-0.0
14	2.898e-03	2.2	6.231e-03	2.1	9.894e-03	2.0	2.119e-02	2.0	8.340e-16	-0.6	9.992e-16	-1.6
16	2.177e-03	2.1	4.692e-03	2.1	7.594e-03	2.0	1.641e-02	1.9	6.630e-16	1.7	7.772e-16	1.9
18	1.695e-03	2.1	3.659e-03	2.1	6.010e-03	2.0	1.294e-02	2.0	7.754e-16	-1.3	1.013e-15	-2.3
20	1.357e-03	2.1	2.933e-03	2.1	4.874e-03	2.0	1.055e-02	1.9	8.042e-16	-0.3	1.110e-15	-0.9
22	1.110e-03	2.1	2.403e-03	2.1	4.031e-03	2.0	8.705e-03	2.0	7.200e-16	1.2	7.772e-16	3.7
24	9.257e-04	2.1	2.004e-03	2.1	3.390e-03	2.0	7.347e-03	2.0	8.701e-16	-2.2	1.110e-15	-4.1
26	7.835e-04	2.1	1.697e-03	2.1	2.890e-03	2.0	6.250e-03	2.0	9.096e-16	-0.6	1.291e-15	-1.9
28	6.717e-04	2.1	1.456e-03	2.1	2.493e-03	2.0	5.406e-03	2.0	8.312e-16	1.2	8.188e-16	6.1
30	5.822e-04	2.1	1.262e-03	2.1	2.172e-03	2.0	4.703e-03	2.0	9.175e-16	-1.4	1.138e-15	-4.8
32	5.095e-04	2.1	1.105e-03	2.1	1.910e-03	2.0	4.143e-03	2.0	6.585e-16	5.1	1.540e-15	-4.7
34	4.496e-04	2.1	9.753e-04	2.1	1.692e-03	2.0	3.666e-03	2.0	6.671e-16	-0.2	1.027e-15	6.7
36	3.997e-04	2.1	8.672e-04	2.1	1.510e-03	2.0	3.275e-03	2.0	6.236e-16	1.2	1.027e-15	-0.0
38	3.577e-04	2.1	7.761e-04	2.1	1.355e-03	2.0	2.937e-03	2.0	7.868e-16	-4.3	1.582e-15	-8.0
40	3.219e-04	2.1	6.986e-04	2.1	1.223e-03	2.0	2.654e-03	2.0	5.428e-16	7.2	1.096e-15	7.2
42	2.913e-04	2.1	6.322e-04	2.0	1.110e-03	2.0	2.406e-03	2.0	7.694e-16	-7.1	1.402e-15	-5.0
44	2.648e-04	2.0	5.748e-04	2.0	1.011e-03	2.0	2.194e-03	2.0	8.321e-16	-1.7	1.110e-15	5.0
46	2.418e-04	2.0	5.249e-04	2.0	9.251e-04	2.0	2.006e-03	2.0	7.315e-16	2.9	1.305e-15	-3.6
48	2.217e-04	2.0	4.812e-04	2.0	8.497e-04	2.0	1.844e-03	2.0	7.514e-16	-0.6	1.874e-15	-8.5
50	2.039e-04	2.0	4.428e-04	2.0	7.831e-04	2.0	1.699e-03	2.0	6.903e-16	2.1	2.984e-15	-11.4

Table 1: L_1/L_∞ errors and observed order of convergence ν for the non-linear models in the Gauss slab geometry case.

S2. Heaviside distribution in slab geometry

Ansatz functions for the Heaviside distribution on the interval $[-1, 1]$

$$\psi_{\text{Heaviside}}(\mu) = \begin{cases} \psi_{vac}(\mu) & \text{if } \mu < 0 \\ 1 & \text{else} \end{cases} \qquad \text{where} \qquad \psi_{vac}(\mu) = \frac{10^{-8}}{2}$$

for all tested models can be found in Figures S2.1-S2.8. Errors and observed orders of convergence are listed in Tables 3 and 4.

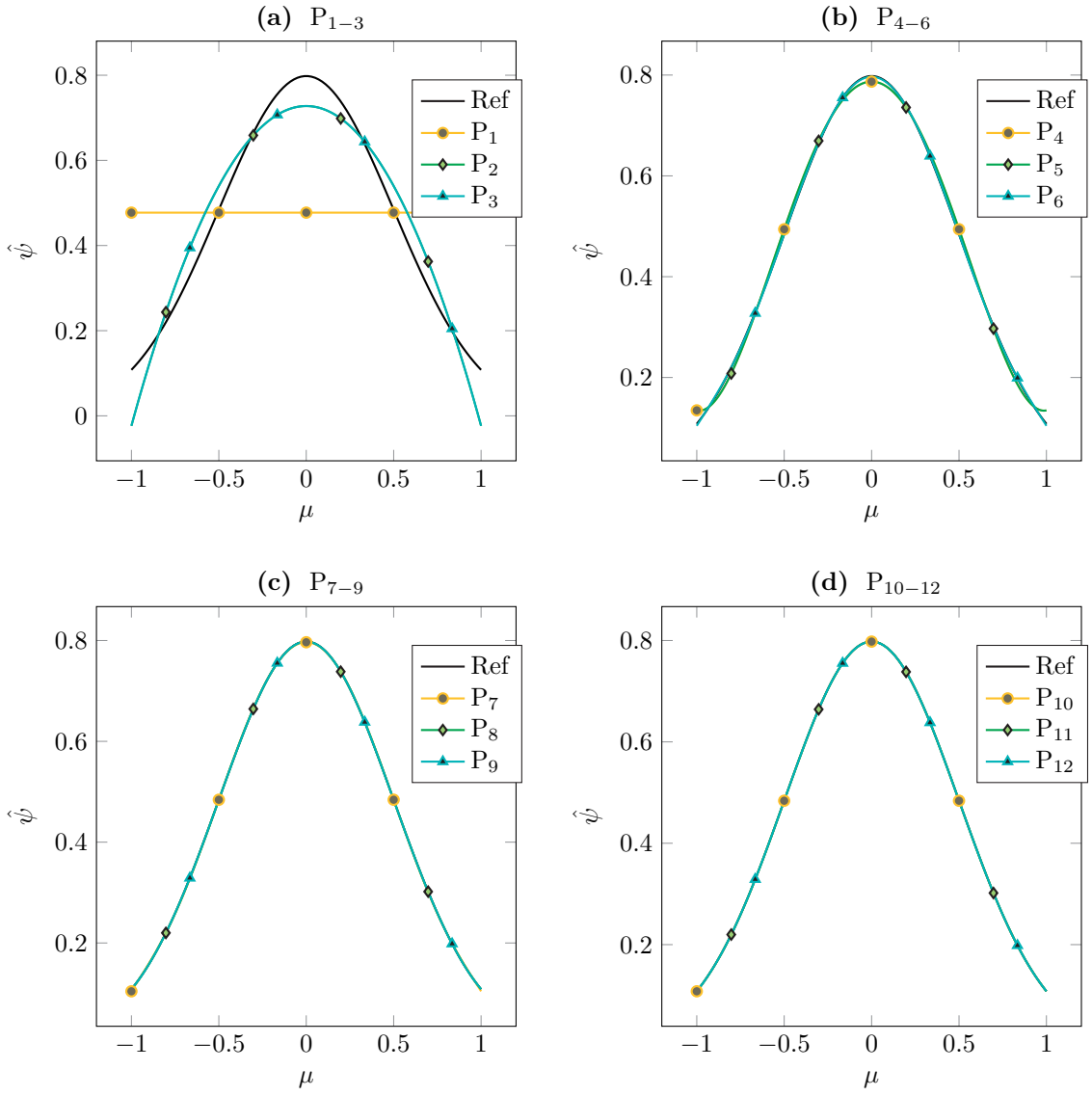

Figure S1.1: Distributions of P_N models for the slab geometry Gauss test.

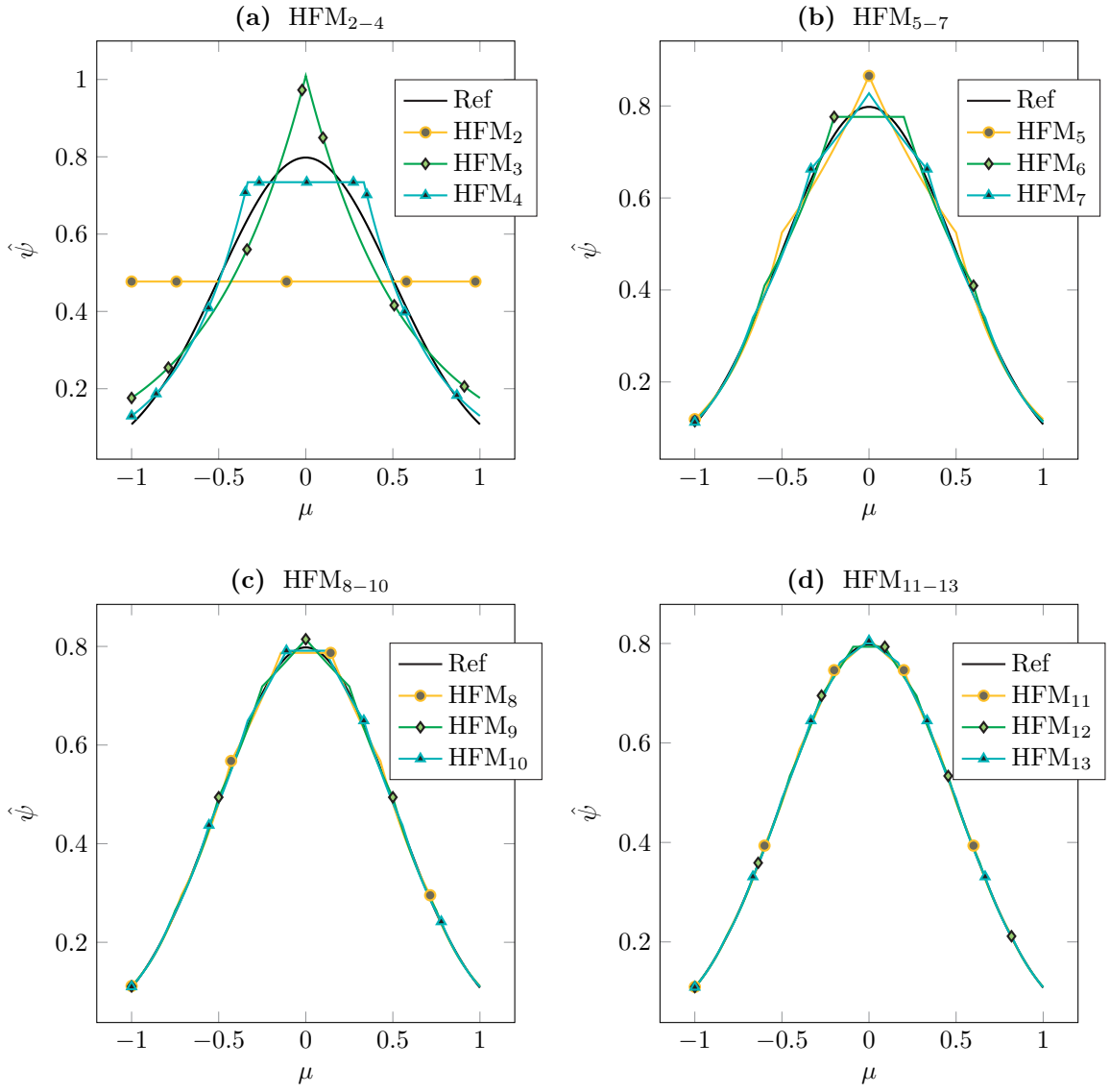

Figure S1.2: Distributions of HFM_n models for the slab geometry Gauss test.

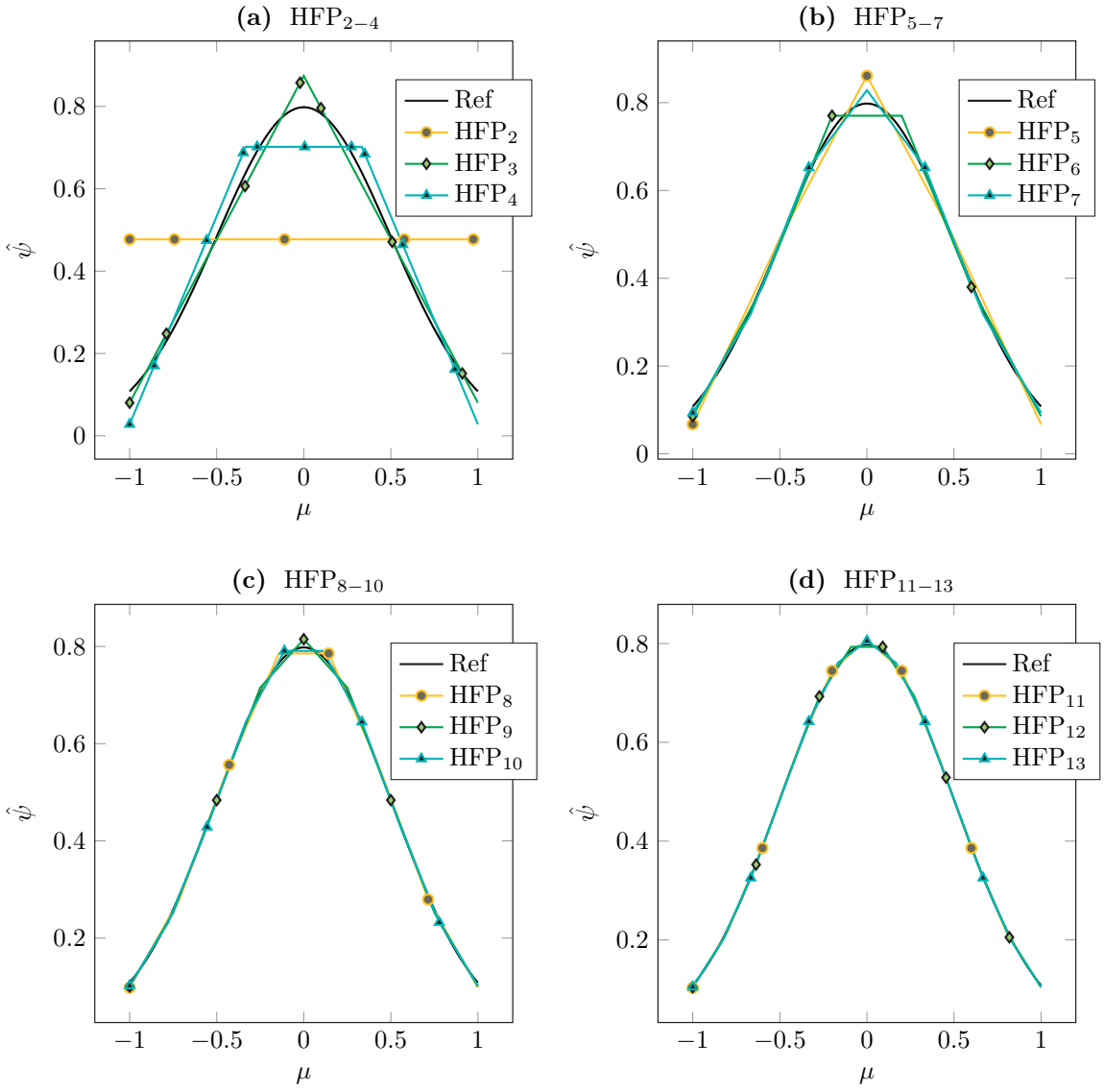

Figure S1.3: Distributions of HFP_n models for the slab geometry Gauss test.

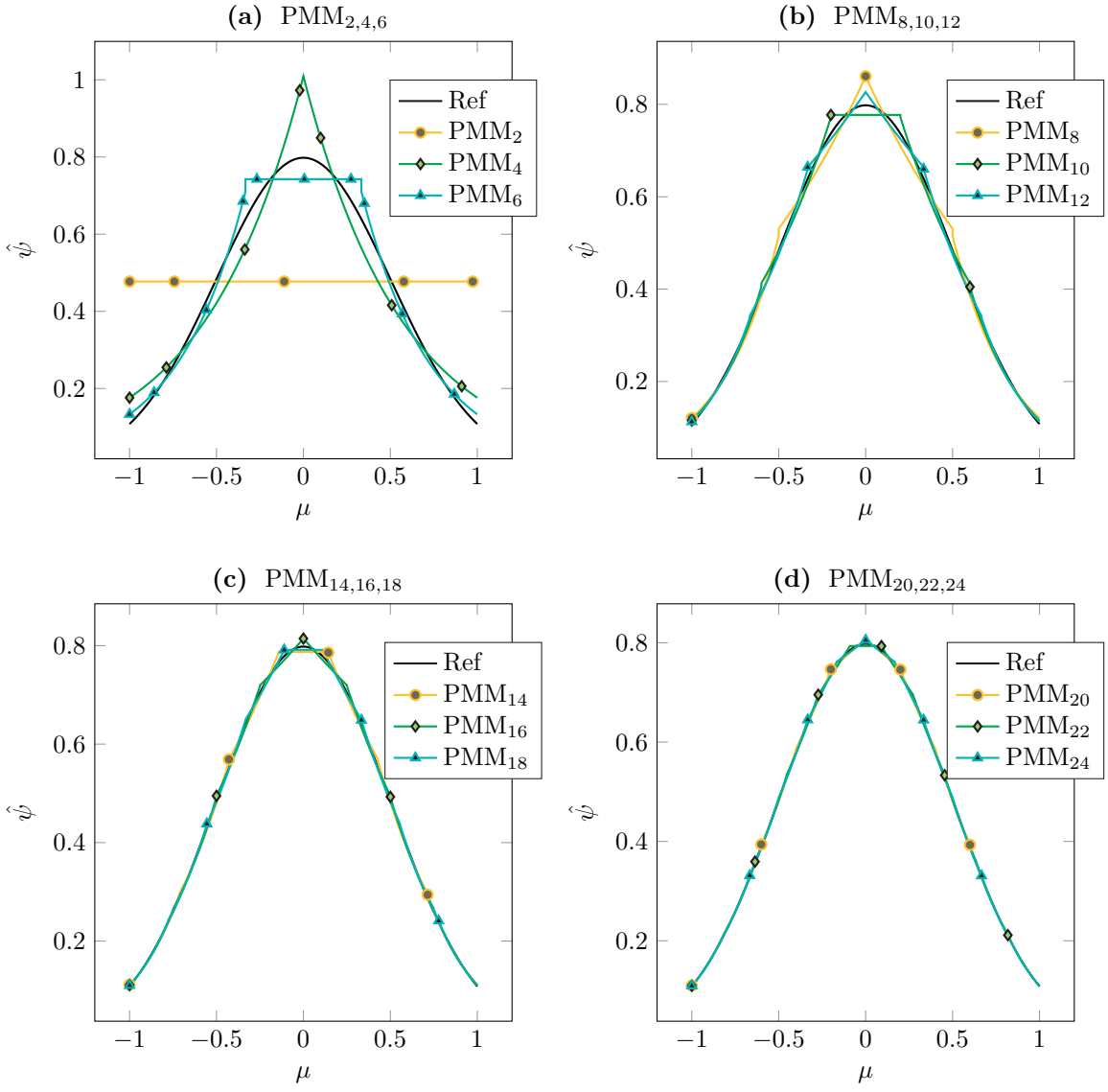

Figure S1.4: Distributions of PMM_n models for the slab geometry Gauss test.

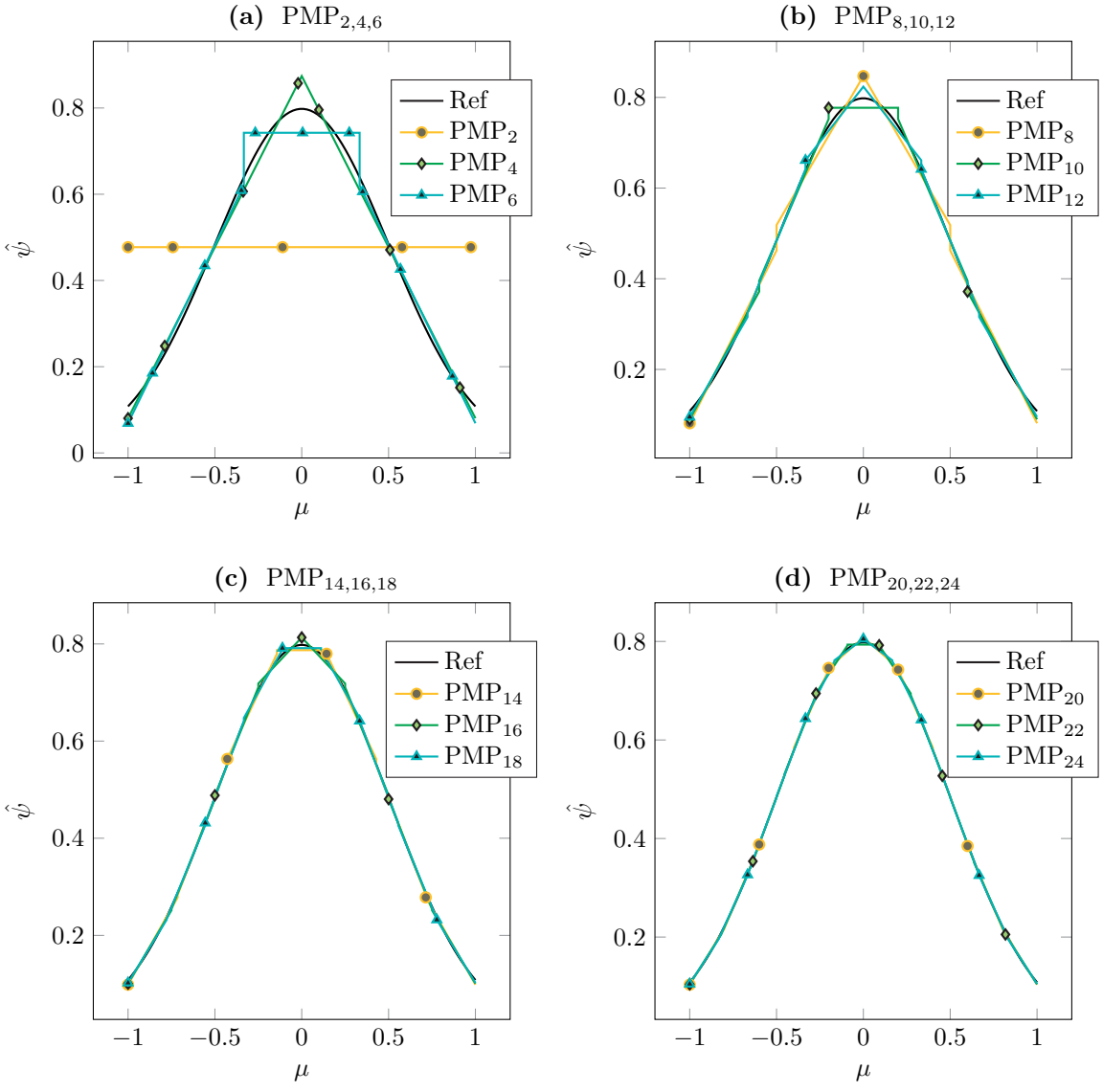

Figure S1.5: Distributions of PMP_n models for the slab geometry Gauss test.

	HFP$_n$				PMP$_n$				P$_N$			
n	E_h^1	ν	E_h^∞	ν	E_h^1	ν	E_h^∞	ν	E_h^1	ν	E_h^∞	ν
2	4.111e-01	—	3.693e-01	—	4.111e-01	—	3.693e-01	—	4.110e-01	—	3.693e-01	—
4	8.936e-02	2.2	9.601e-02	1.9	3.666e-02	3.5	7.626e-02	2.3	9.429e-02	2.1	1.315e-01	1.5
6	1.987e-02	3.7	3.369e-02	2.6	4.450e-02	-0.5	1.036e-01	-0.8	1.506e-02	4.5	2.683e-02	3.9
8	9.315e-03	2.6	1.960e-02	1.9	2.616e-02	1.8	4.921e-02	2.6	1.834e-03	7.3	3.868e-03	6.7
10	5.298e-03	2.5	1.238e-02	2.1	1.540e-02	2.4	4.057e-02	0.9	1.802e-04	10.4	4.320e-04	9.8
12	3.444e-03	2.4	8.461e-03	2.1	1.005e-02	2.3	2.586e-02	2.5	1.483e-05	13.7	3.940e-05	13.1
14	2.415e-03	2.3	6.127e-03	2.1	7.901e-03	1.6	2.119e-02	1.3	1.049e-06	17.2	3.038e-06	16.6
16	1.793e-03	2.2	4.634e-03	2.1	6.156e-03	1.9	1.542e-02	2.4	6.507e-08	20.8	2.028e-07	20.3
18	1.383e-03	2.2	3.624e-03	2.1	4.767e-03	2.2	1.294e-02	1.5	3.596e-09	24.6	1.195e-08	24.0
20	1.101e-03	2.2	2.911e-03	2.1	3.774e-03	2.2	1.014e-02	2.3	1.789e-10	28.5	6.294e-10	27.9
22	8.965e-04	2.2	2.388e-03	2.1	3.194e-03	1.8	8.705e-03	1.6	8.097e-12	32.5	2.999e-11	31.9
24	7.447e-04	2.1	1.994e-03	2.1	2.705e-03	1.9	7.146e-03	2.3	3.363e-13	36.6	1.305e-12	36.0
26	6.285e-04	2.1	1.690e-03	2.1	2.285e-03	2.1	6.250e-03	1.7	1.290e-14	40.7	5.285e-14	40.1
28	5.376e-04	2.1	1.450e-03	2.1	1.947e-03	2.2	5.296e-03	2.2	7.057e-16	39.2	2.082e-15	43.6
30	4.651e-04	2.1	1.258e-03	2.1	1.716e-03	1.8	4.703e-03	1.7	5.974e-16	2.4	7.772e-16	14.3
32	4.064e-04	2.1	1.102e-03	2.1	1.515e-03	1.9	4.078e-03	2.2	5.975e-16	-0.0	8.049e-16	-0.5
34	3.582e-04	2.1	9.729e-04	2.1	1.336e-03	2.1	3.666e-03	1.8	6.035e-16	-0.2	1.041e-15	-4.2
36	3.181e-04	2.1	8.653e-04	2.1	1.183e-03	2.1	3.235e-03	2.2	6.054e-16	-0.1	1.277e-15	-3.6
38	2.844e-04	2.1	7.746e-04	2.0	1.069e-03	1.9	2.937e-03	1.8	6.178e-16	-0.4	1.443e-15	-2.3
40	2.557e-04	2.1	6.974e-04	2.0	9.680e-04	1.9	2.628e-03	2.2	6.198e-16	-0.1	1.762e-15	-3.9
42	2.312e-04	2.1	6.312e-04	2.0	8.752e-04	2.1	2.406e-03	1.8	6.262e-16	-0.2	1.554e-15	2.6
44	2.101e-04	2.1	5.740e-04	2.0	7.937e-04	2.1	2.176e-03	2.2	6.288e-16	-0.1	1.499e-15	0.8
46	1.917e-04	2.1	5.242e-04	2.0	7.297e-04	1.9	2.006e-03	1.8	6.297e-16	-0.0	1.235e-15	4.4
48	1.757e-04	2.1	4.806e-04	2.0	6.715e-04	2.0	1.832e-03	2.1	6.467e-16	-0.6	2.151e-15	-13.0
50	1.616e-04	2.1	4.423e-04	2.0	6.175e-04	2.1	1.699e-03	1.8	6.598e-16	-0.5	1.846e-15	3.7

Table 2: L_1/L_∞ errors and observed order of convergence ν for the linear models in the Gauss slab geometry case.

	HFM$_n$				PMM$_n$				M$_N$			
n	E_h^1	ν	E_h^∞	ν	E_h^1	ν	E_h^∞	ν	E_h^1	ν	E_h^∞	ν
2	5.446e-01	—	8.478e-01	—	5.446e-01	—	8.478e-01	—	5.447e-01	—	8.475e-01	—
6	1.604e-01	1.1	6.788e-01	0.2	1.815e-01	1.0	8.478e-01	-0.0	1.603e-01	1.1	6.453e-01	0.2
10	9.085e-02	1.1	6.788e-01	-0.0	1.089e-01	1.0	8.478e-01	0.0	1.017e-01	0.9	6.308e-01	0.0
14	6.298e-02	1.1	6.788e-01	-0.0	7.780e-02	1.0	8.478e-01	-0.0	7.052e-02	1.1	6.352e-01	-0.0
18	4.817e-02	1.1	6.788e-01	-0.0	6.051e-02	1.0	8.478e-01	-0.0	5.208e-02	1.2	6.236e-01	0.1
22	3.899e-02	1.1	6.788e-01	-0.0	4.951e-02	1.0	8.478e-01	-0.0	5.099e-02	0.1	6.329e-01	-0.1
26	3.276e-02	1.0	6.788e-01	-0.0	4.189e-02	1.0	8.478e-01	-0.0	3.935e-02	1.6	6.288e-01	0.0
30	2.824e-02	1.0	6.788e-01	-0.0	3.631e-02	1.0	8.478e-01	0.0	3.210e-02	1.4	6.272e-01	0.0
34	2.481e-02	1.0	6.788e-01	-0.0	3.204e-02	1.0	8.478e-01	0.0	3.567e-02	-0.8	6.269e-01	0.0
38	2.213e-02	1.0	6.788e-01	-0.0	2.866e-02	1.0	8.478e-01	0.0	2.512e-02	3.2	6.263e-01	0.0
42	1.997e-02	1.0	6.788e-01	-0.0	2.593e-02	1.0	8.478e-01	-0.0	2.349e-02	0.7	6.262e-01	0.0
46	1.820e-02	1.0	6.788e-01	-0.0	2.368e-02	1.0	8.478e-01	-0.0	3.065e-02	-2.9	6.279e-01	-0.0
50	1.671e-02	1.0	6.788e-01	-0.0	2.178e-02	1.0	8.478e-01	-0.0	2.940e-02	0.5	6.280e-01	-0.0

Table 3: L_1/L_∞ errors and observed order of convergence ν for the non-linear models in the Heaviside slab geometry case.

	HFP$_n$				PMP$_n$				P$_N$			
n	E_h^1	ν	E_h^∞	ν	E_h^1	ν	E_h^∞	ν	E_h^1	ν	E_h^∞	ν
2	4.167e-01	—	4.882e-01	—	4.167e-01	—	4.882e-01	—	4.167e-01	—	4.999e-01	—
6	1.271e-01	1.1	4.907e-01	-0.0	1.389e-01	1.0	4.882e-01	-0.0	2.165e-01	0.6	4.998e-01	0.0
10	7.191e-02	1.1	4.907e-01	-0.0	8.333e-02	1.0	4.882e-01	-0.0	1.522e-01	0.7	4.997e-01	0.0
14	4.985e-02	1.1	4.907e-01	-0.0	5.952e-02	1.0	4.882e-01	-0.0	1.191e-01	0.7	4.996e-01	0.0
18	3.813e-02	1.1	4.907e-01	-0.0	4.630e-02	1.0	4.882e-01	-0.0	9.874e-02	0.7	4.994e-01	0.0
22	3.086e-02	1.1	4.907e-01	-0.0	3.788e-02	1.0	4.882e-01	-0.0	8.472e-02	0.8	4.993e-01	0.0
26	2.593e-02	1.0	4.907e-01	-0.0	3.205e-02	1.0	4.882e-01	-0.0	7.433e-02	0.8	4.992e-01	0.0
30	2.235e-02	1.0	4.907e-01	-0.0	2.778e-02	1.0	4.882e-01	-0.0	6.653e-02	0.8	4.991e-01	0.0
34	1.964e-02	1.0	4.907e-01	-0.0	2.451e-02	1.0	4.882e-01	-0.0	6.017e-02	0.8	4.989e-01	0.0
38	1.752e-02	1.0	4.907e-01	0.0	2.193e-02	1.0	4.882e-01	-0.0	5.522e-02	0.8	4.988e-01	0.0
42	1.581e-02	1.0	4.907e-01	-0.0	1.984e-02	1.0	4.882e-01	-0.0	5.087e-02	0.8	4.987e-01	0.0
46	1.440e-02	1.0	4.907e-01	-0.0	1.812e-02	1.0	4.882e-01	-0.0	4.739e-02	0.8	4.985e-01	0.0
50	1.323e-02	1.0	4.907e-01	0.0	1.667e-02	1.0	4.882e-01	-0.0	4.433e-02	0.8	4.984e-01	0.0

Table 4: L_1/L_∞ errors and observed order of convergence ν for the linear models in the Heaviside slab geometry case.

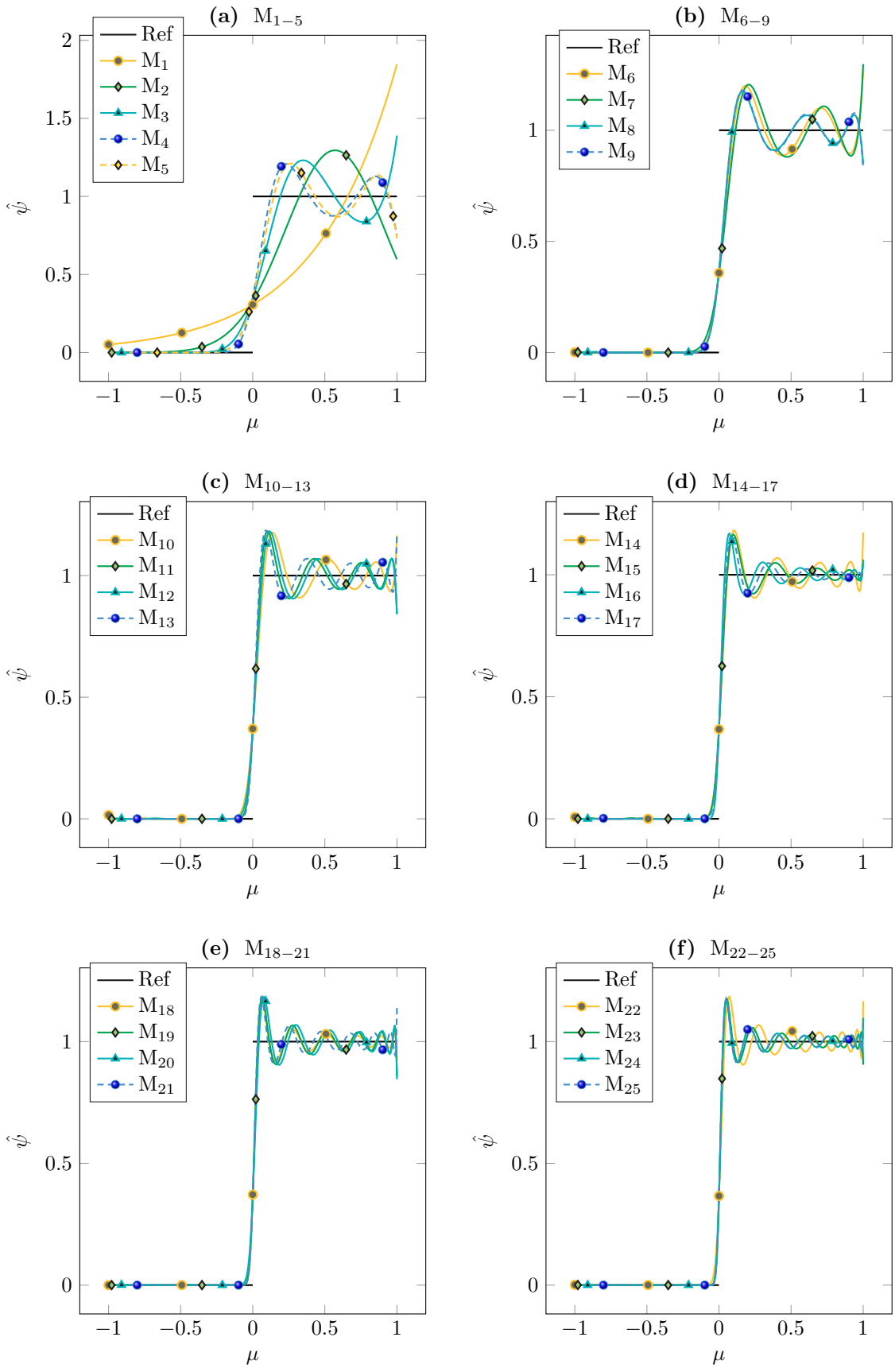

Figure S2.1: Distributions of M_N models for the slab geometry Heaviside test. Continued in Figure S2.2.

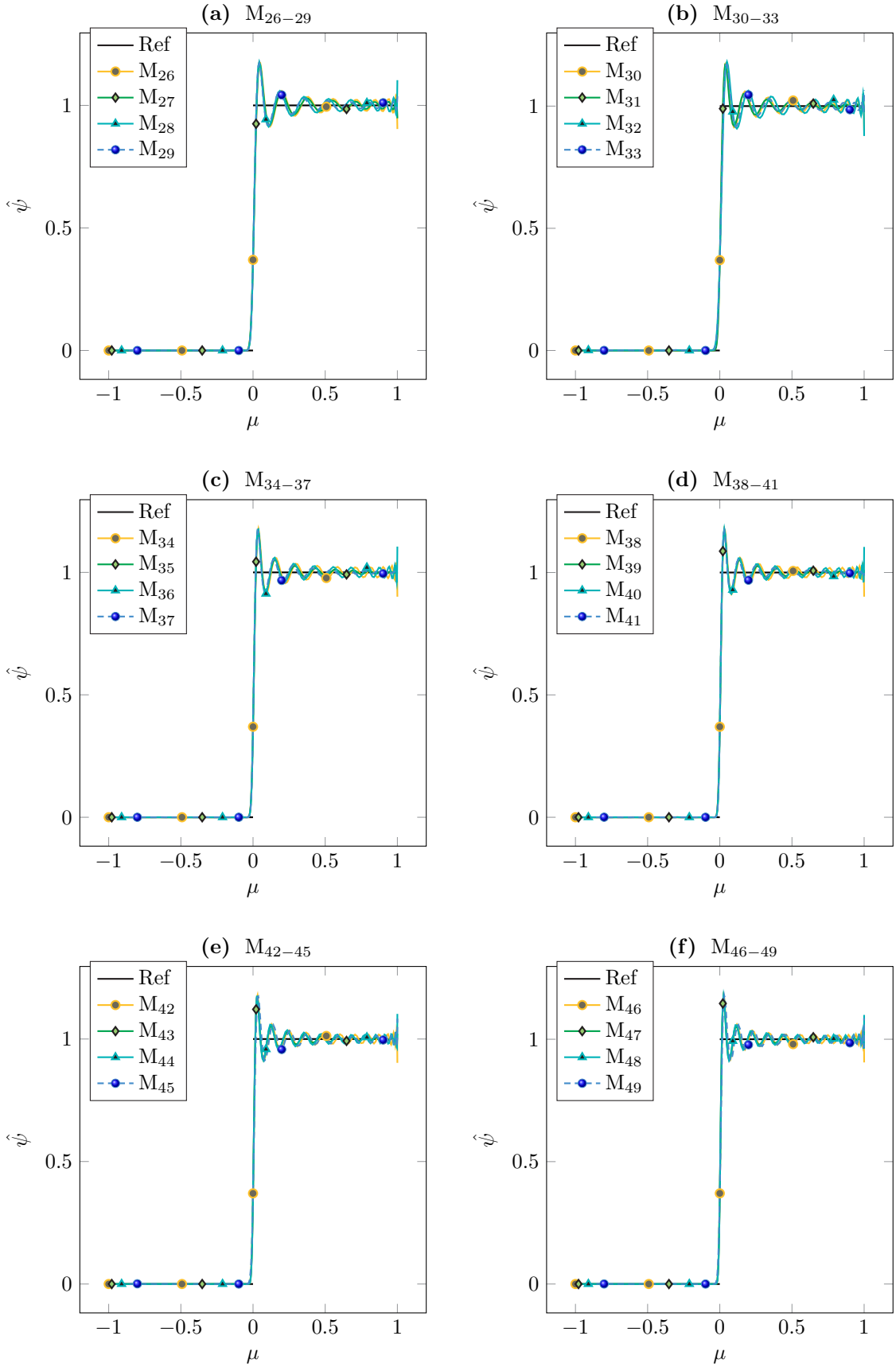

Figure S2.2: Distributions of M_N models for the slab geometry Heaviside test (continued).

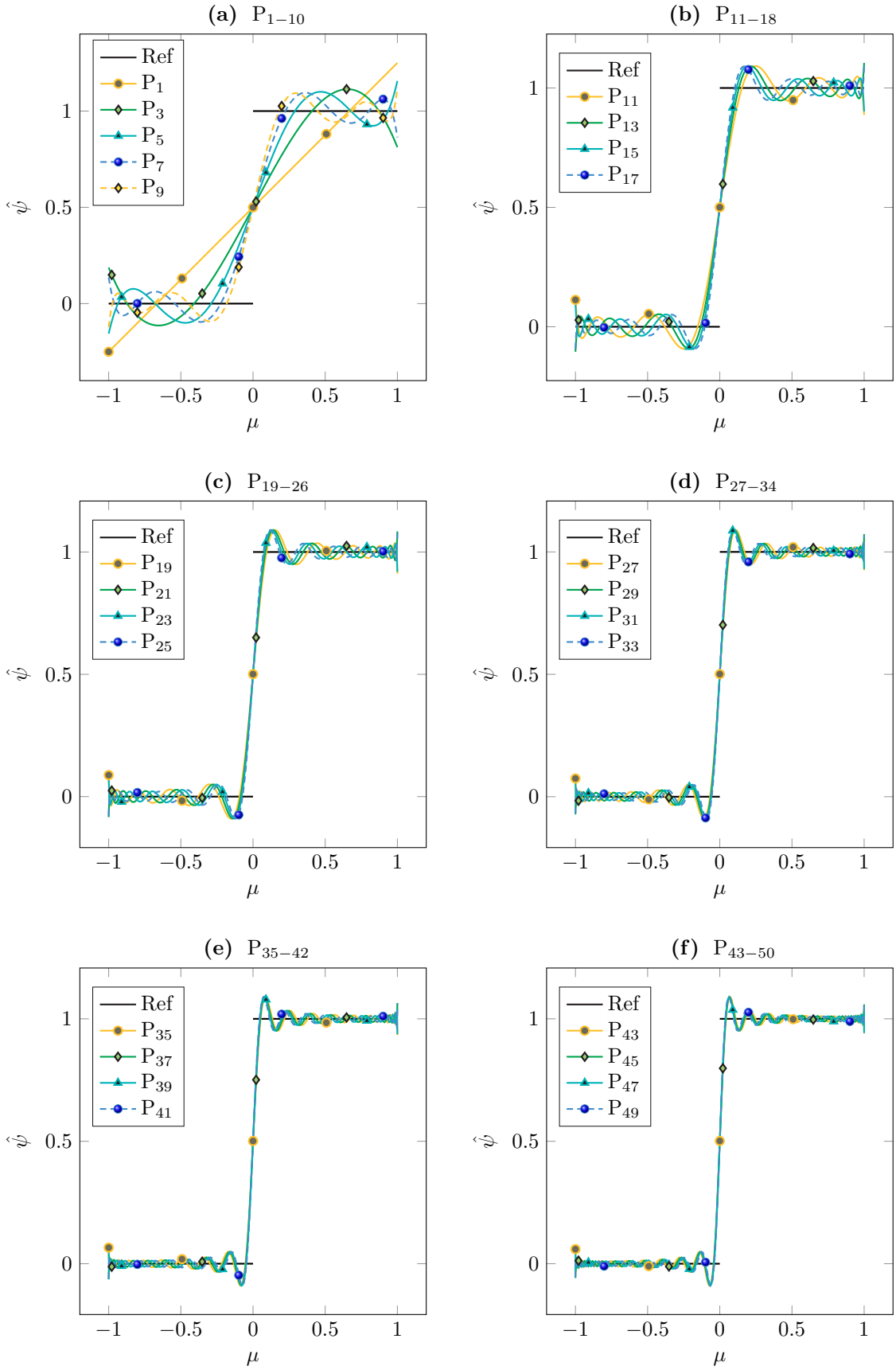

Figure S2.3: Distributions of P_N models for the slab geometry Heaviside test. Even order polynomials do not contribute to the ansatz, so models P_{2k} are equivalent to models P_{2k-1} and thus only models with odd order are shown.

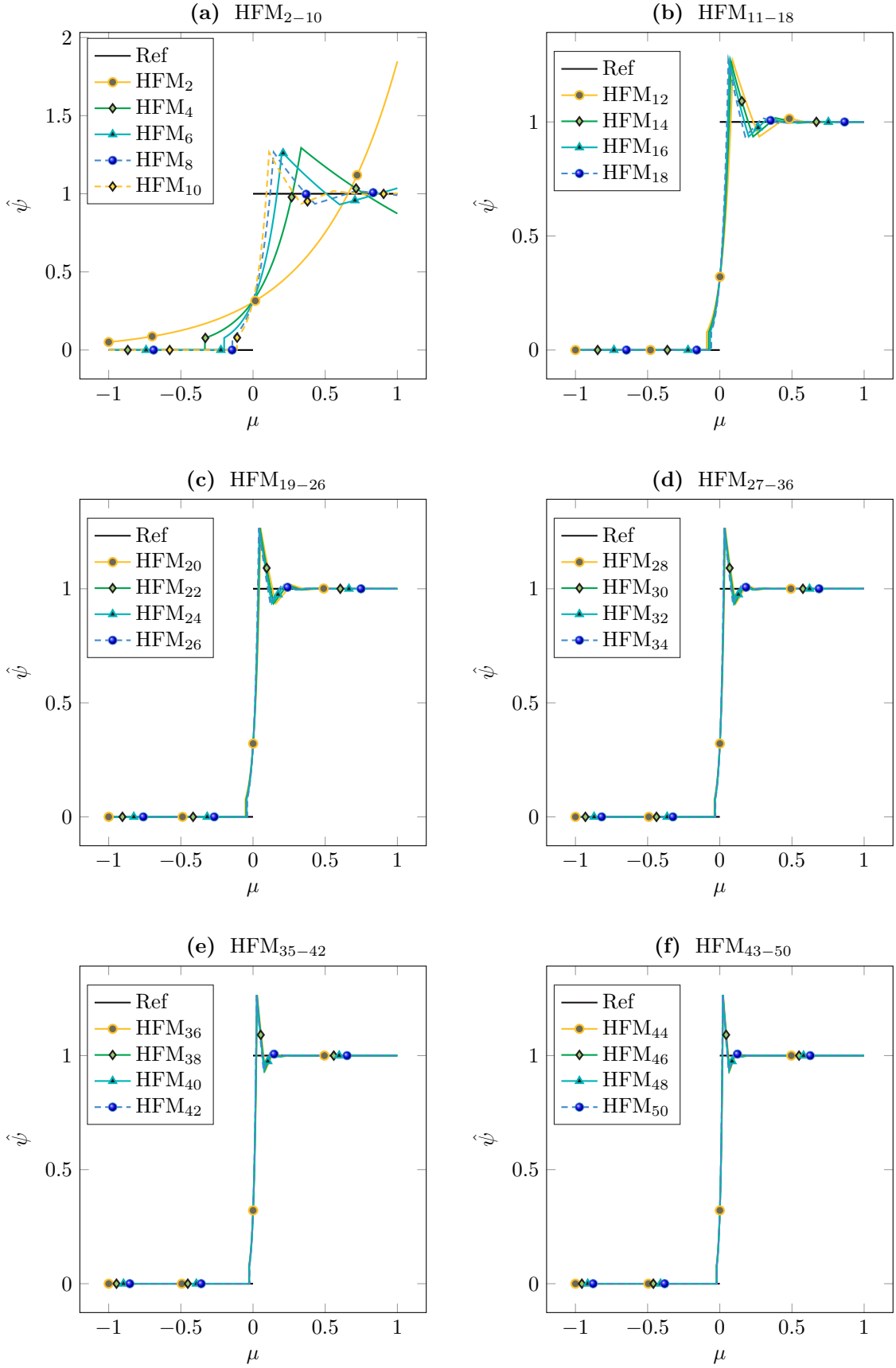

Figure S2.4: Distributions of HFM_n models for the slab geometry Heaviside test. Models HFM_{2k+1} using an even number of intervals are close to the reference solution, so only models HFM_{2k} with an odd number of intervals are shown.

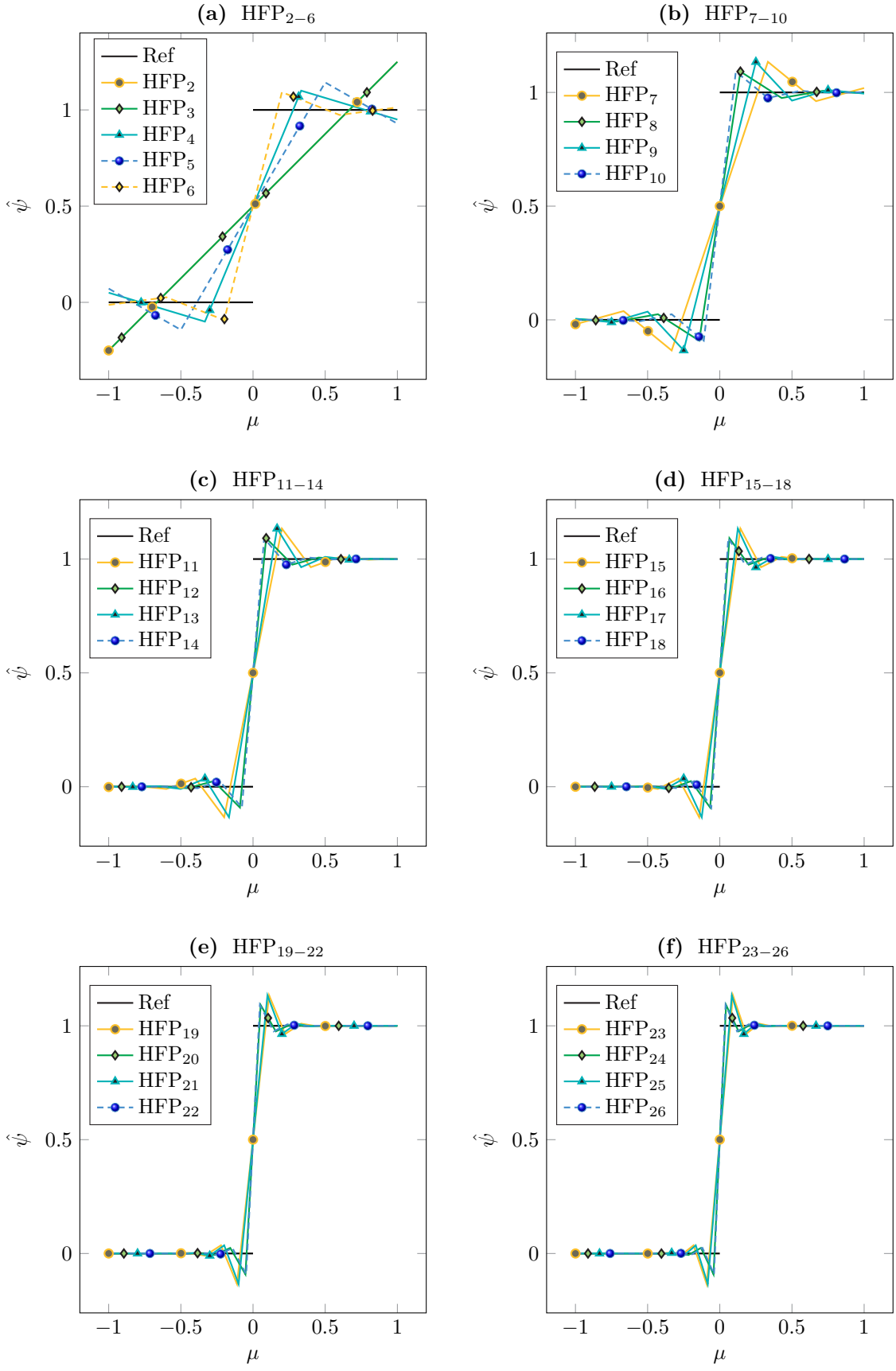

Figure S2.5: Distributions of HFP_n models for the slab geometry Heaviside test. Continued in Figure S2.6

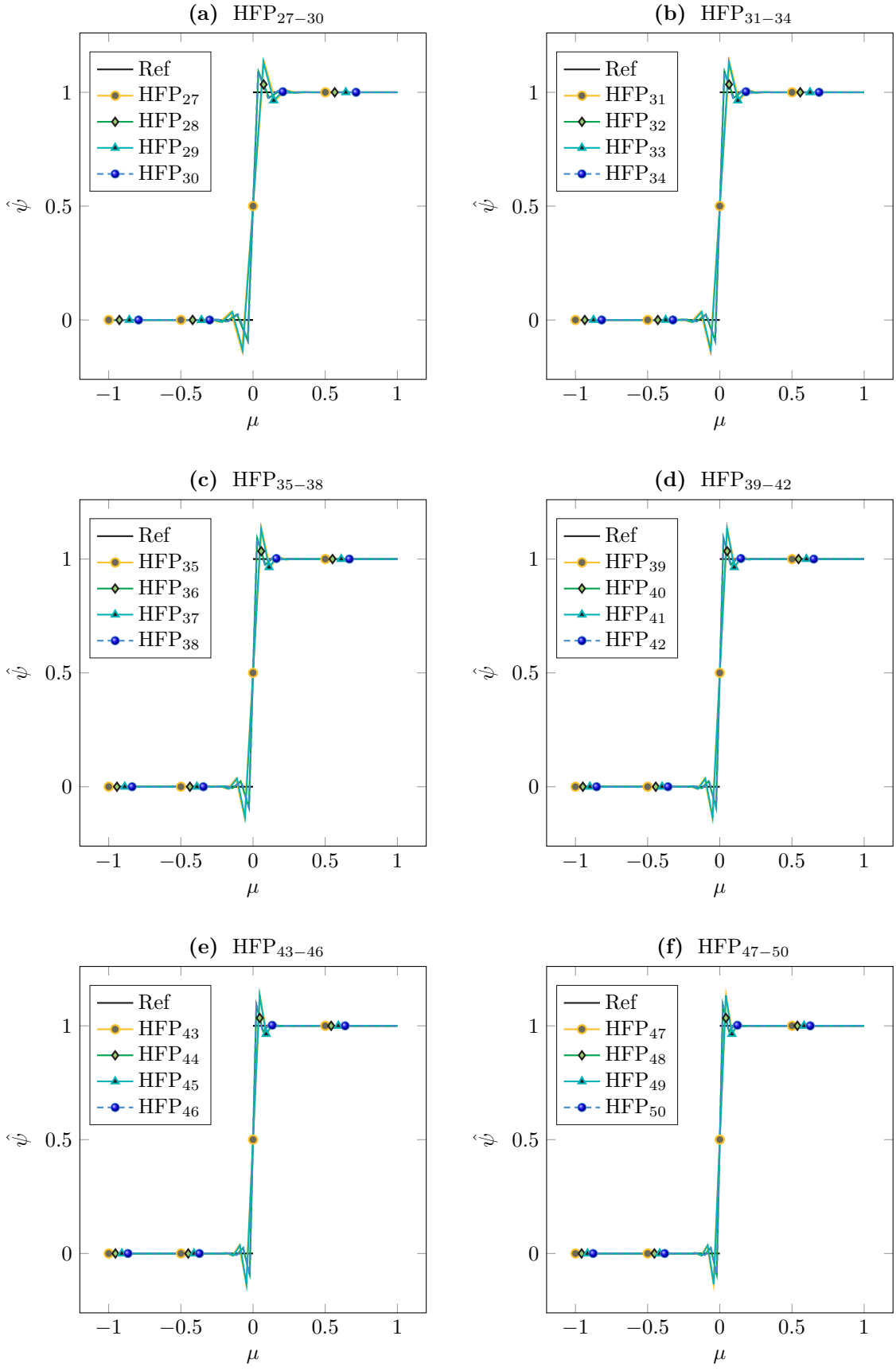

Figure S2.6: Distributions of HFP_n models for the slab geometry Heaviside test (continued).

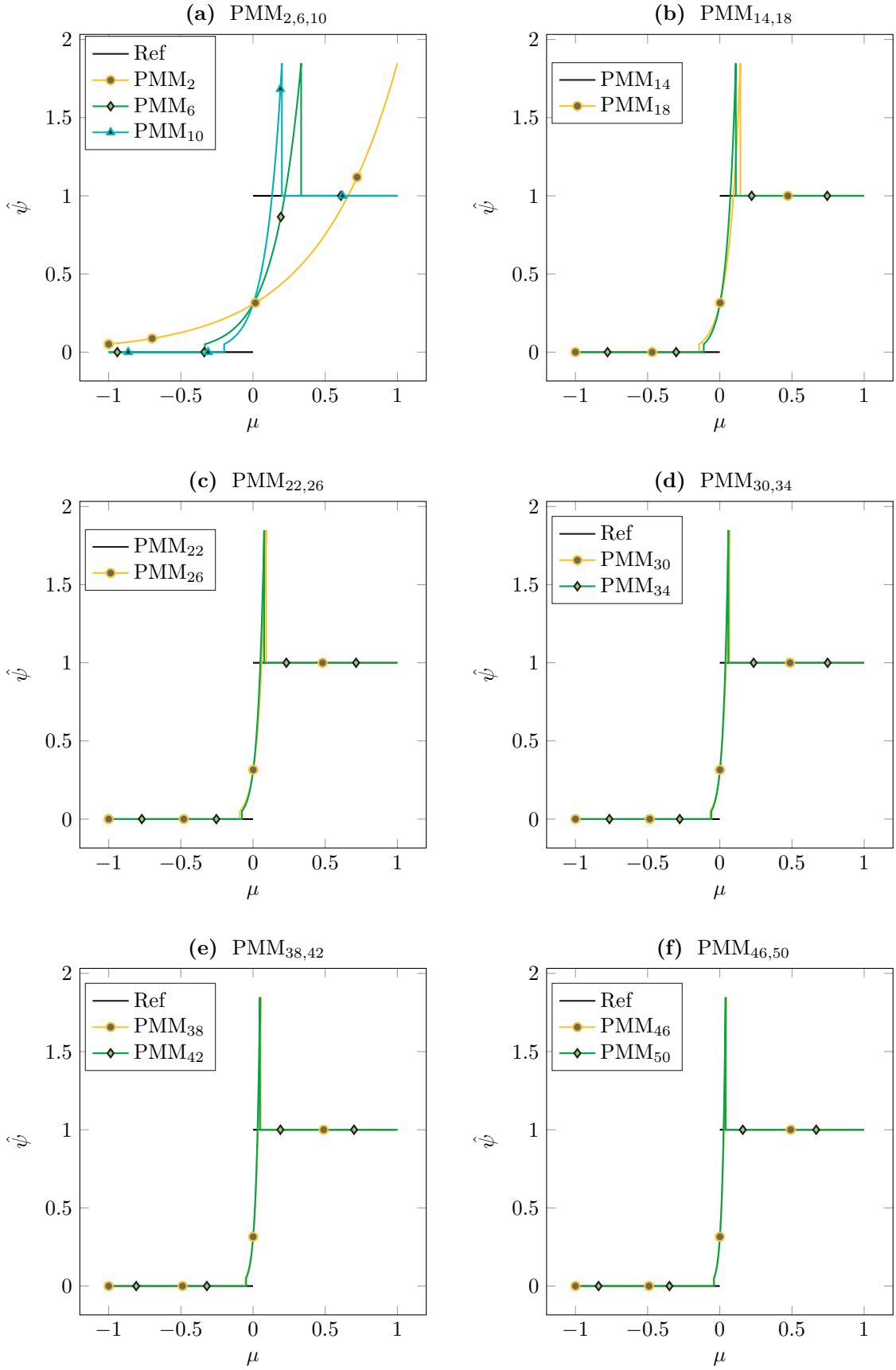

Figure S2.7: Distributions of PMM_n models for the slab geometry Heaviside test. Models PMM_{4k} using an even number of intervals are (almost) exact, so only PMM_{4k+2} models are shown.

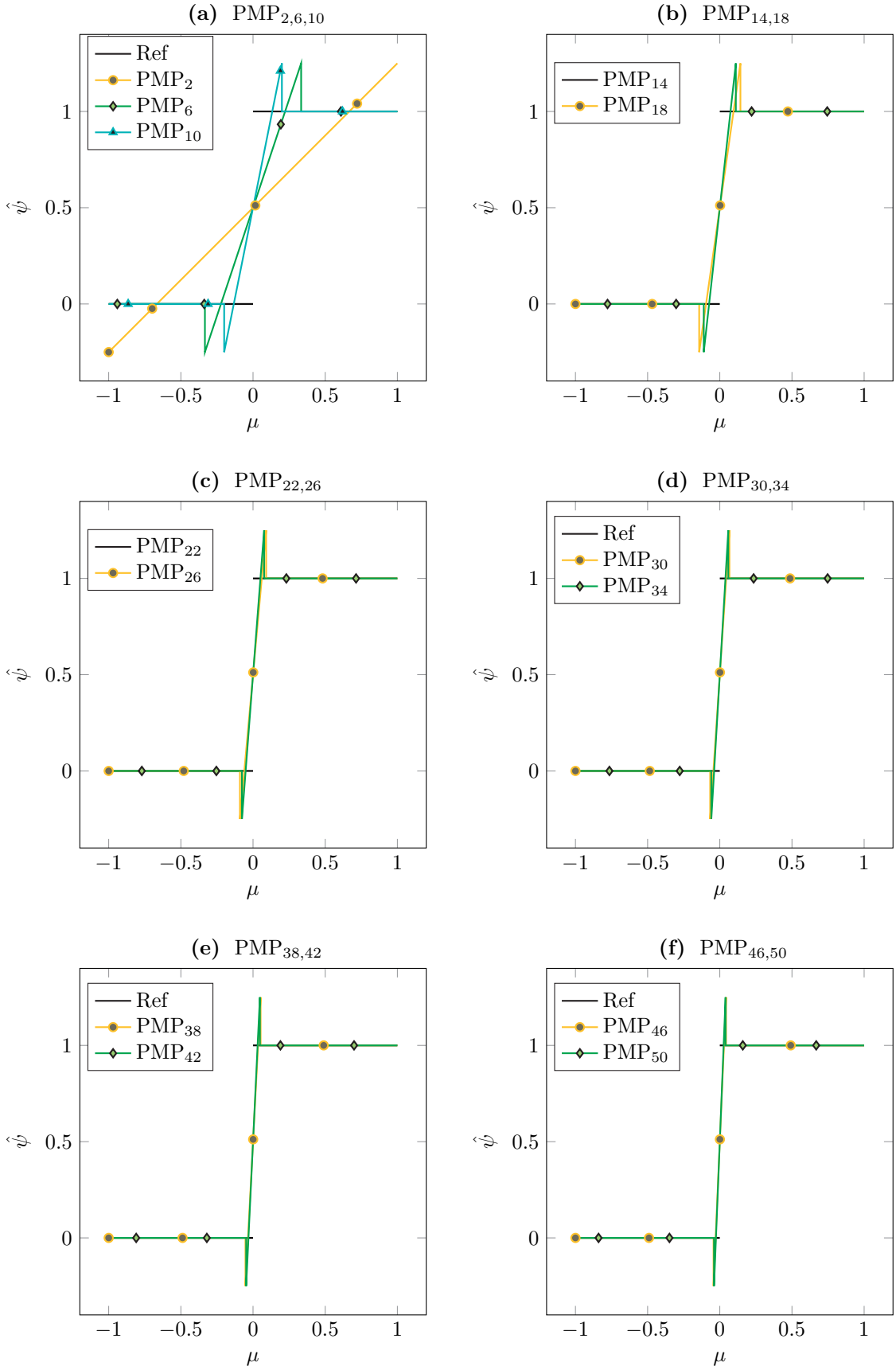

Figure S2.8: Distributions of PMP_n models for the slab geometry Heaviside test. Models PMP_{4k} using an even number of intervals are (almost) exact, so only PMP_{4k+2} models are shown.

S3. Crossing beams in slab geometry

Ansatz functions for the crossing beams test case on the interval $[-1, 1]$

$$\psi_{\text{CrossingBeams}}(\mu) = \sqrt{\frac{a}{\pi}} \left(\exp\left(-a(\mu+1)^2\right) + \exp\left(-a(\mu-0.5)^2\right) \right) \text{ where } a = 10^3$$

for all tested models can be found in S3.1-S3.9. Errors and observed orders of convergence are listed in Tables 5 and 6.

	HFM_n				PMM_n				M_N			
n	E_h^1	ν	E_h^∞	ν	E_h^1	ν	E_h^∞	ν	E_h^1	ν	E_h^∞	ν
2	2.711e+00	—	1.710e+01	—	2.711e+00	—	1.710e+01	—	2.711e+00	—	1.710e+01	—
6	1.371e+00	0.6	1.410e+01	0.2	1.624e+00	0.5	1.559e+01	0.1	2.496e-02	4.3	3.821e-01	3.5
10	9.925e-01	0.6	1.478e+01	-0.1	1.371e+00	0.3	1.410e+01	0.2	1.462e-04	10.1	3.080e-03	9.4
14	7.647e-01	0.8	1.512e+01	-0.1	1.153e+00	0.5	1.280e+01	0.3	1.208e-04	0.6	3.906e-03	-0.7
18	6.143e-01	0.9	1.327e+01	0.5	9.725e-01	0.7	1.555e+01	-0.8	1.832e-04	-1.7	4.859e-03	-0.9
22	5.036e-01	1.0	1.128e+01	0.8	8.292e-01	0.8	1.700e+01	-0.4	1.145e-04	2.3	1.827e-03	4.9
26	4.187e-01	1.1	9.613e+00	1.0	7.185e-01	0.9	1.736e+01	-0.1	6.457e-05	3.4	5.931e-03	-7.0
30	3.522e-01	1.2	8.275e+00	1.0	6.325e-01	0.9	1.702e+01	0.1	5.229e-05	1.5	1.704e-03	8.7
34	2.984e-01	1.3	7.314e+00	1.0	5.642e-01	0.9	1.628e+01	0.4	5.243e-05	-0.0	9.098e-04	5.0
38	2.537e-01	1.5	6.519e+00	1.0	5.081e-01	0.9	1.532e+01	0.5	3.451e-05	3.8	5.939e-04	3.8
42	2.162e-01	1.6	5.775e+00	1.2	4.604e-01	1.0	1.425e+01	0.7	2.305e-05	4.0	9.416e-04	-4.6
46	1.846e-01	1.7	5.098e+00	1.4	4.189e-01	1.0	1.315e+01	0.9	2.133e-05	0.9	1.569e-03	-5.6
50	1.584e-01	1.8	4.496e+00	1.5	3.822e-01	1.1	1.208e+01	1.0	2.946e-05	-3.9	5.172e-04	13.3
54	1.366e-01	1.9	3.967e+00	1.6	3.492e-01	1.2	1.106e+01	1.1	3.101e-05	-0.7	1.052e-03	-9.2
58	1.187e-01	2.0	3.508e+00	1.7	3.194e-01	1.2	1.011e+01	1.3	1.498e-05	10.2	2.587e-04	19.6
62	1.040e-01	2.0	3.113e+00	1.8	2.925e-01	1.3	9.244e+00	1.3	7.827e-06	9.7	5.934e-04	-12.4
66	9.167e-02	2.0	2.772e+00	1.9	2.682e-01	1.4	8.456e+00	1.4	1.368e-05	-8.9	2.493e-04	13.9
70	8.139e-02	2.0	2.479e+00	1.9	2.462e-01	1.5	7.745e+00	1.5	1.670e-05	-3.4	3.107e-04	-3.7
74	7.273e-02	2.0	2.226e+00	1.9	2.263e-01	1.5	7.107e+00	1.5	1.268e-05	4.9	6.640e-04	-13.7
78	6.536e-02	2.0	2.008e+00	2.0	2.083e-01	1.6	6.533e+00	1.6	5.265e-06	16.7	1.216e-04	32.2
82	5.905e-02	2.0	1.819e+00	2.0	1.921e-01	1.6	6.019e+00	1.6	8.192e-06	-8.8	5.415e-04	-29.9
86	5.361e-02	2.0	1.654e+00	2.0	1.776e-01	1.7	5.558e+00	1.7	1.048e-05	-5.2	2.869e-04	13.3
90	4.889e-02	2.0	1.510e+00	2.0	1.644e-01	1.7	5.143e+00	1.7	7.829e-06	6.4	1.390e-04	15.9
94	4.476e-02	2.0	1.384e+00	2.0	1.525e-01	1.7	4.770e+00	1.7	4.125e-06	14.7	7.144e-05	15.3
98	4.113e-02	2.0	1.273e+00	2.0	1.418e-01	1.7	4.433e+00	1.8	2.846e-06	8.9	1.093e-04	-10.2
102	3.793e-02	2.0	1.174e+00	2.0	1.321e-01	1.8	4.129e+00	1.8	5.665e-06	-17.2	9.507e-05	3.5
106	3.508e-02	2.0	1.086e+00	2.0	1.234e-01	1.8	3.854e+00	1.8	5.657e-06	0.0	1.003e-04	-1.4
110	3.255e-02	2.0	1.008e+00	2.0	1.154e-01	1.8	3.604e+00	1.8	4.925e-06	3.7	3.404e-04	-33.0
114	3.028e-02	2.0	9.378e-01	2.0	1.081e-01	1.8	3.376e+00	1.8	2.813e-06	15.7	2.504e-04	8.6
118	2.823e-02	2.0	8.746e-01	2.0	1.015e-01	1.8	3.169e+00	1.8	3.217e-06	-3.9	6.908e-05	37.3
122	2.639e-02	2.0	8.176e-01	2.0	9.550e-02	1.8	2.980e+00	1.8	4.037e-06	-6.8	8.492e-05	-6.2
126	2.472e-02	2.0	7.659e-01	2.0	8.997e-02	1.8	2.806e+00	1.9	2.563e-06	14.1	4.593e-05	19.1
130	2.321e-02	2.0	7.190e-01	2.0	8.489e-02	1.9	2.647e+00	1.9	1.650e-06	14.1	7.787e-05	-16.9
134	2.183e-02	2.0	6.763e-01	2.0	8.022e-02	1.9	2.501e+00	1.9	1.917e-06	-5.0	9.687e-05	-7.2
138	2.057e-02	2.0	6.372e-01	2.0	7.592e-02	1.9	2.366e+00	1.9	2.976e-06	-14.9	7.876e-05	7.0
142	1.942e-02	2.0	6.014e-01	2.0	7.195e-02	1.9	2.241e+00	1.9	2.726e-06	3.1	9.254e-05	-5.6
146	1.836e-02	2.0	5.686e-01	2.0	6.827e-02	1.9	2.126e+00	1.9	1.864e-06	13.7	1.040e-04	-4.2
150	1.738e-02	2.0	5.384e-01	2.0	6.487e-02	1.9	2.020e+00	1.9	1.492e-06	8.2	1.503e-04	-13.6
154	1.648e-02	2.0	5.105e-01	2.0	6.171e-02	1.9	1.921e+00	1.9	1.833e-06	-7.8	3.748e-05	52.8
158	1.565e-02	2.0	4.847e-01	2.0	5.877e-02	1.9	1.829e+00	1.9	1.961e-06	-2.6	3.417e-05	3.6
162	1.488e-02	2.0	4.609e-01	2.0	5.603e-02	1.9	1.743e+00	1.9	1.294e-06	16.6	5.212e-05	-16.9
166	1.417e-02	2.0	4.387e-01	2.0	5.348e-02	1.9	1.663e+00	1.9	8.168e-07	18.9	4.604e-05	5.1
170	1.350e-02	2.0	4.181e-01	2.0	5.109e-02	1.9	1.589e+00	1.9	1.347e-06	-21.0	1.018e-04	-33.3
174	1.288e-02	2.0	3.989e-01	2.0	4.886e-02	1.9	1.519e+00	1.9	1.581e-06	-6.9	2.812e-05	55.3
178	1.231e-02	2.0	3.811e-01	2.0	4.677e-02	1.9	1.454e+00	1.9	1.453e-06	3.7	7.288e-05	-41.9
182	1.177e-02	2.0	3.644e-01	2.0	4.481e-02	1.9	1.393e+00	1.9	7.440e-07	30.1	1.276e-05	78.4
186	1.126e-02	2.0	3.487e-01	2.0	4.297e-02	1.9	1.335e+00	1.9	7.415e-07	0.2	5.649e-05	-68.4
190	1.079e-02	2.0	3.341e-01	2.0	4.124e-02	1.9	1.281e+00	1.9	1.120e-06	-19.4	2.066e-05	47.3
194	1.035e-02	2.0	3.203e-01	2.0	3.961e-02	1.9	1.230e+00	1.9	1.242e-06	-5.0	4.009e-05	-31.8
198	9.931e-03	2.0	3.074e-01	2.0	3.808e-02	1.9	1.182e+00	1.9	9.004e-07	15.8	7.924e-05	-33.4

Table 5: L_1/L_∞ errors and observed order of convergence ν for the non-linear models in the Crossing Beams slab geometry case.

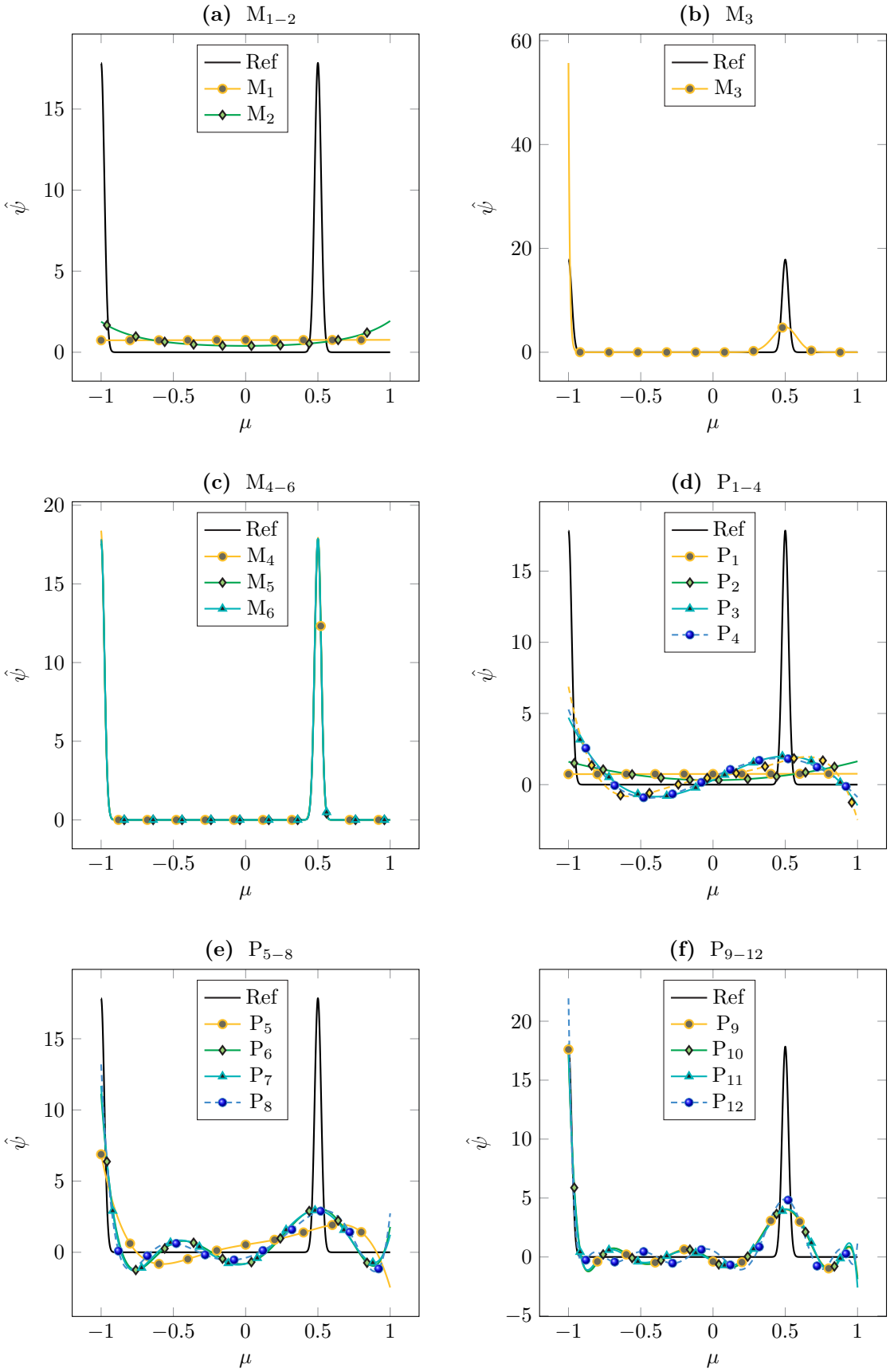

Figure S3.1: Distributions of M_N and P_N models for the slab geometry crossing beams test. P_N models are continued in Figure S3.2. Higher order M_N models are omitted as they are close to the reference solution.

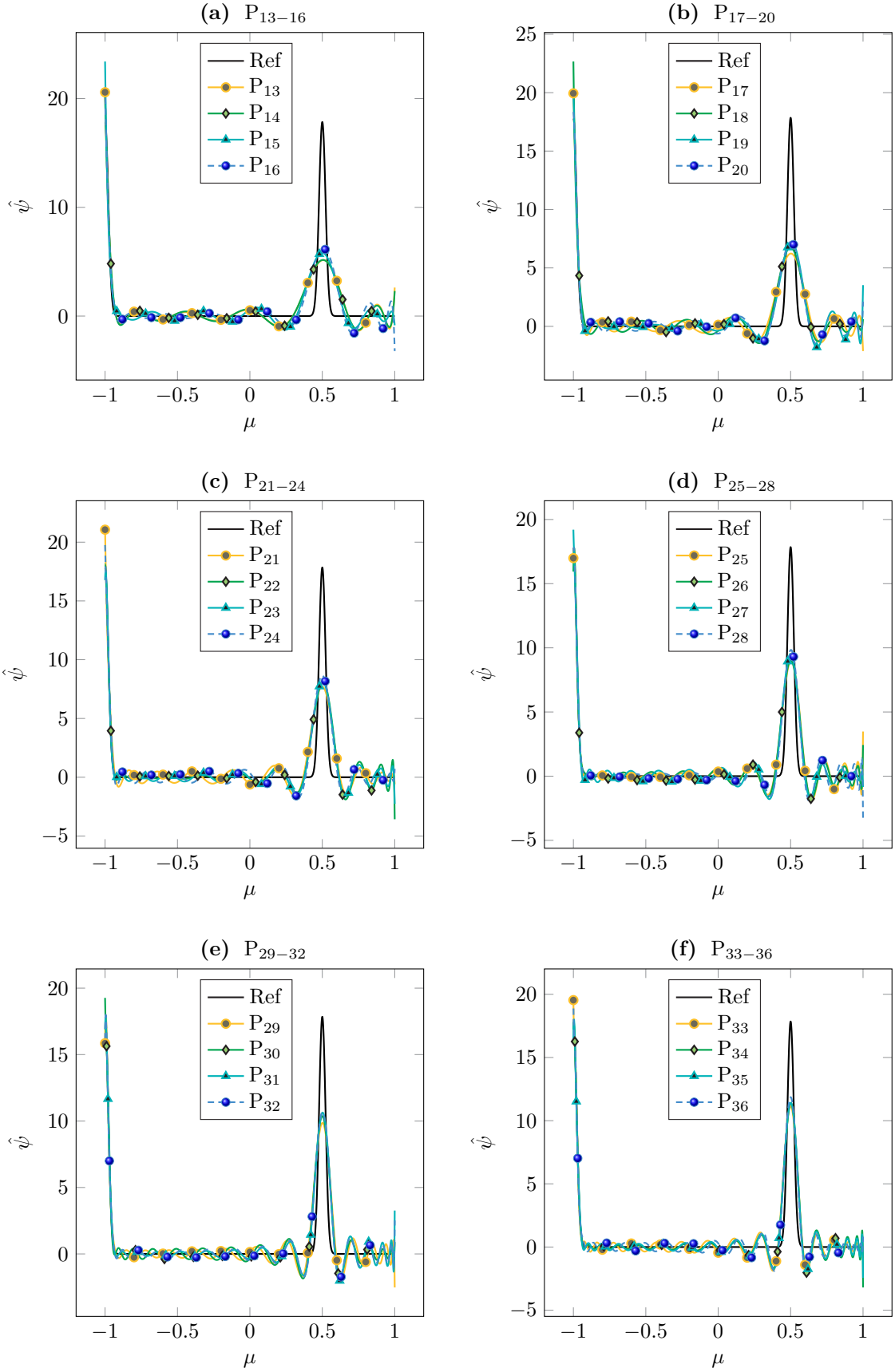

Figure S3.2: Distributions of P_N models for the slab geometry crossing beams test. Lower order models can be found in Figure S3.1, higher order models in Figure S3.3.

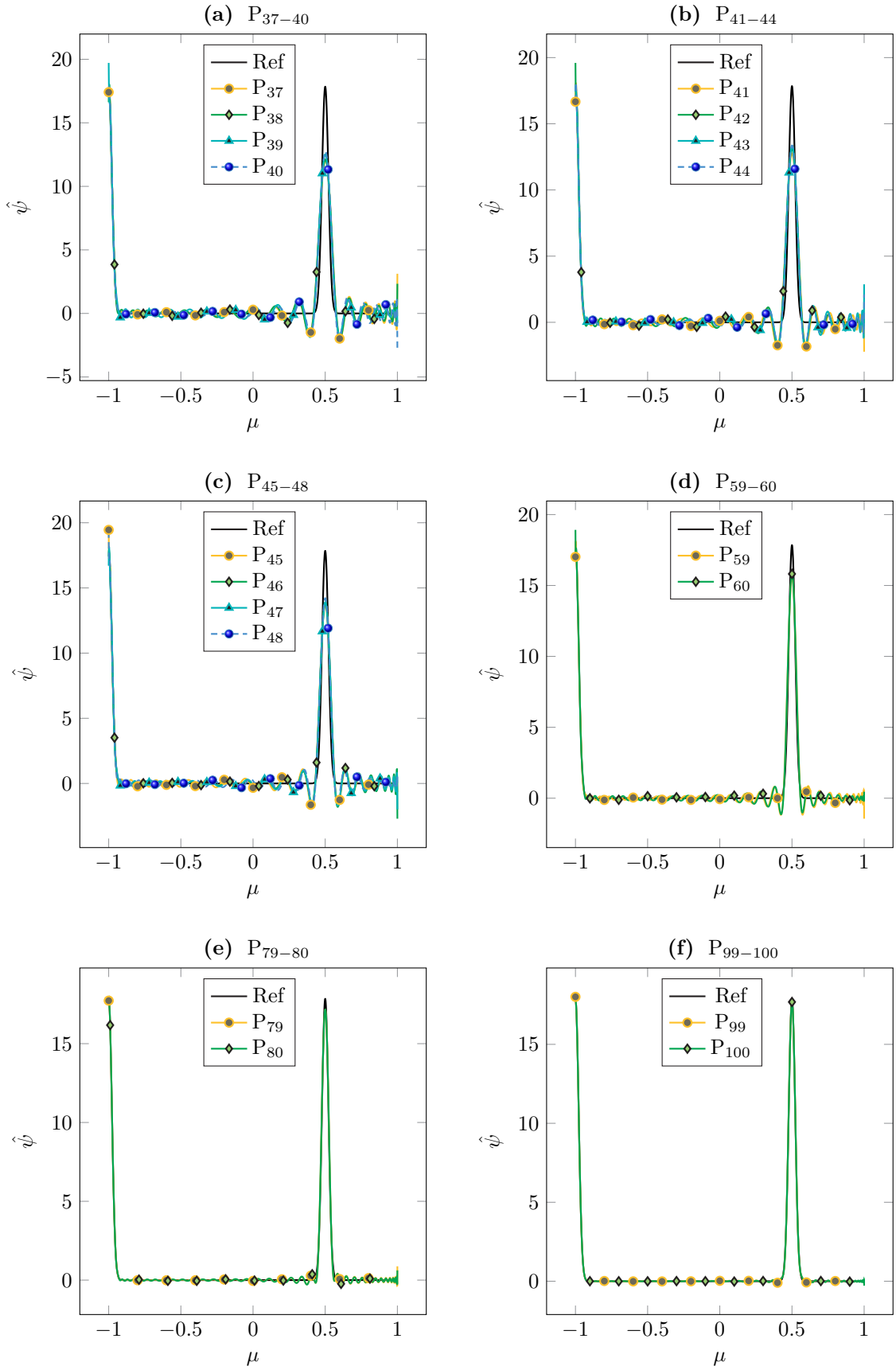

Figure S3.3: Distributions of selected high-order P_N models for the slab geometry crossing beams test. Lower order models can be found in Figures S3.1 and S3.2.

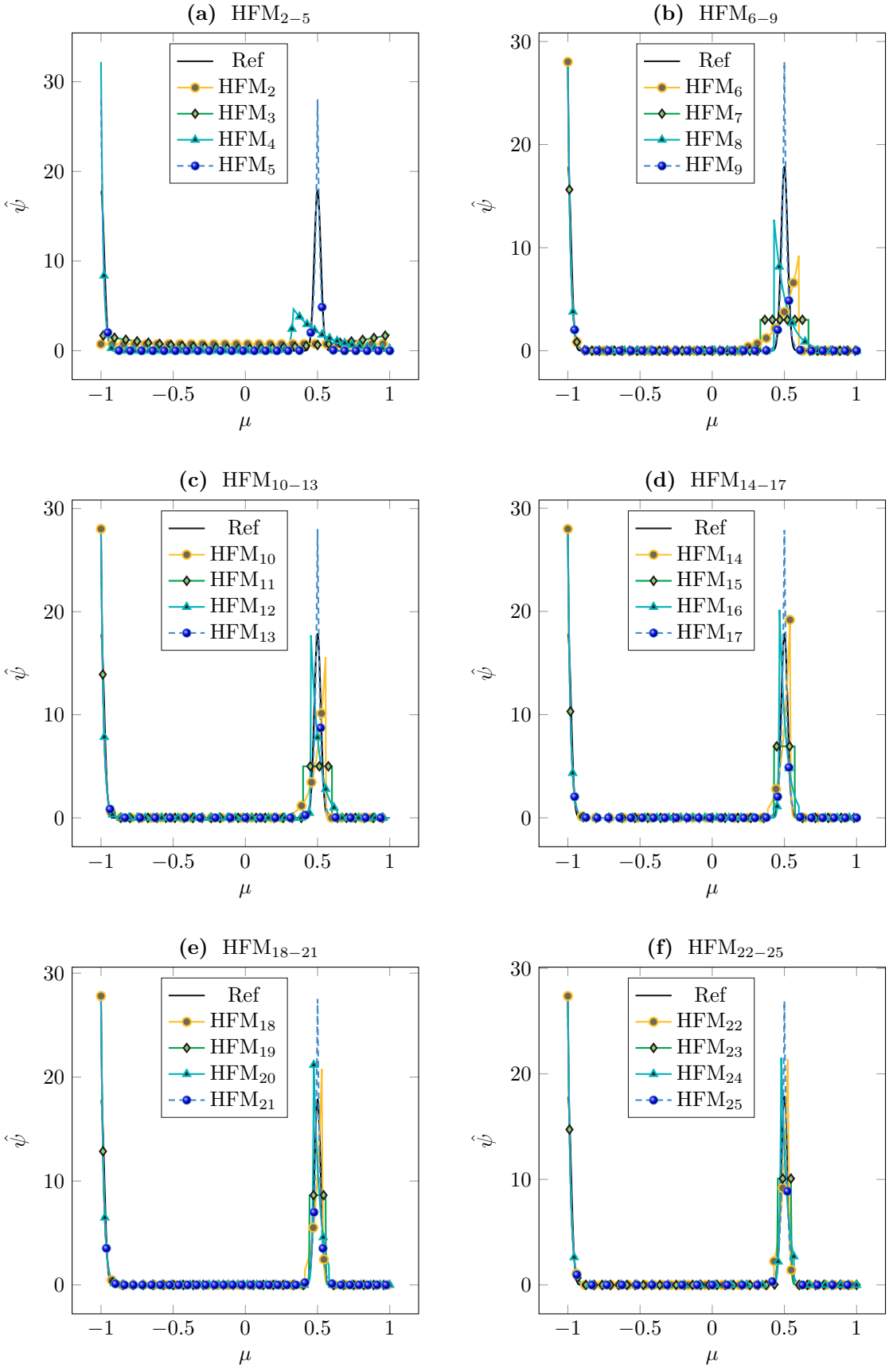

Figure S3.4: Distributions of HFM_n models for the slab geometry crossing beams test. Continued in Figure S3.5.

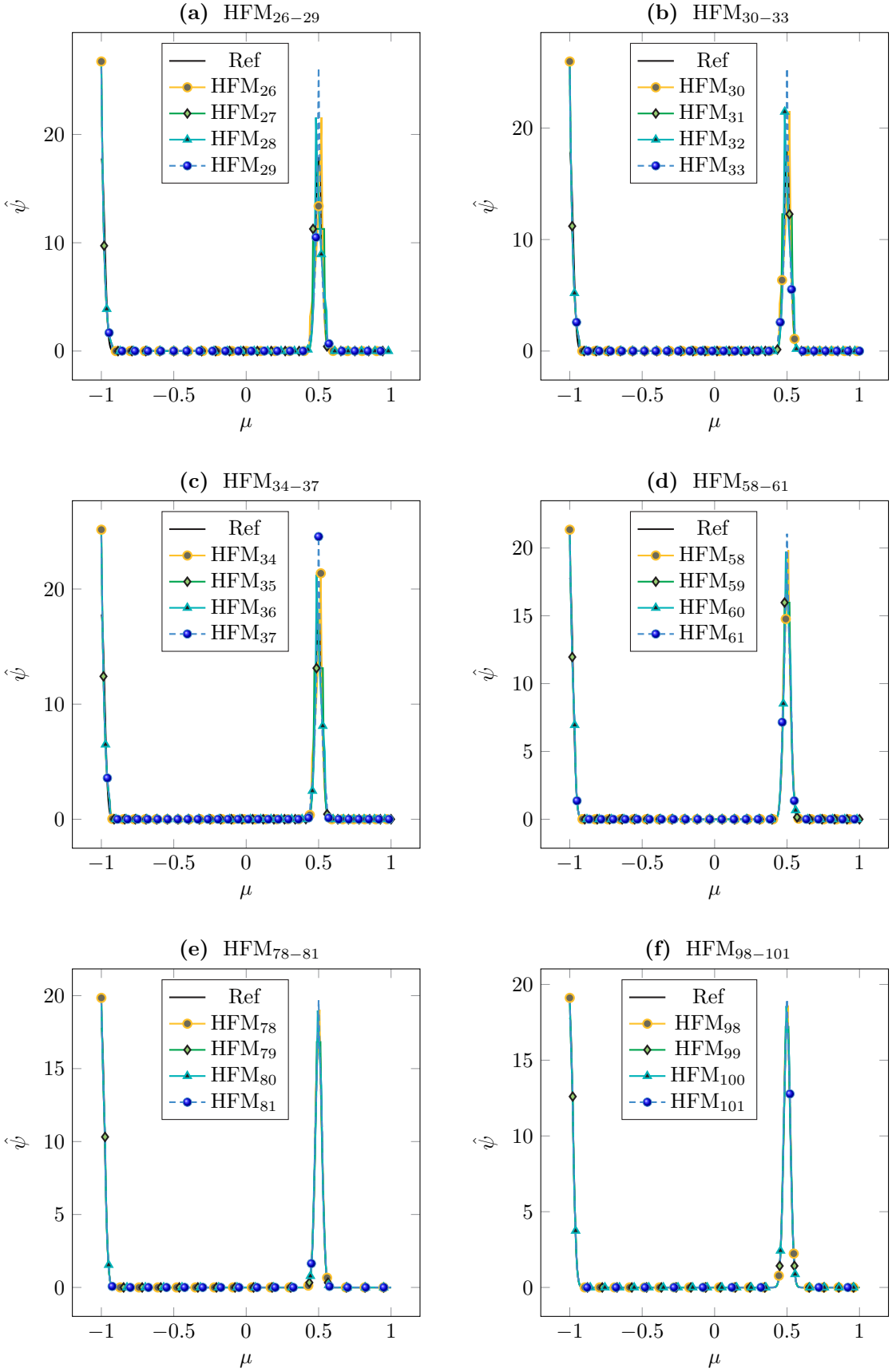

Figure S3.5: Distributions of HFM_n models for the slab geometry crossing beams test. Lower order models can be found in Figure S3.4.

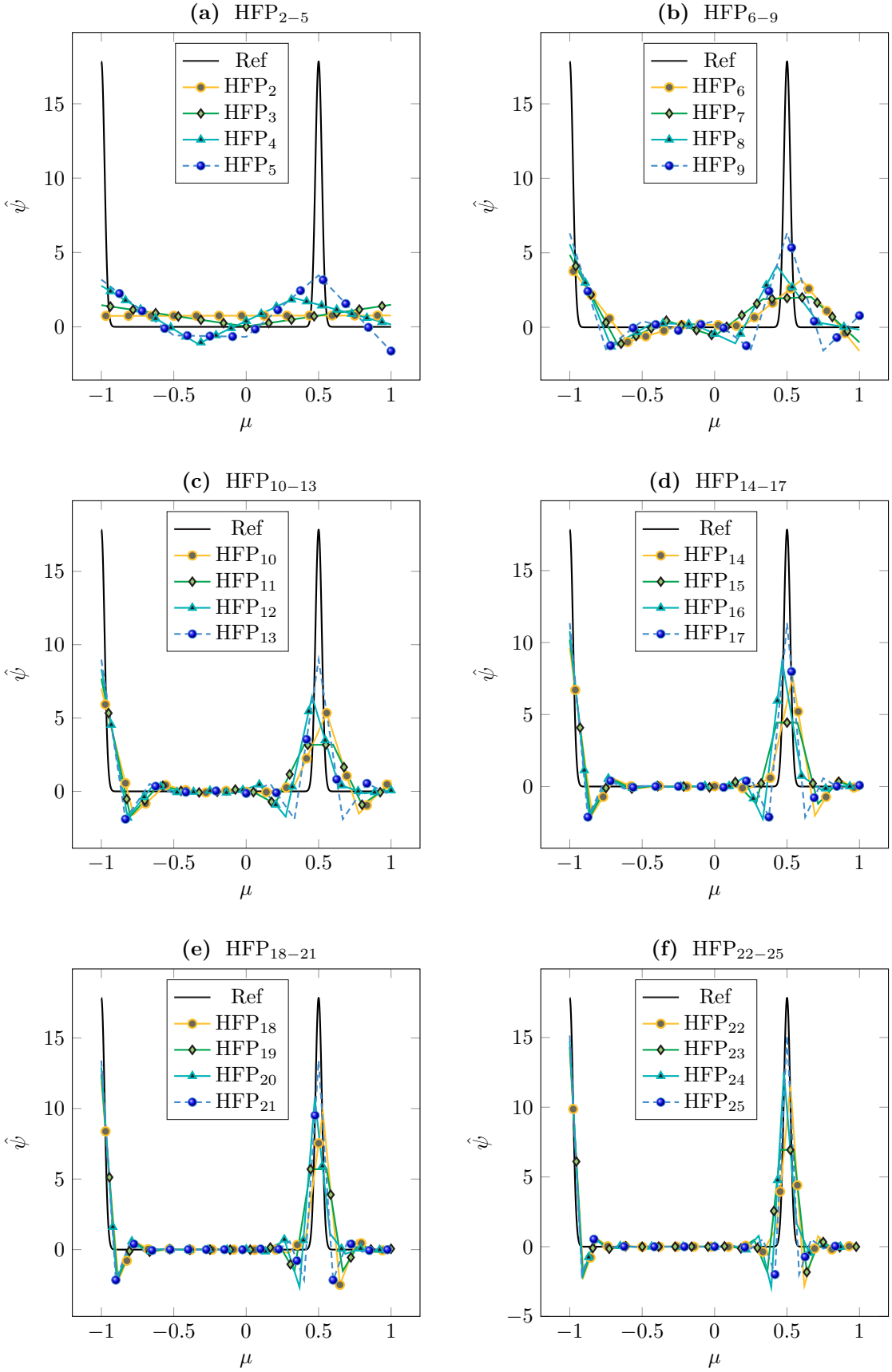

Figure S3.6: Distributions of HFP_n models for the slab geometry crossing beams test. High order models can be found in Figure S3.7.

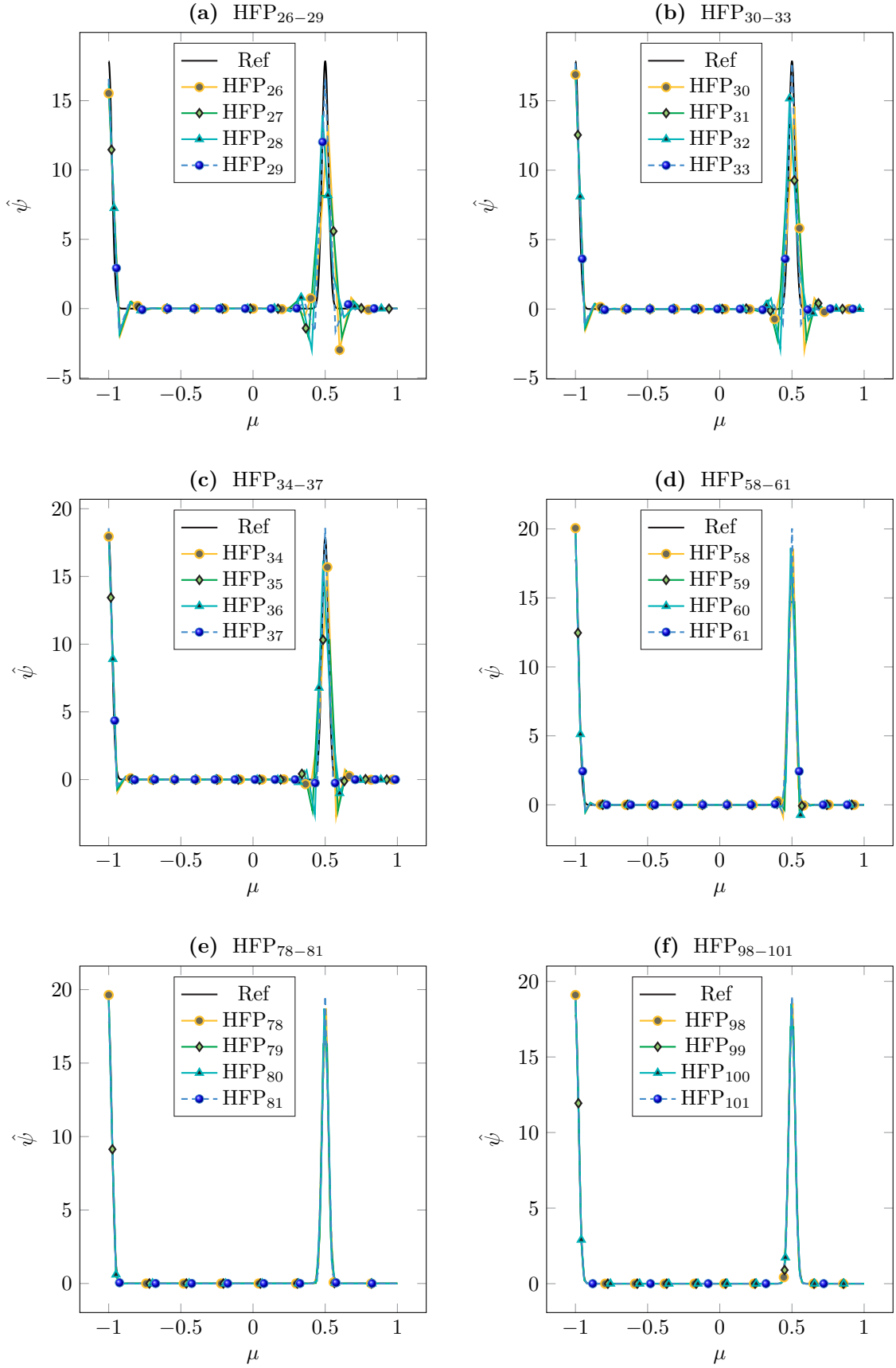

Figure S3.7: Distributions of HFP_n models for the slab geometry crossing beams test. Lower order models can be found in Figure S3.6.

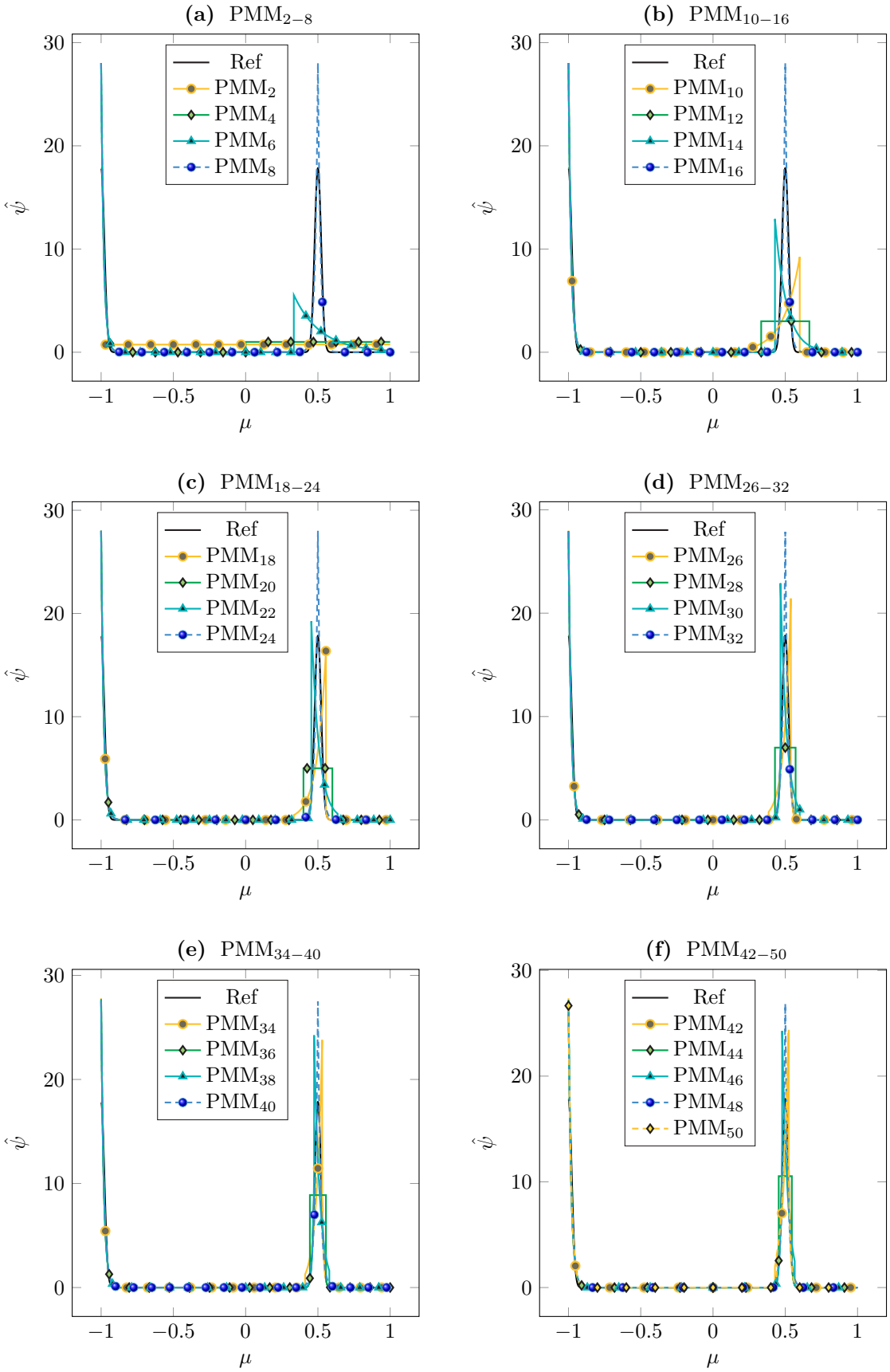

Figure S3.8: Distributions of PMM_n models for the slab geometry crossing beams test. High order models can be found in Figure S3.10.

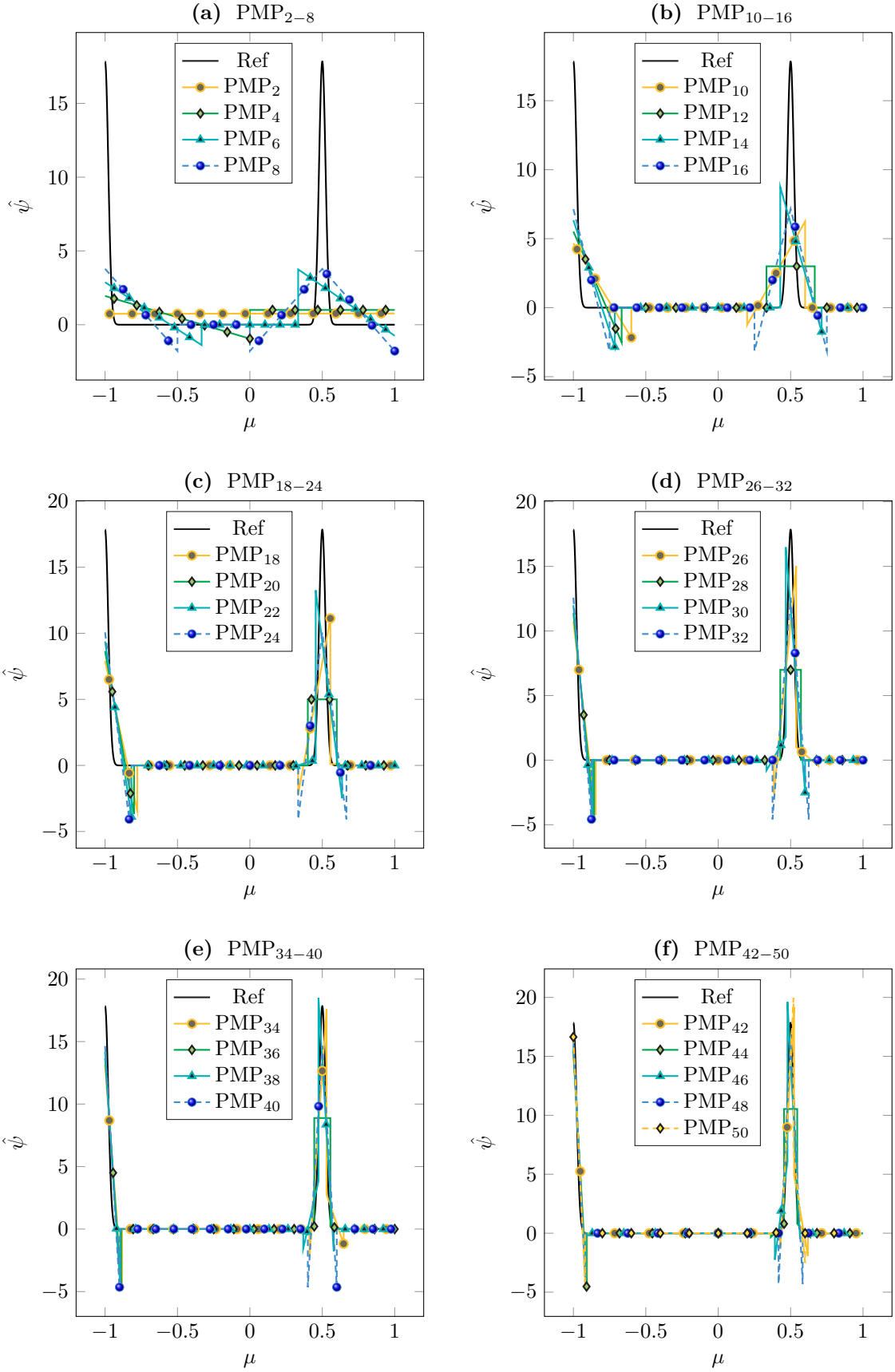

Figure S3.9: Distributions of PMP_n models for the slab geometry crossing beams test. High order models can be found in Figure S3.10.

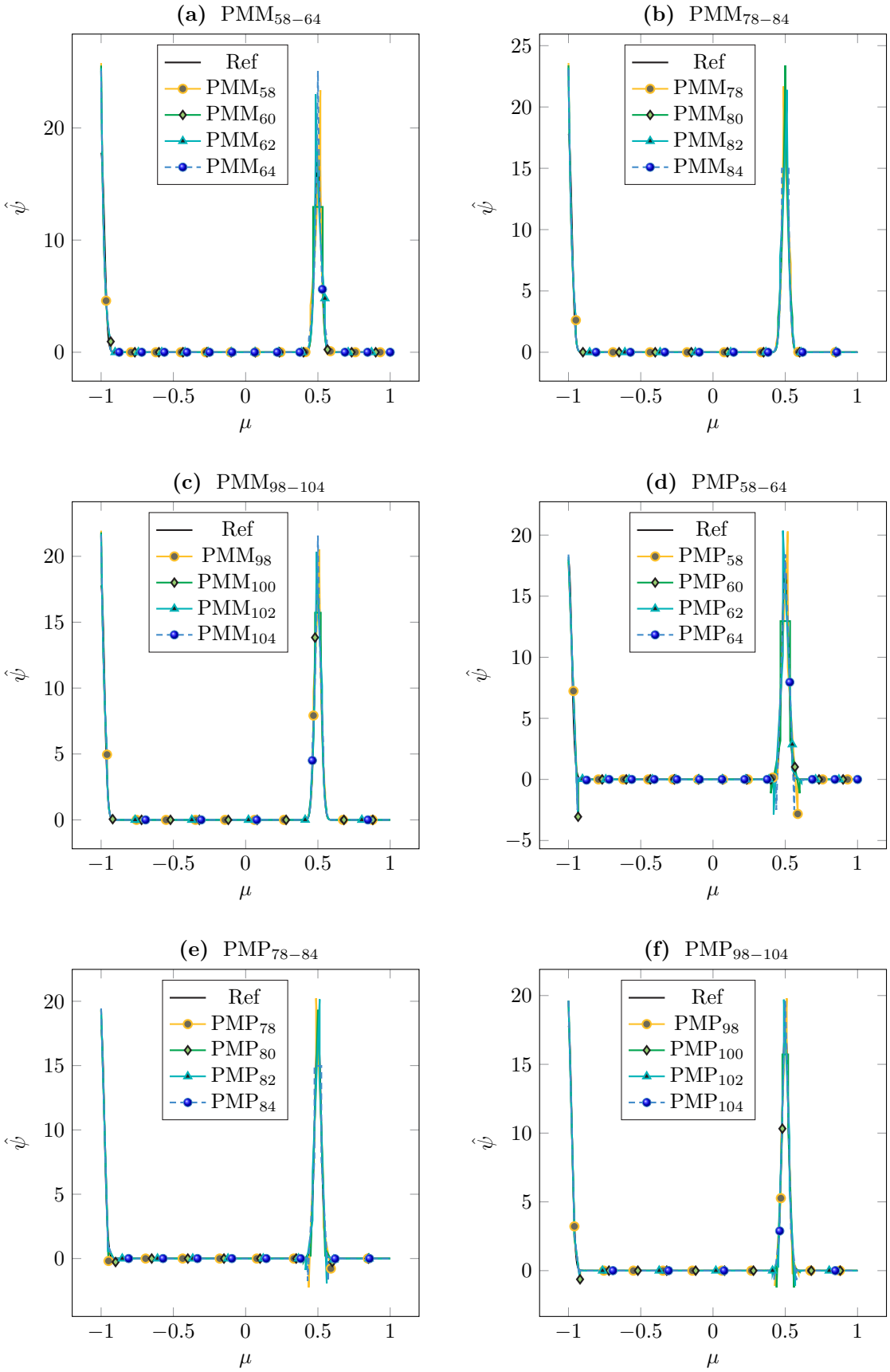

Figure S3.10: Distributions of PMM_n and PMP_n models for the slab geometry crossing beams test. Lower order models can be found in Figures S3.8 and S3.9.

	HFP$_n$				PMP$_n$				P$_N$			
n	E_h^1	ν	E_h^∞	ν	E_h^1	ν	E_h^∞	ν	E_h^1	ν	E_h^∞	ν
2	2.711e+00	—	1.710e+01	—	2.711e+00	—	1.710e+01	—	2.711e+00	—	1.710e+01	—
6	2.712e+00	-0.0	1.543e+01	0.1	2.532e+00	0.1	1.522e+01	0.1	2.807e+00	-0.0	1.615e+01	0.1
10	2.332e+00	0.3	1.374e+01	0.2	2.099e+00	0.4	1.347e+01	0.2	2.272e+00	0.4	1.383e+01	0.3
14	1.932e+00	0.6	1.201e+01	0.4	1.734e+00	0.6	1.174e+01	0.4	1.970e+00	0.4	1.271e+01	0.3
18	1.578e+00	0.8	1.038e+01	0.6	1.434e+00	0.8	1.031e+01	0.5	1.877e+00	0.2	1.161e+01	0.4
22	1.278e+00	1.1	8.935e+00	0.7	1.198e+00	0.9	1.100e+01	-0.3	1.748e+00	0.4	1.013e+01	0.7
26	1.027e+00	1.3	7.679e+00	0.9	1.015e+00	1.0	1.098e+01	0.0	1.403e+00	1.3	8.864e+00	0.8
30	8.176e-01	1.6	6.609e+00	1.0	8.688e-01	1.1	1.061e+01	0.2	1.407e+00	-0.0	7.982e+00	0.7
34	6.440e-01	1.9	5.706e+00	1.2	7.480e-01	1.2	1.011e+01	0.4	1.260e+00	0.9	6.700e+00	1.4
38	5.038e-01	2.2	4.945e+00	1.3	6.462e-01	1.3	9.571e+00	0.5	1.044e+00	1.7	5.758e+00	1.4
42	4.065e-01	2.1	4.303e+00	1.4	5.598e-01	1.4	9.032e+00	0.6	1.004e+00	0.4	5.080e+00	1.3
46	3.394e-01	2.0	3.758e+00	1.5	4.865e-01	1.5	8.508e+00	0.7	8.766e-01	1.5	4.142e+00	2.2
50	2.868e-01	2.0	3.290e+00	1.6	4.249e-01	1.6	8.001e+00	0.7	6.943e-01	2.8	3.465e+00	2.1
54	2.434e-01	2.1	2.888e+00	1.7	3.732e-01	1.7	7.514e+00	0.8	6.576e-01	0.7	2.995e+00	1.9
58	2.096e-01	2.1	2.539e+00	1.8	3.284e-01	1.8	7.050e+00	0.9	5.524e-01	2.4	2.363e+00	3.3
62	1.820e-01	2.1	2.235e+00	1.9	2.903e-01	1.9	6.608e+00	1.0	4.230e-01	4.0	1.927e+00	3.1
66	1.565e-01	2.4	2.116e+00	0.9	2.584e-01	1.9	6.192e+00	1.0	3.931e-01	1.2	1.630e+00	2.7
70	1.336e-01	2.7	2.021e+00	0.8	2.318e-01	1.8	5.801e+00	1.1	3.182e-01	3.6	1.243e+00	4.6
74	1.139e-01	2.9	1.911e+00	1.0	2.095e-01	1.8	5.434e+00	1.2	2.353e-01	5.4	1.142e+00	1.5
78	9.826e-02	2.8	1.795e+00	1.2	1.906e-01	1.8	5.093e+00	1.2	2.147e-01	1.7	8.169e-01	6.4
82	8.590e-02	2.7	1.679e+00	1.3	1.747e-01	1.7	4.776e+00	1.3	1.672e-01	5.0	6.017e-01	6.1
86	7.587e-02	2.6	1.565e+00	1.5	1.610e-01	1.7	4.482e+00	1.3	1.194e-01	7.1	6.532e-01	-1.7
90	6.759e-02	2.5	1.457e+00	1.6	1.492e-01	1.7	4.209e+00	1.4	1.071e-01	2.4	3.825e-01	11.8
94	6.057e-02	2.5	1.355e+00	1.7	1.390e-01	1.6	3.956e+00	1.4	8.007e-02	6.7	2.676e-01	8.2
98	5.452e-02	2.5	1.260e+00	1.7	1.301e-01	1.6	3.723e+00	1.5	5.529e-02	8.9	3.372e-01	-5.5
102	4.927e-02	2.5	1.173e+00	1.8	1.224e-01	1.5	3.506e+00	1.5	4.876e-02	3.1	1.836e-01	15.2
106	4.469e-02	2.5	1.092e+00	1.8	1.153e-01	1.5	3.306e+00	1.5	3.496e-02	8.7	1.126e-01	12.7
110	4.069e-02	2.5	1.018e+00	1.9	1.087e-01	1.6	3.121e+00	1.6	2.339e-02	10.9	1.575e-01	-9.1
114	3.723e-02	2.5	9.508e-01	1.9	1.027e-01	1.6	2.949e+00	1.6	2.027e-02	4.0	7.851e-02	19.5
118	3.421e-02	2.5	8.890e-01	1.9	9.723e-02	1.6	2.790e+00	1.6	1.391e-02	10.9	4.769e-02	14.5
122	3.157e-02	2.4	8.326e-01	2.0	9.219e-02	1.6	2.643e+00	1.6	9.051e-03	12.9	6.660e-02	-10.0
126	2.923e-02	2.4	7.809e-01	2.0	8.755e-02	1.6	2.506e+00	1.7	7.688e-03	5.1	2.982e-02	24.9
130	2.715e-02	2.4	7.336e-01	2.0	8.322e-02	1.6	2.378e+00	1.7	5.041e-03	13.5	1.813e-02	15.9
134	2.528e-02	2.4	6.903e-01	2.0	7.919e-02	1.6	2.259e+00	1.7	3.217e-03	14.8	2.552e-02	-11.3
138	2.359e-02	2.3	6.506e-01	2.0	7.544e-02	1.7	2.149e+00	1.7	2.659e-03	6.5	9.998e-03	31.9
142	2.208e-02	2.3	6.140e-01	2.0	7.195e-02	1.7	2.046e+00	1.7	1.665e-03	16.4	6.166e-03	16.9
146	2.070e-02	2.3	5.804e-01	2.0	6.871e-02	1.7	1.950e+00	1.7	1.055e-03	16.4	8.847e-03	-13.0
150	1.945e-02	2.3	5.494e-01	2.0	6.570e-02	1.7	1.860e+00	1.7	8.382e-04	8.5	3.280e-03	36.7
154	1.832e-02	2.3	5.207e-01	2.0	6.282e-02	1.7	1.776e+00	1.8	5.010e-04	19.6	2.248e-03	14.4
158	1.728e-02	2.3	4.942e-01	2.0	6.006e-02	1.8	1.697e+00	1.8	3.194e-04	17.6	2.771e-03	-8.2
162	1.634e-02	2.2	4.697e-01	2.0	5.740e-02	1.8	1.623e+00	1.8	2.405e-04	11.4	1.039e-03	39.2
166	1.549e-02	2.2	4.469e-01	2.0	5.486e-02	1.9	1.554e+00	1.8	1.374e-04	23.0	7.637e-04	12.6
170	1.469e-02	2.2	4.257e-01	2.0	5.242e-02	1.9	1.488e+00	1.8	8.922e-05	18.1	7.818e-04	-1.0
174	1.396e-02	2.2	4.060e-01	2.0	5.010e-02	2.0	1.427e+00	1.8	6.274e-05	15.1	2.972e-04	41.6
178	1.328e-02	2.2	3.876e-01	2.0	4.788e-02	2.0	1.369e+00	1.8	3.436e-05	26.5	2.342e-04	10.5
182	1.265e-02	2.2	3.704e-01	2.0	4.577e-02	2.0	1.315e+00	1.8	2.293e-05	18.2	1.977e-04	7.6
186	1.206e-02	2.2	3.543e-01	2.0	4.375e-02	2.1	1.264e+00	1.8	1.487e-05	19.9	7.646e-05	43.7
190	1.152e-02	2.2	3.393e-01	2.0	4.184e-02	2.1	1.215e+00	1.8	7.849e-06	30.0	6.460e-05	7.9
194	1.100e-02	2.2	3.252e-01	2.0	4.001e-02	2.1	1.169e+00	1.8	5.404e-06	17.9	4.451e-05	17.9
198	1.052e-02	2.2	3.119e-01	2.0	3.829e-02	2.2	1.126e+00	1.9	3.205e-06	25.6	1.759e-05	45.5

Table 6: L_1/L_∞ errors and observed order of convergence ν for the linear models in the Crossing Beams slab geometry case.

S4. Gauss distribution in three dimensions

Ansatz functions for a Gauss distribution on the unit sphere

$$\psi_{\text{Gauss}}(\Omega) = \frac{1}{2\pi\sigma^2\left(1-\exp\left(-2\sigma^{-2}\right)\right)} \exp\left(\frac{(\Omega_x - \overline{\Omega_x})^2 + \Omega_y^2 + \Omega_z^2}{-2\sigma^2}\right) \text{ where } \sigma = 0.5, \overline{\Omega_x} = 1,$$

for all tested models can be found in Figures S4.1-S4.5. M_N and PMM_n models are omitted as they are exact. Errors and observed orders of convergence are listed in Tables 7 and 8.

	HFM_n					PMM_n					M_N			
n	E_h^1	ν	E_h^∞	ν	n	E_h^1	ν	E_h^∞	ν	n	E_h^1	ν	E_h^∞	ν
6	2.06e-01	—	7.47e-01	—	32	6.46e-14	—	1.89e-13	—	4	3.24e-13	—	2.47e-13	—
18	7.80e-02	0.9	1.94e-01	1.2	128	9.46e-14	-0.3	1.15e-13	0.4	16	4.38e-13	-0.2	3.92e-13	-0.3
66	2.21e-02	1.0	5.07e-02	1.0	512	2.93e-13	-0.8	8.40e-13	-1.4	64	1.19e-13	0.9	4.53e-14	1.6
258	5.45e-03	1.0	1.55e-02	0.9	2048	5.33e-13	-0.4	3.20e-12	-1.0	256	1.13e-13	0.0	3.69e-14	0.1
1026	1.34e-03	1.0	4.13e-03	1.0	8192	1.46e-12	-0.7	1.74e-11	-1.2	961	1.06e-13	0.0	3.01e-14	0.2

Table 7: L_1/L_∞ errors and observed order of convergence ν for the non-linear models in the Gauss 3D case.

	HFP_n					PMP_n					P_N			
n	E_h^1	ν	E_h^∞	ν	n	E_h^1	ν	E_h^∞	ν	n	E_h^1	ν	E_h^∞	ν
6	3.76e-01	—	1.20e-01	—	32	2.54e-01	—	1.18e-01	—	4	8.79e-01	—	3.78e-01	—
18	2.30e-01	0.4	1.55e-01	-0.2	128	6.43e-02	1.0	6.66e-02	0.4	16	2.08e-01	1.0	9.03e-02	1.0
66	4.73e-02	1.2	4.93e-02	0.9	512	1.68e-02	1.0	2.25e-02	0.8	64	1.50e-03	3.6	7.31e-04	3.5
258	1.05e-02	1.1	1.53e-02	0.9	2048	4.19e-03	1.0	6.50e-03	0.9	256	1.04e-09	10.2	8.17e-10	9.9
1026	2.53e-03	1.0	4.10e-03	1.0	8192	1.04e-03	1.0	1.88e-03	0.9	961	7.00e-10	0.3	4.45e-10	0.5

Table 8: L_1/L_∞ errors and observed order of convergence ν for the linear models in the Gauss 3D case.

S5. Square distribution in three dimensions

Ansatz functions for a discontinuous square distribution on the unit sphere

$$\psi_{\text{Square}}(\Omega) = \begin{cases} 1 & \text{if } \Omega_x > 0 \wedge |\Omega_y| < 0.5 \wedge |\Omega_z| < 0.5 \\ \psi_{vac}(\Omega) & \text{else,} \end{cases} \quad \text{where} \quad \psi_{vac}(\Omega) = \frac{10^{-8}}{4\pi},$$

for all tested models can be found in Figures S5.1-S5.15. Errors and observed orders of convergence are listed in Tables 9 and 10.

	HFM_n					PMM_n					M_N			
n	E_h^1	ν	E_h^∞	ν	n	E_h^1	ν	E_h^∞	ν	n	E_h^1	ν	E_h^∞	ν
18	6.12e-01	—	9.80e-01	—	32	4.98e-01	—	9.21e-01	—	4	6.63e-01	—	9.16e-01	—
66	3.25e-01	0.5	9.42e-01	0.0	128	3.89e-01	0.2	9.21e-01	0.0	16	3.53e-01	0.5	9.83e-01	-0.1
258	2.80e-01	0.1	9.22e-01	0.0	512	2.00e-01	0.5	9.49e-01	-0.0	121	1.78e-01	0.3	7.57e-01	0.1
1026	8.18e-02	0.9	9.37e-01	-0.0	2048	1.41e-01	0.2	9.14e-01	0.0	289	1.45e-01	0.2	6.83e-01	0.1
4098	6.21e-02	0.2	9.06e-01	0.0	8192	4.67e-02	0.8	9.76e-01	-0.0	529	9.20e-02	0.7	6.48e-01	0.1
16386	3.23e-02	0.5	8.87e-01	0.0	32768	2.90e-02	0.3	1.63e+00	-0.4	961	8.86e-02	0.1	6.20e-01	0.1
65538	2.01e-02	0.3	8.12e-01	0.1	131072	8.73e-03	0.9	2.19e+00	-0.2	1296	7.74e-02	0.5	6.29e-01	-0.0

Table 9: L_1/L_∞ errors and observed order of convergence ν for the non-linear models in the Square 3D case.

S6. Crossing beams in three dimensions

Ansatz functions a distribution modelling two crossing beams of particles

$$\psi_{\text{CrossingBeams}}(\Omega) = \max\left(\frac{a}{\pi}\left(\exp(-a\left\|\Omega-(1,0,0)^T\right\|_2^2) + \exp(-a\left\|\Omega-(0,1,0)^T\right\|_2^2)\right), \psi_{vac}(\Omega)\right), \quad \text{(S6.1)}$$

where $a = 100$, for all tested models can be found in Figures S6.1- S6.11. Errors and observed orders of convergence are listed in Tables 11 and 12.

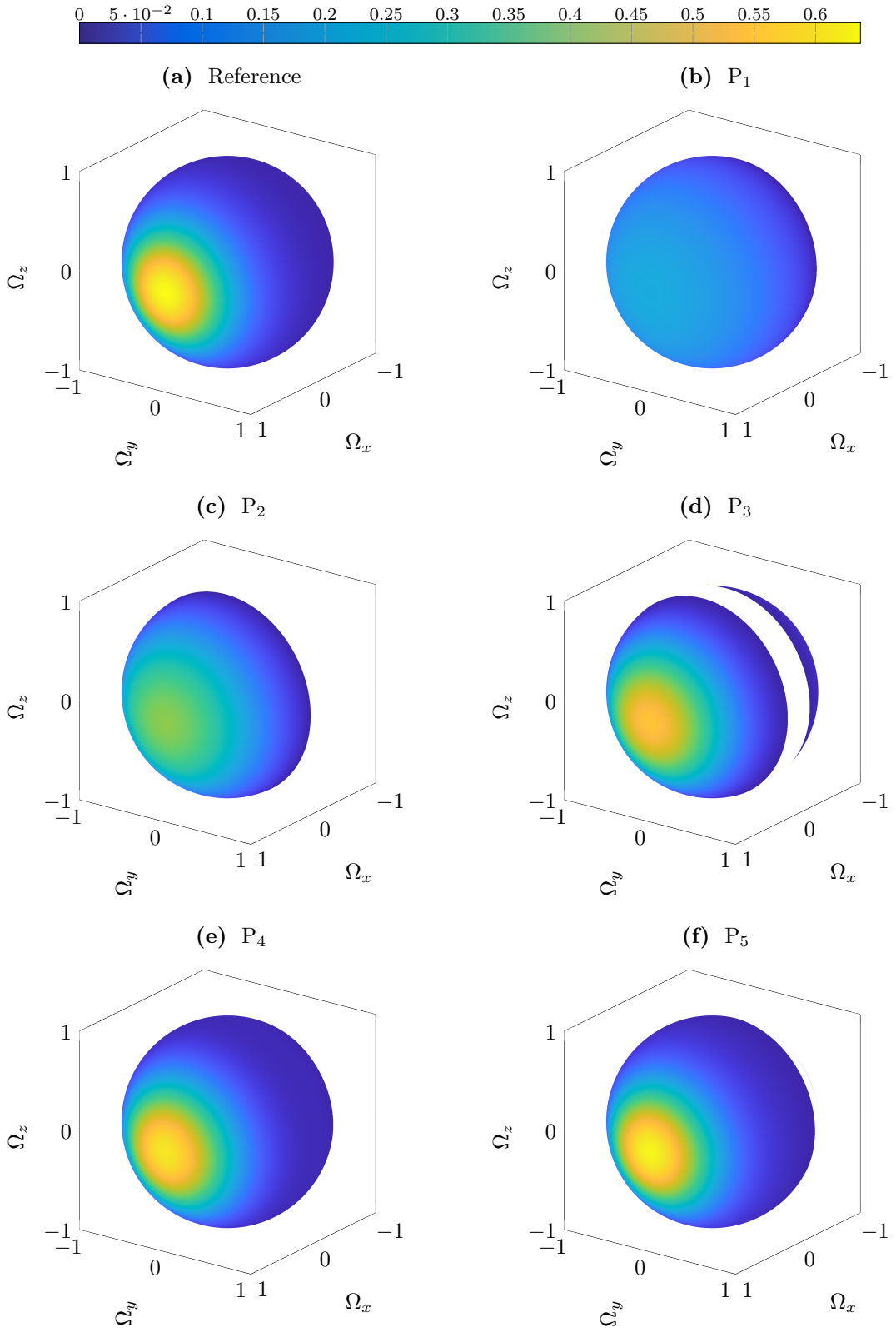

Figure S4.1: Distributions of P_N models for the three-dimensional Gauss test. Unphysical negative values are shown in white. Continued in Figure S4.2.

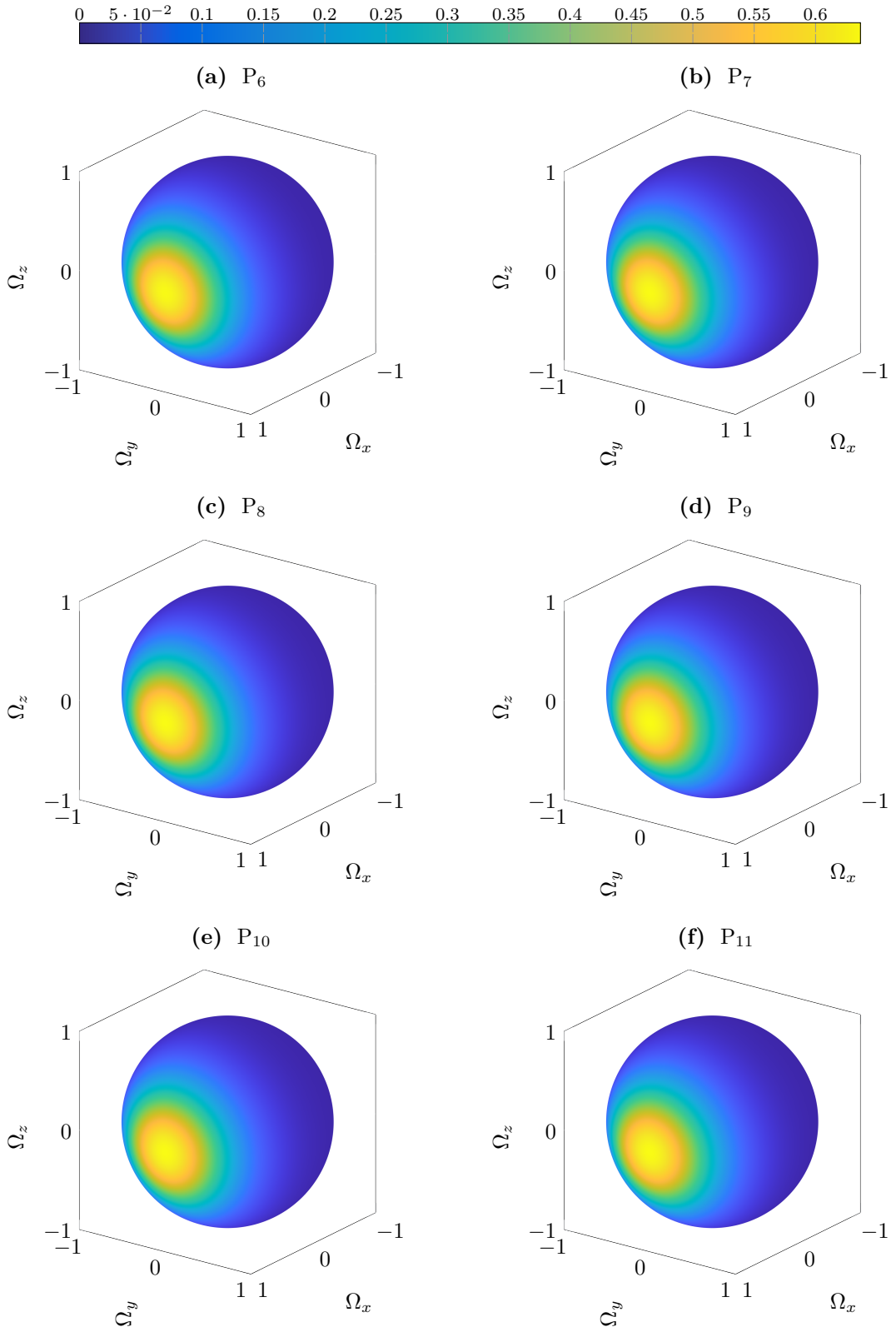

Figure S4.2: Distributions of P_N models for the three-dimensional Gauss test. Unphysical negative values are shown in white. Reference solution can be found in Figure S4.1.

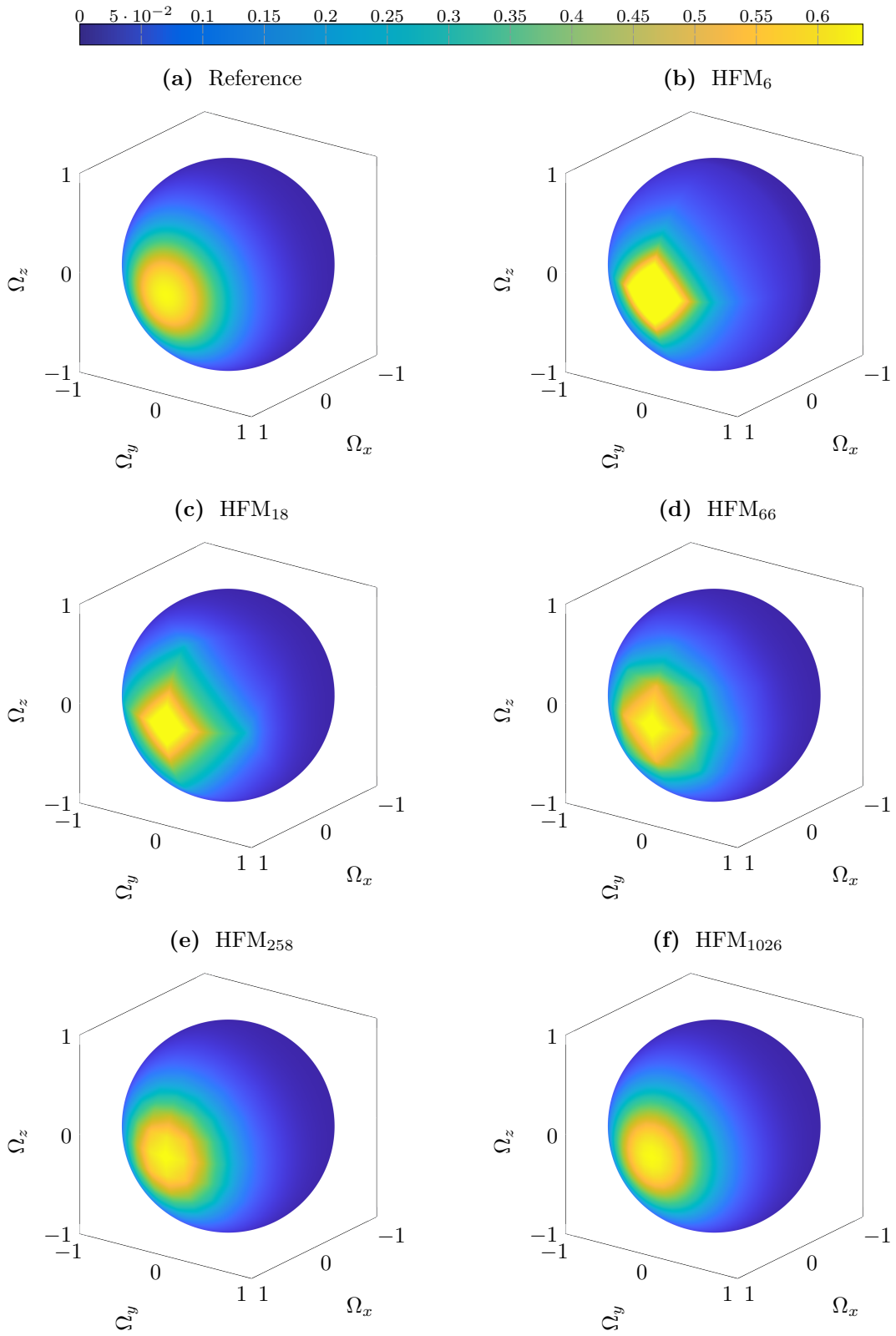

Figure S4.3: Distributions of HFM$_n$ models for the three-dimensional Gauss test.

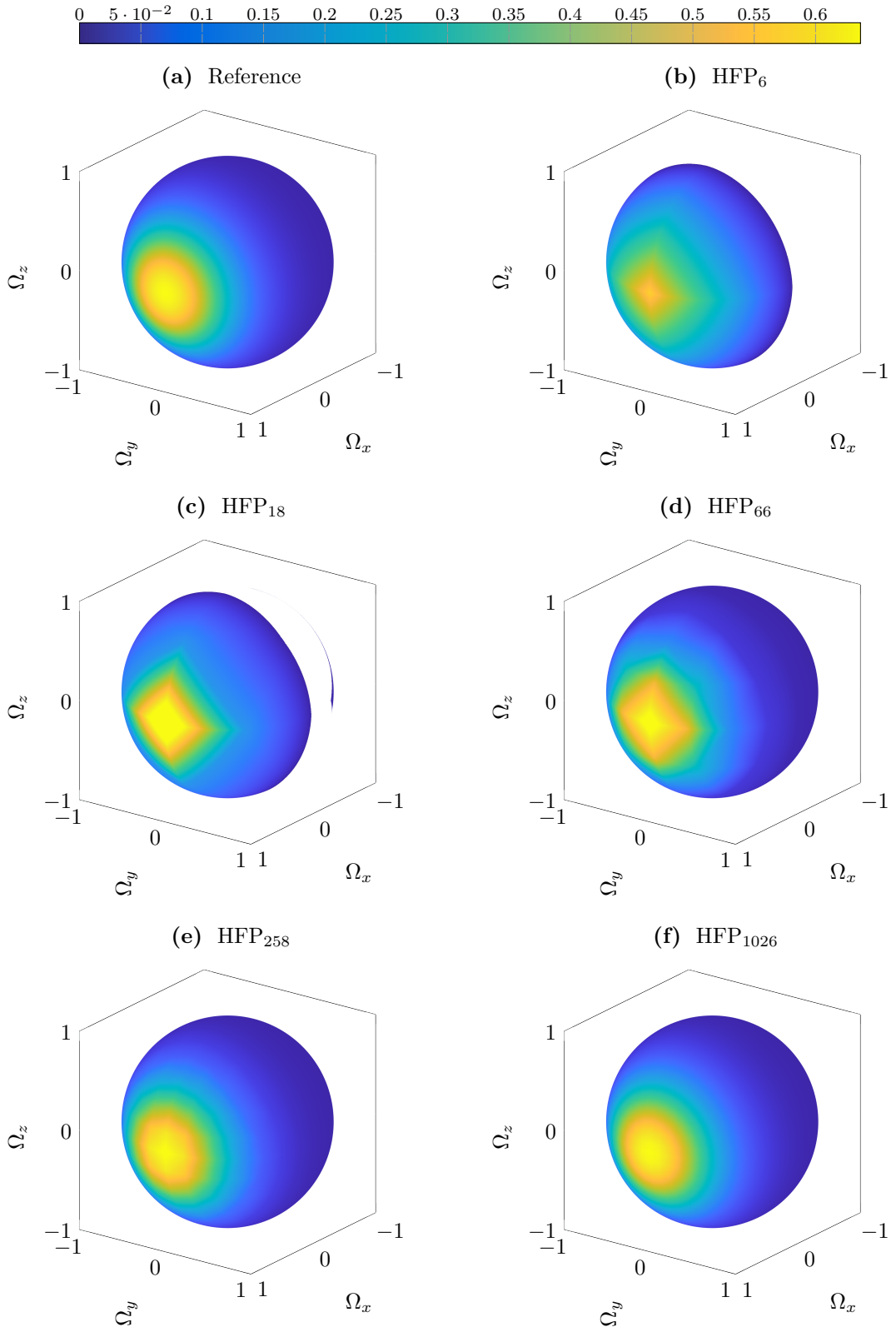

Figure S4.4: Distributions of HFP_n models for the three-dimensional Gauss test. Unphysical negative values are shown in white.

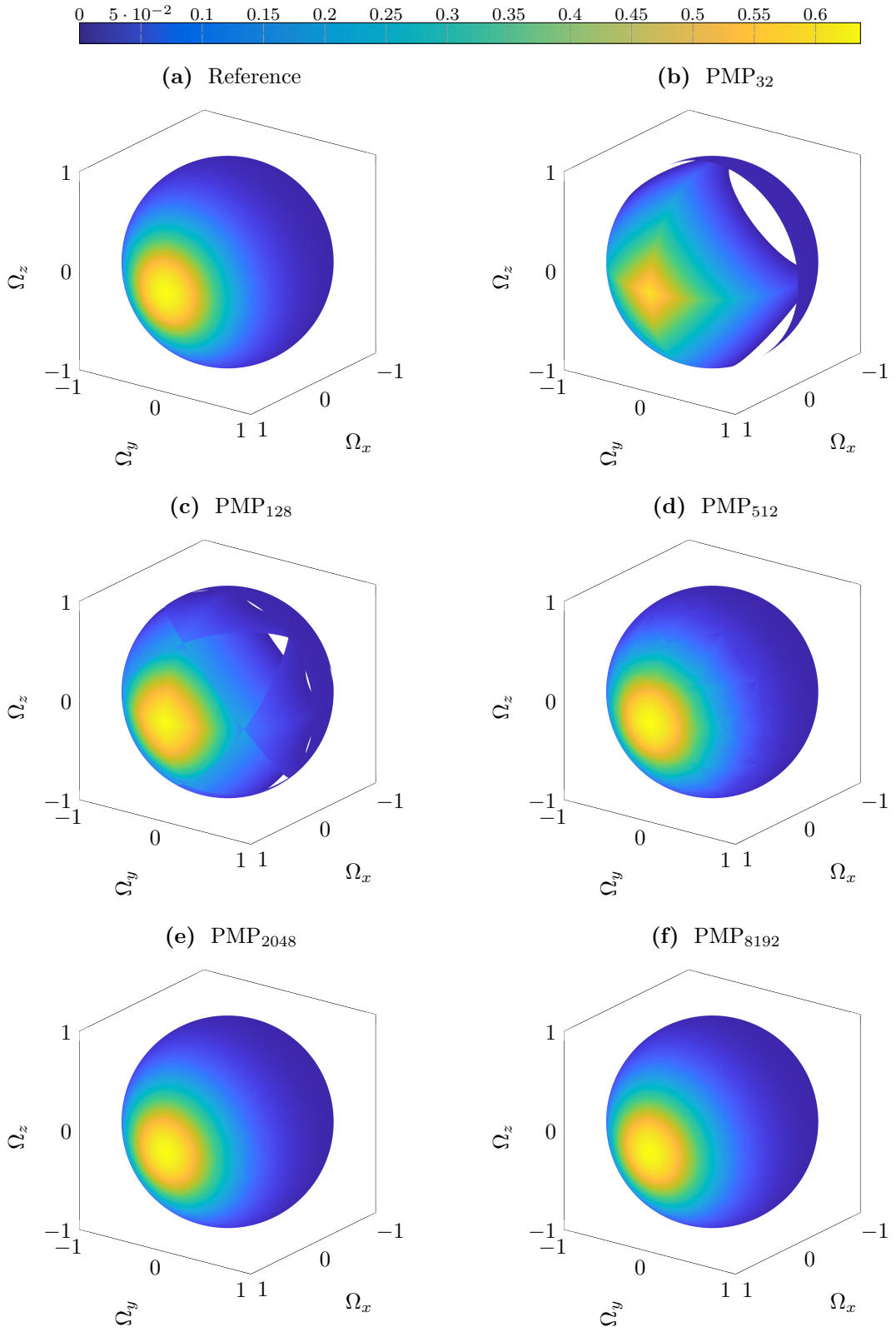

Figure S4.5: Distributions of PMP_n models for the three-dimensional Gauss test. Unphysical negative values are shown in white.

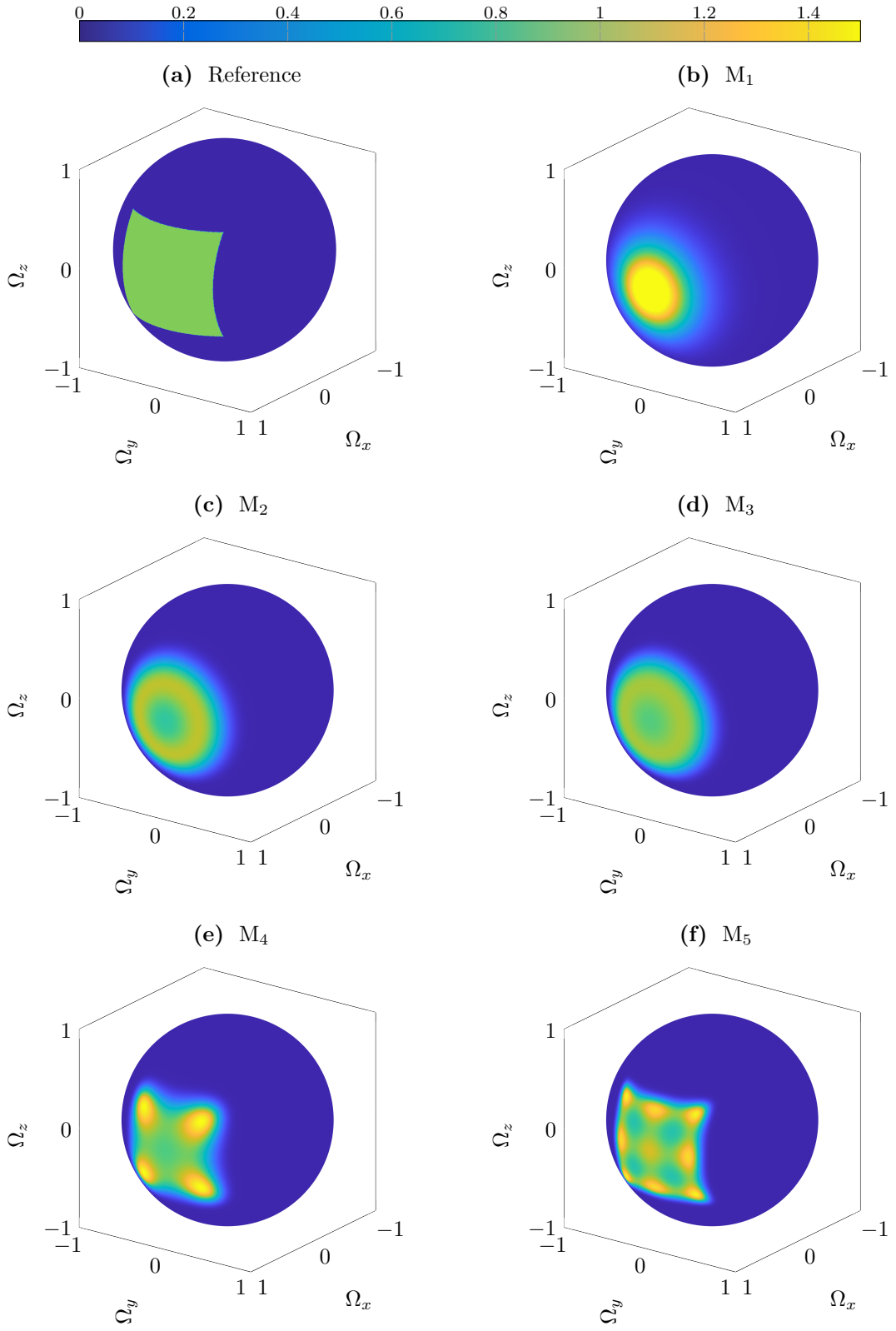

Figure S5.1: Distributions of M_N models for the three-dimensional Square test. Continued in Figure S5.2.

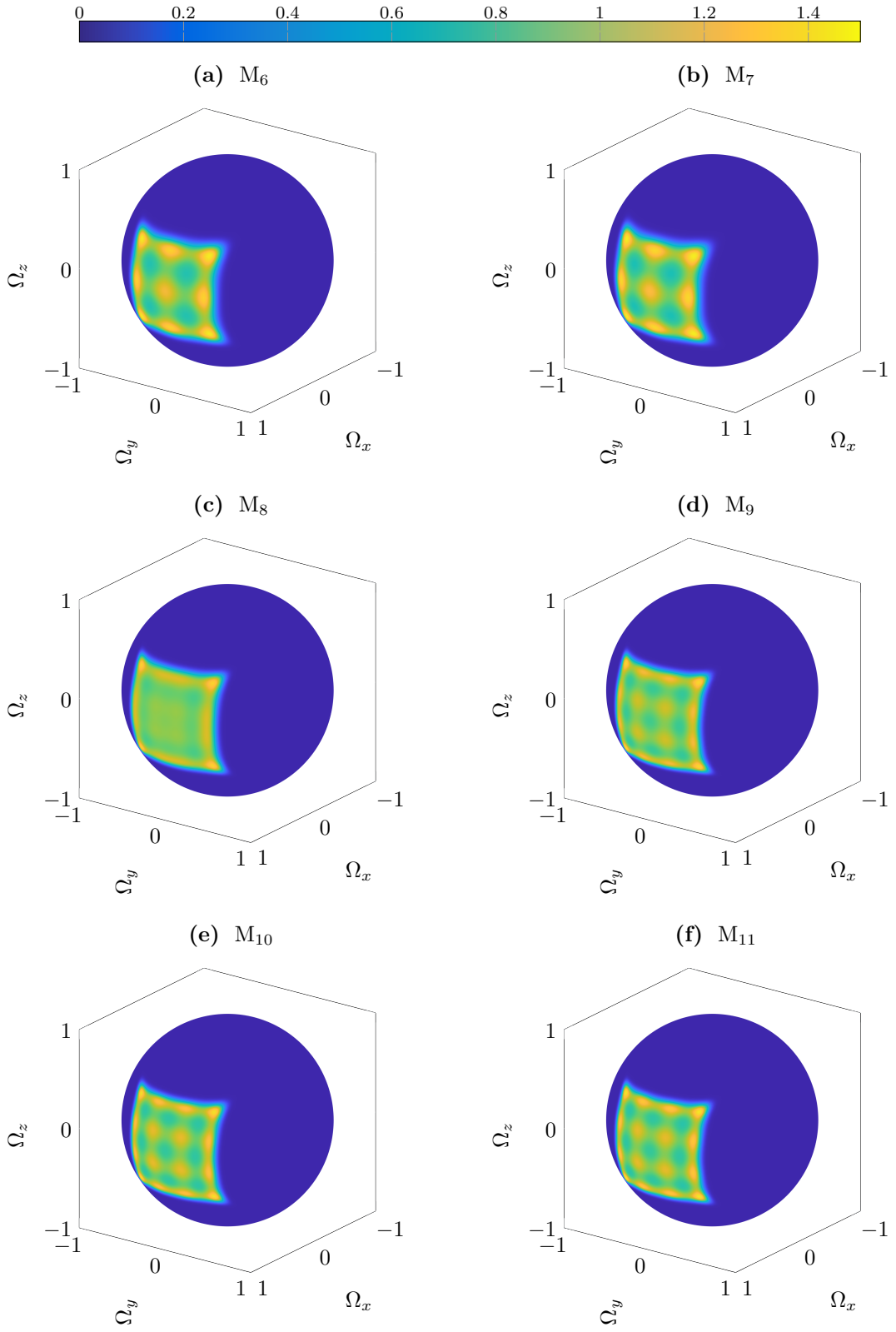

Figure S5.2: Distributions of M_N models for the three-dimensional Square test. Reference solution can be found in Figure S5.1. Continued in Figure S5.3.

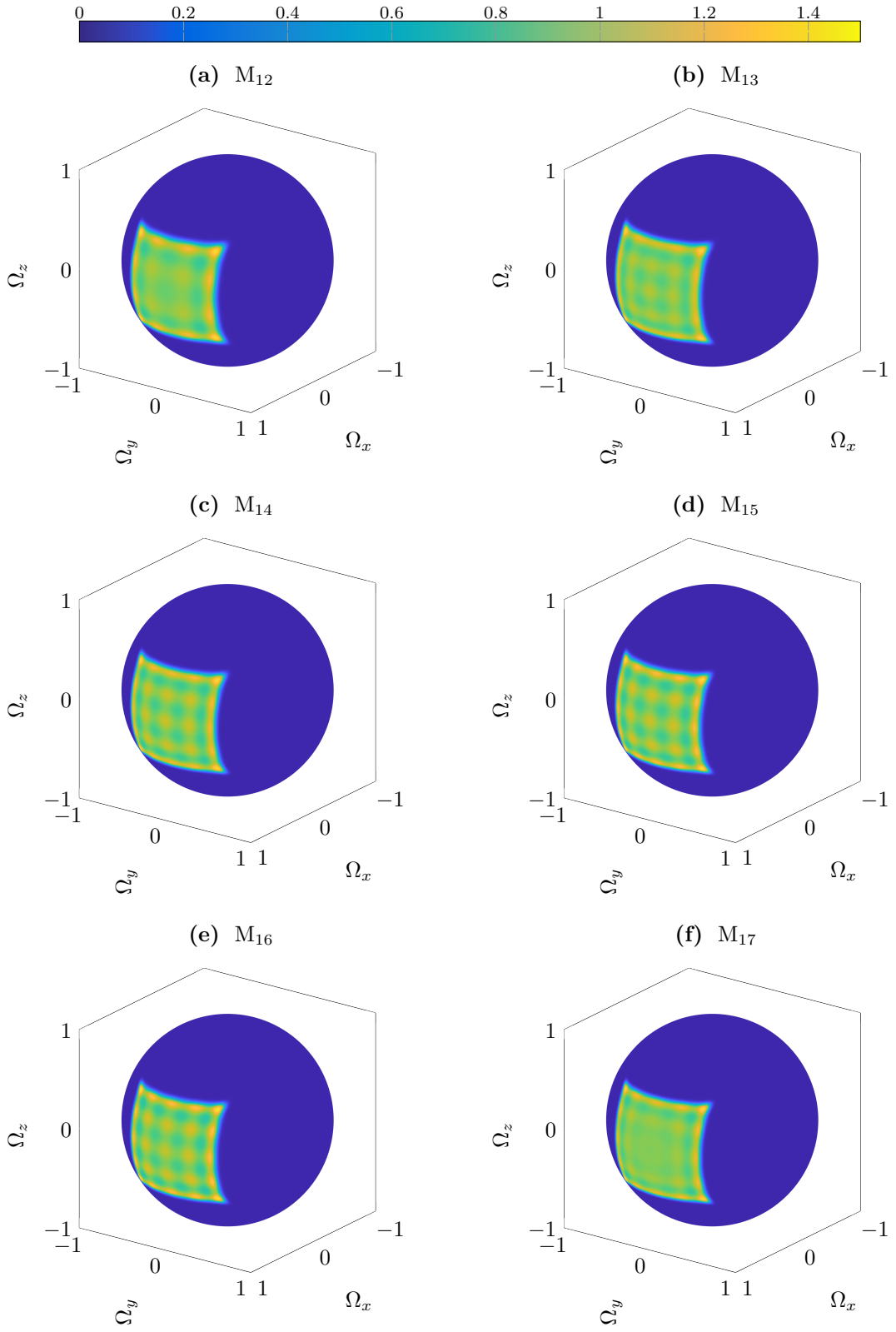

Figure S5.3: Distributions of M_N models for the three-dimensional Square test. Reference solution can be found in Figure S5.1. Continued in Figure S5.4.

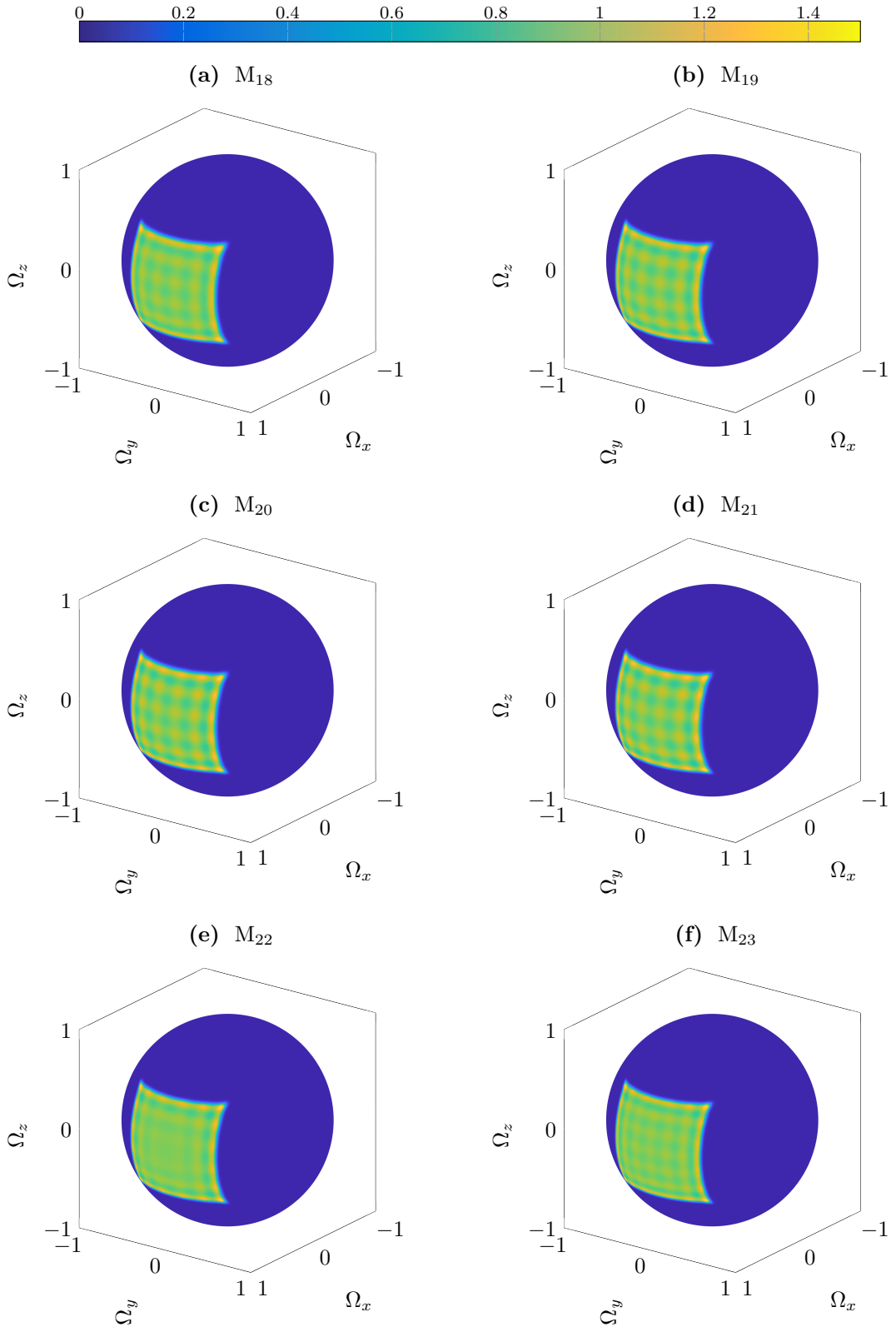

Figure S5.4: Distributions of M_N models for the three-dimensional Square test. Reference solution can be found in Figure S5.1. Continued in Figure S5.5.

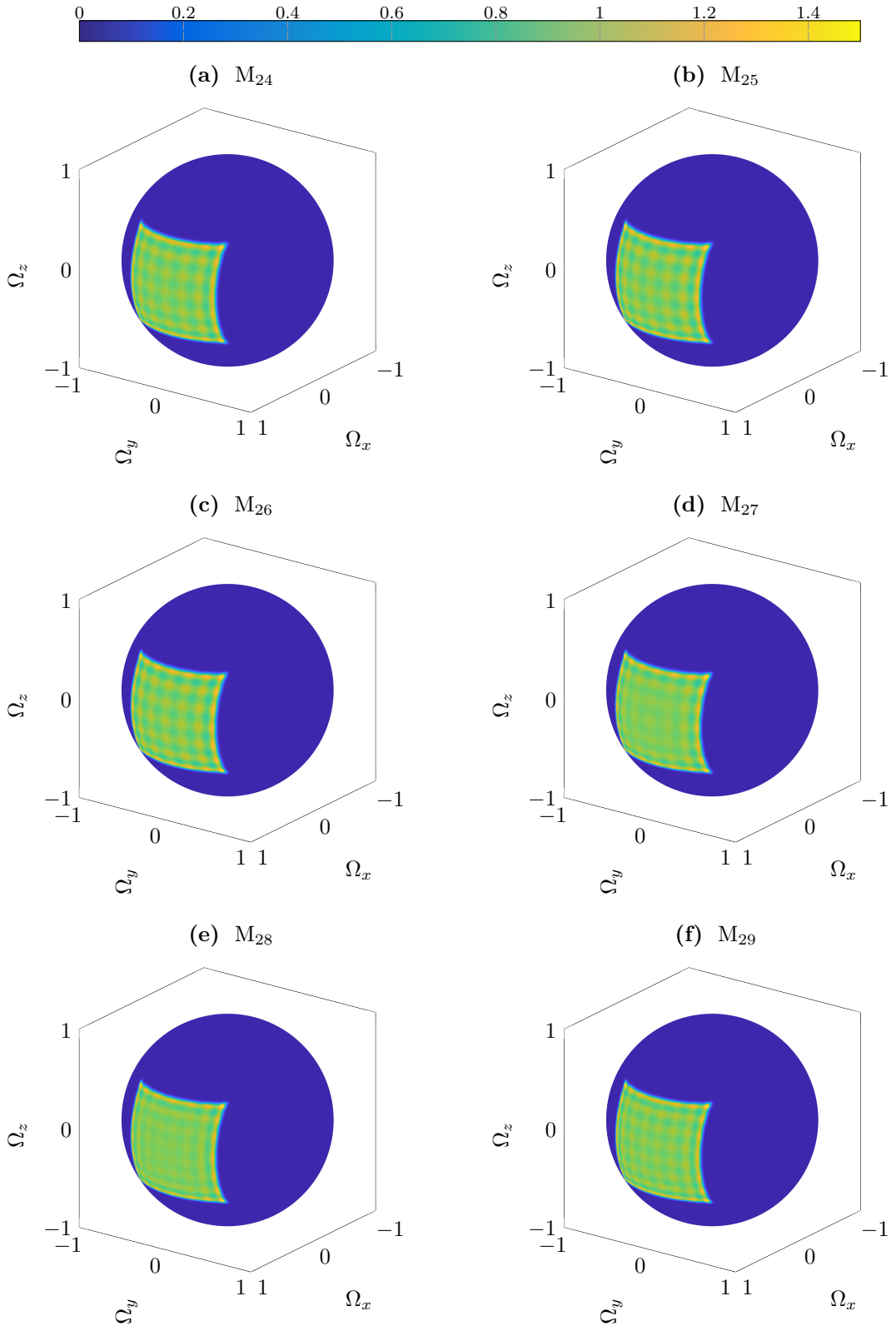

Figure S5.5: Distributions of M_N models for the three-dimensional Square test. Reference solution can be found in Figure S5.1.

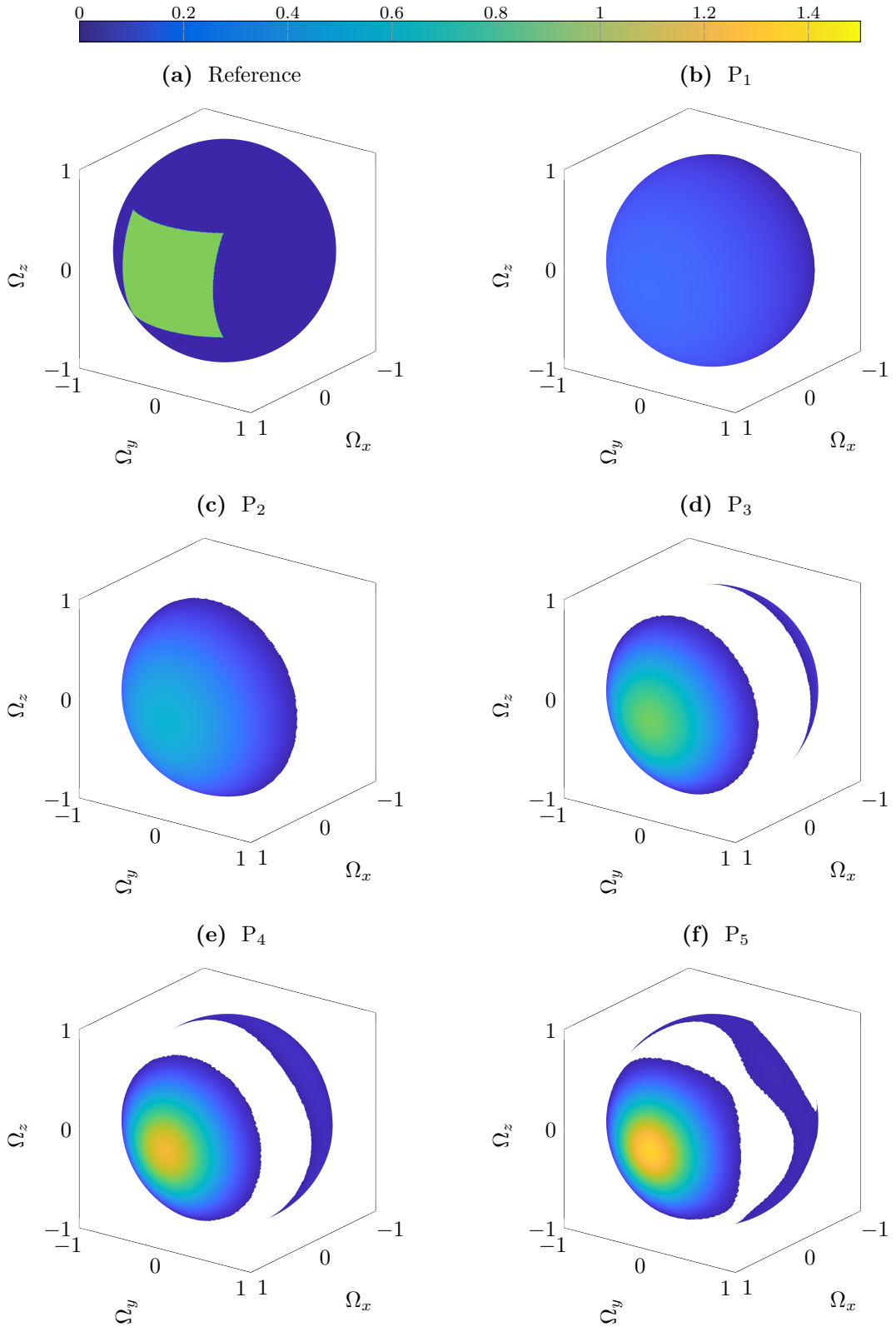

Figure S5.6: Distributions of P_N models for the three-dimensional Square test. Unphysical negative values are shown in white. Continued in Figure S5.7.

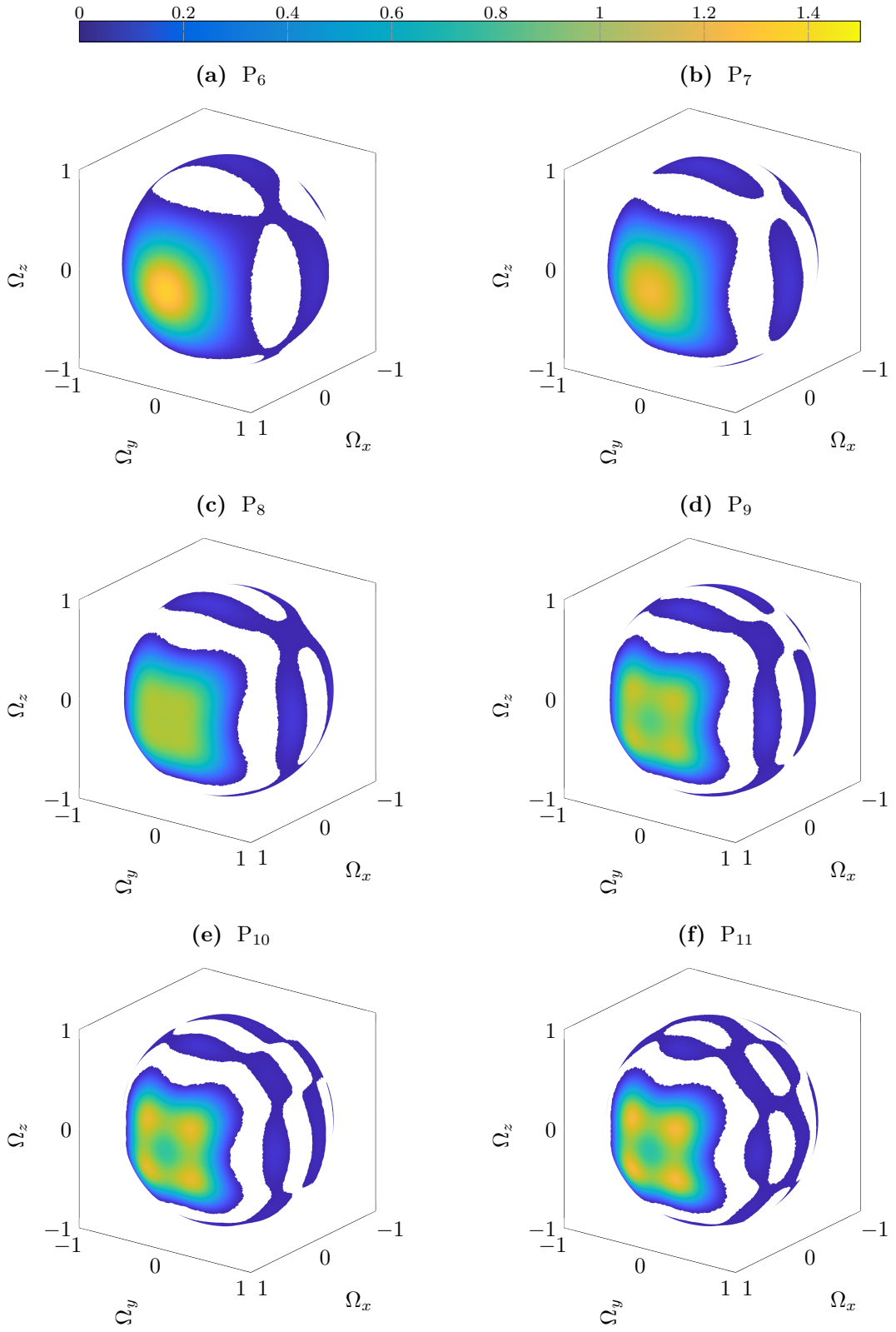

Figure S5.7: Distributions of P_N models for the three-dimensional Square test. Unphysical negative values are shown in white. Reference solution can be found in Figure S5.6. Continued in Figure S5.8.

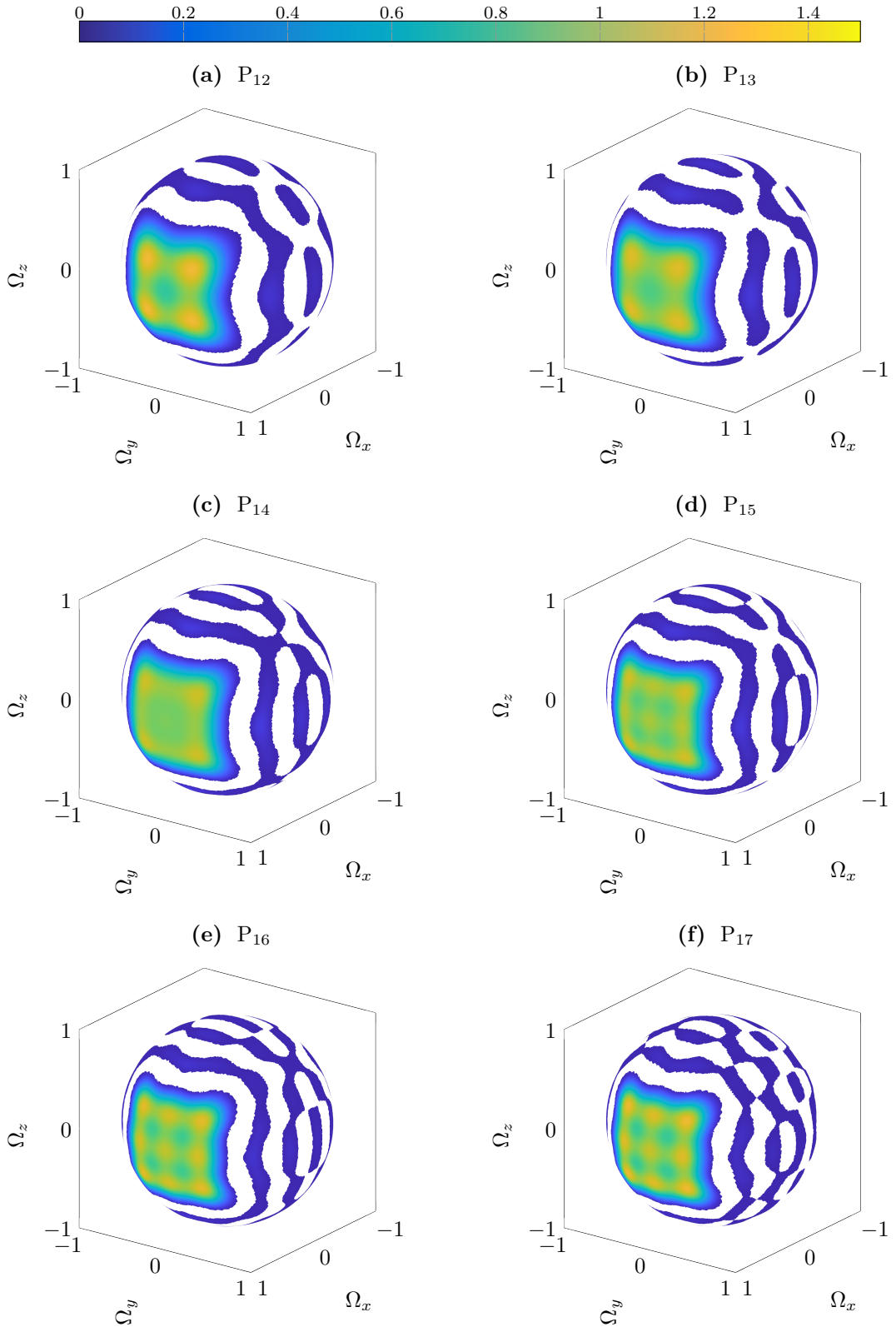

Figure S5.8: Distributions of P_N models for the three-dimensional Square test. Unphysical negative values are shown in white. Reference solution can be found in Figure S5.6. Continued in Figure S5.9.

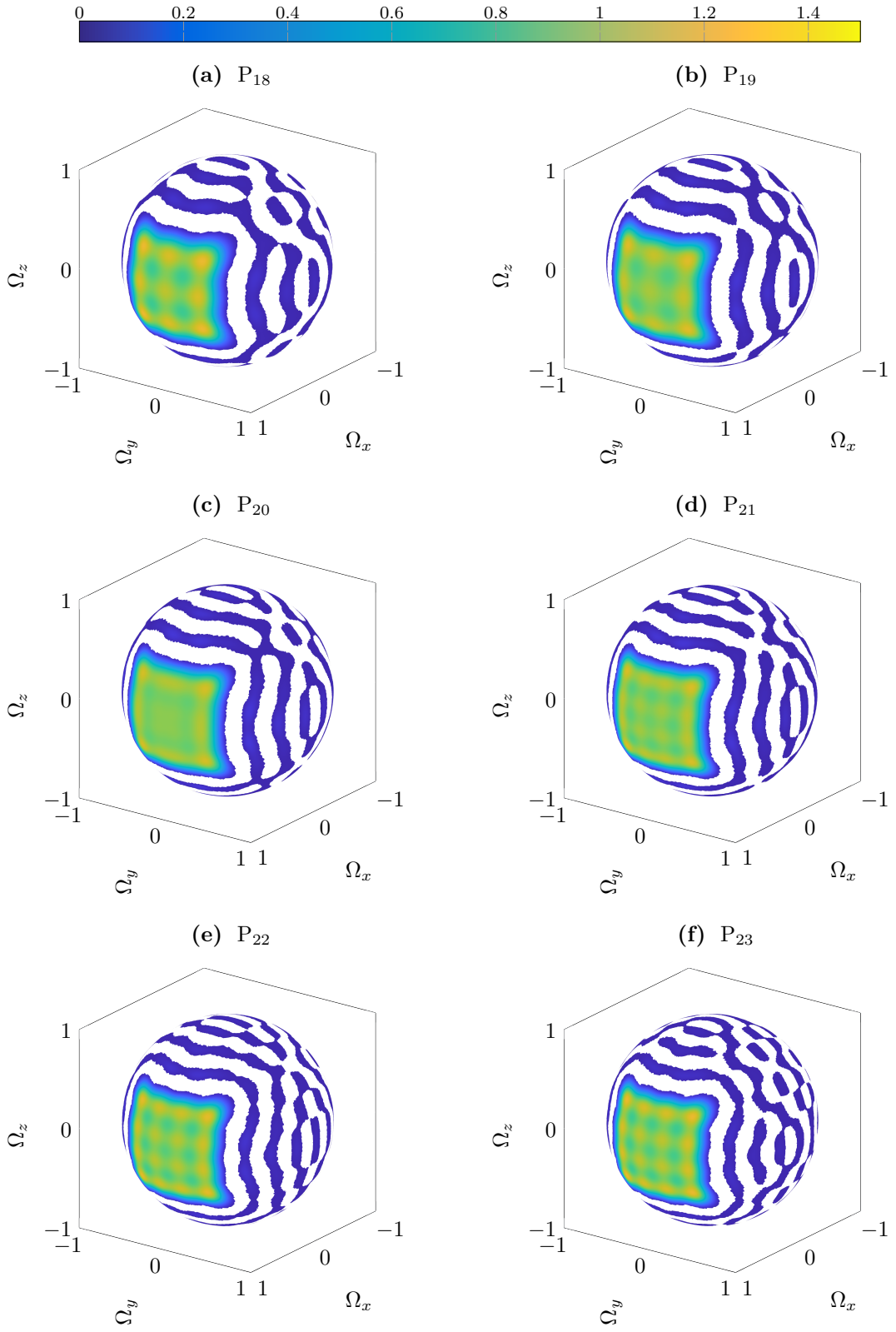

Figure S5.9: Distributions of P_N models for the three-dimensional Square test. Unphysical negative values are shown in white. Reference solution can be found in Figure S5.6. Continued in Figure S5.10.

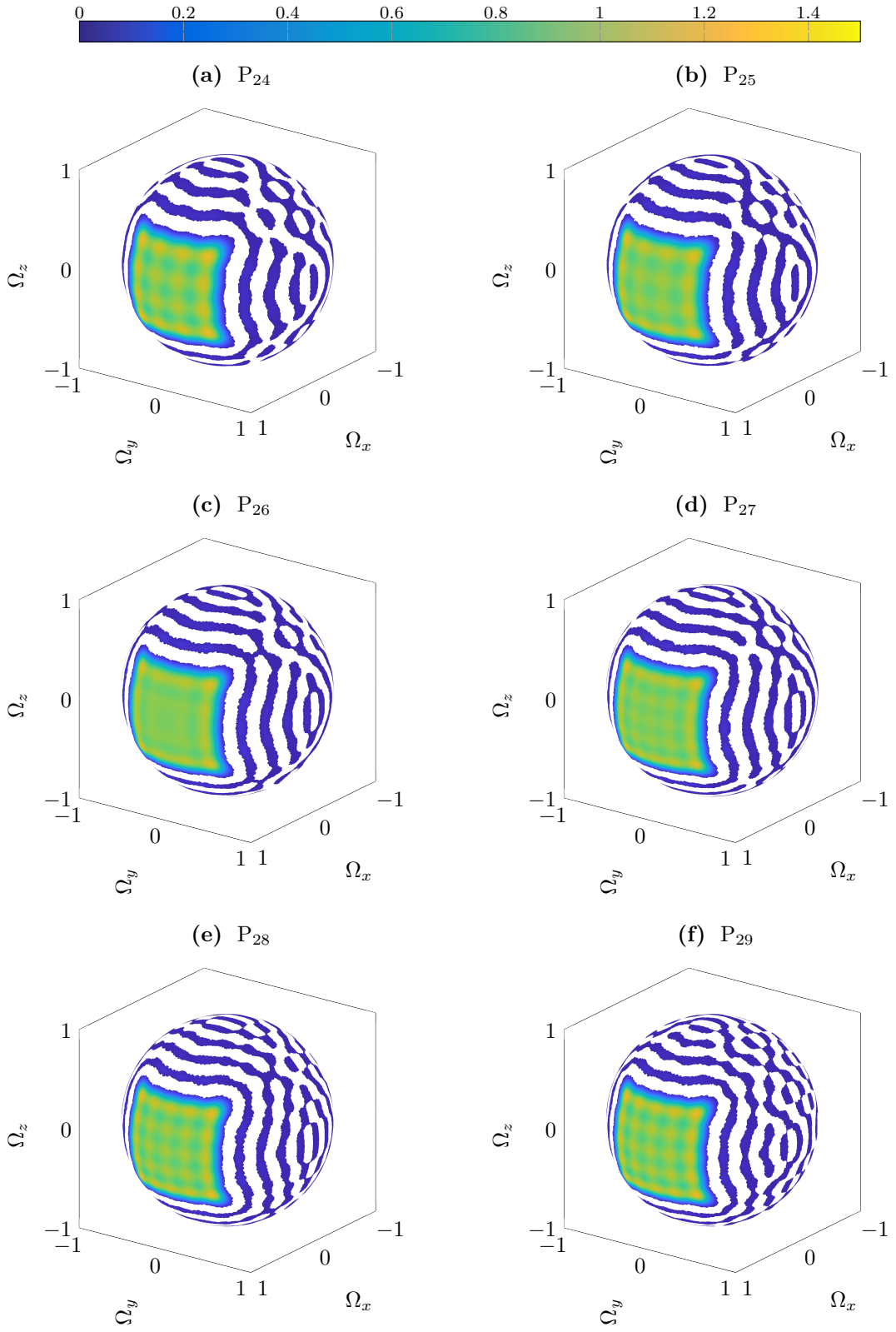

Figure S5.10: Distributions of P_N models for the three-dimensional Square test. Unphysical negative values are shown in white. Reference solution can be found in Figure S5.6.

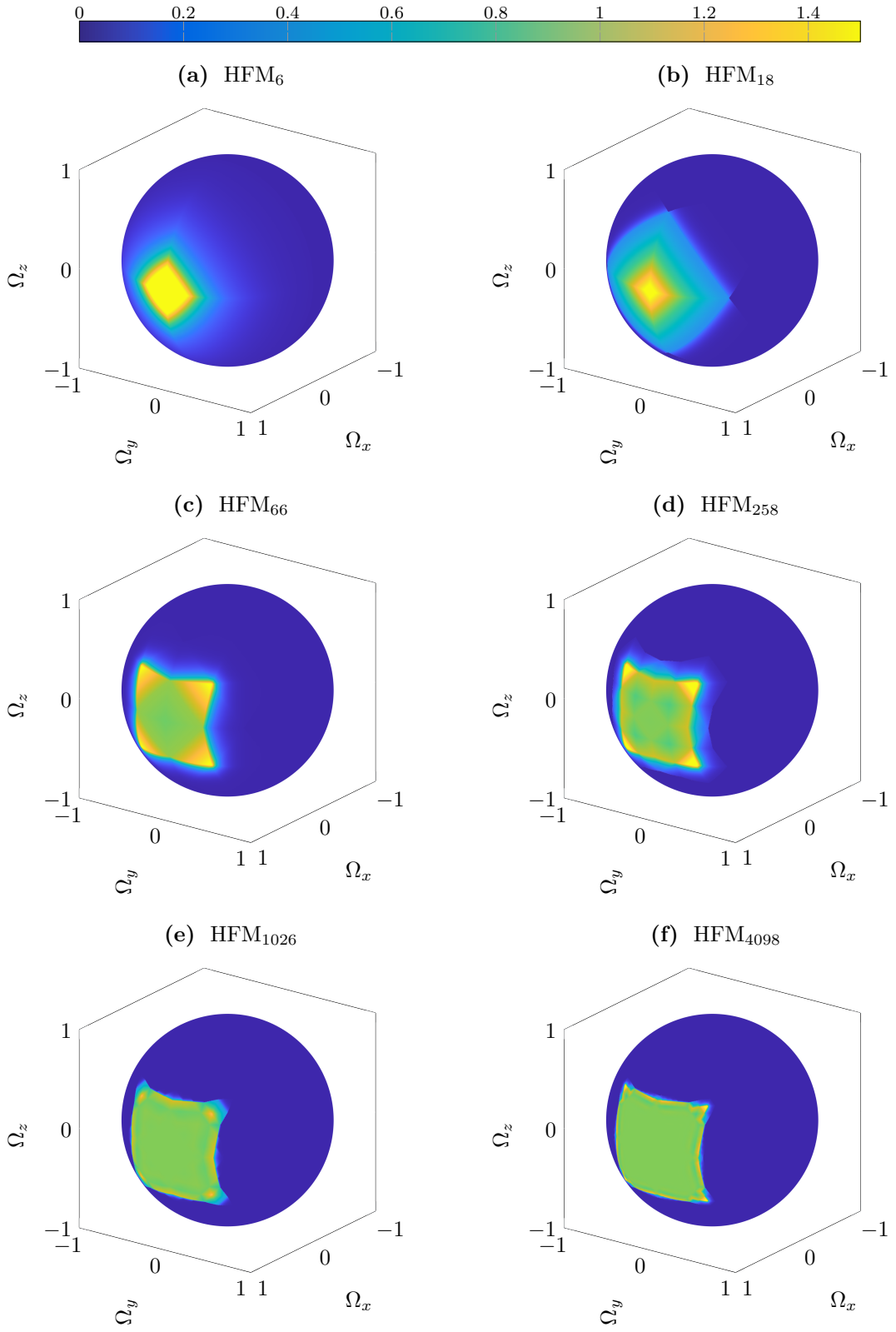

Figure S5.11: Distributions of HFM_n models for the three-dimensional Square test. Reference solution can be found in Figure S5.6. Continued in Figure S5.15.

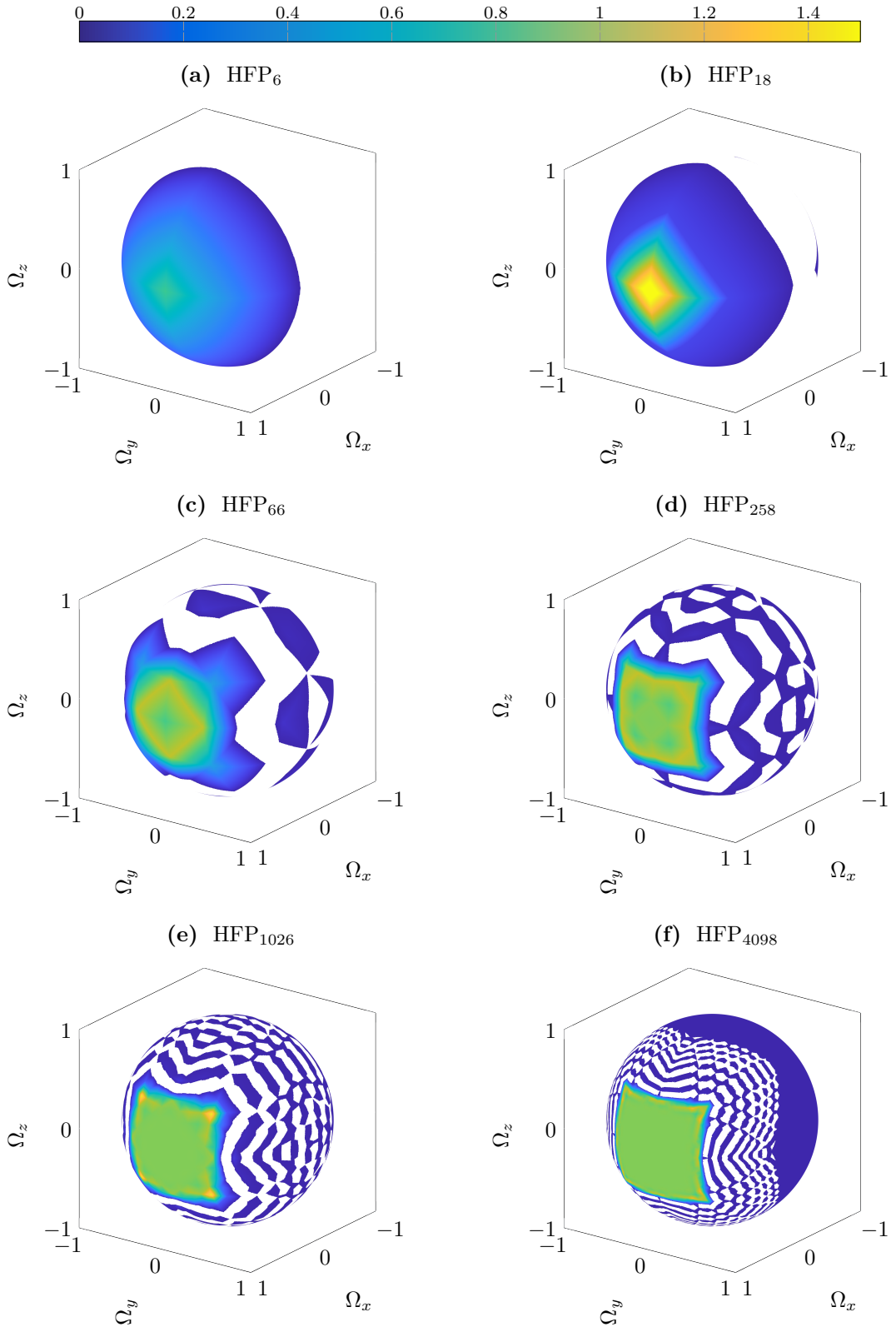

Figure S5.12: Distributions of HFP_n models for the three-dimensional Square test. Unphysical negative values are shown in white. Reference solution can be found in Figure S5.6. Continued in Figure S5.15.

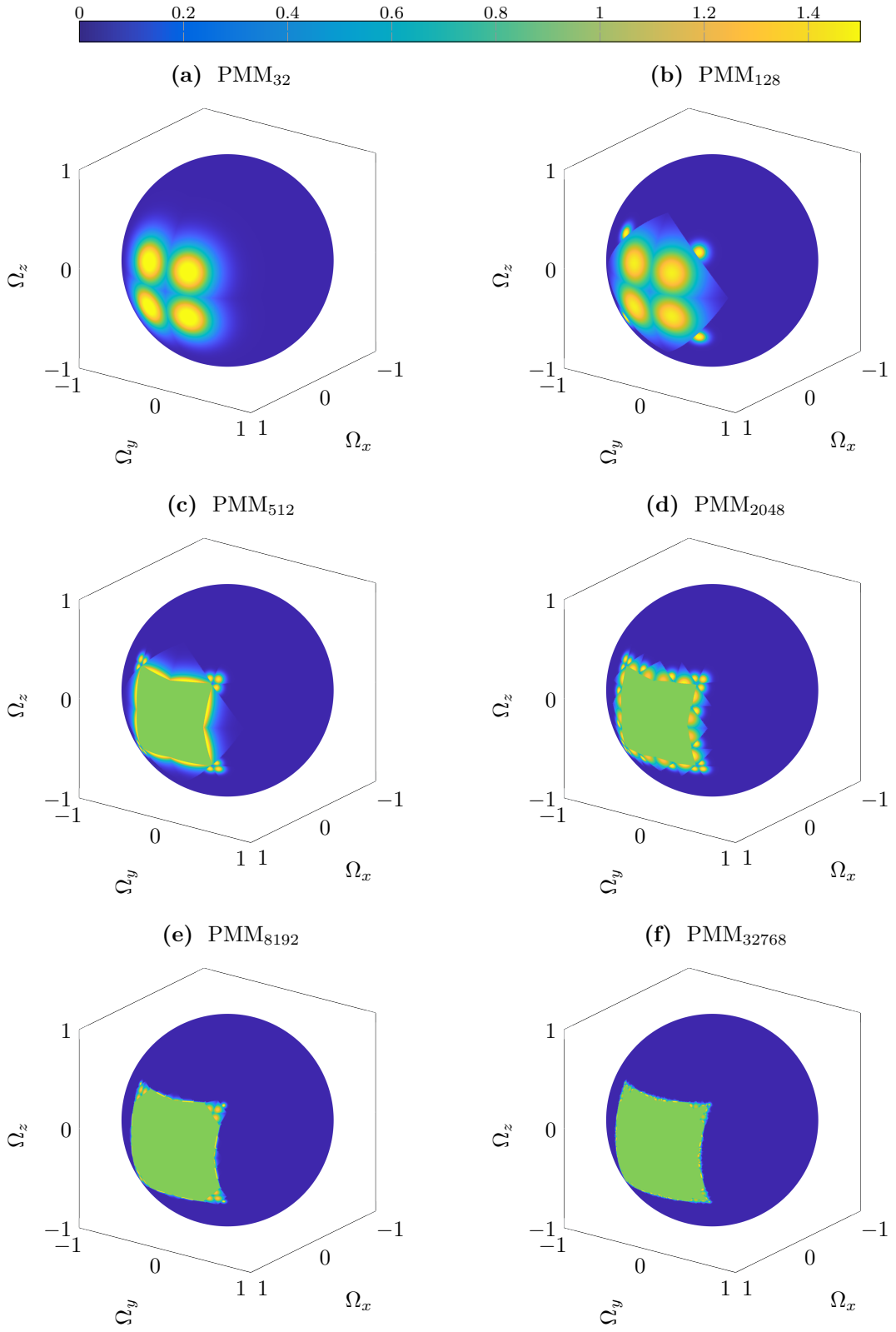

Figure S5.13: Distributions of PMM_n models for the three-dimensional Square test. Reference solution can be found in Figure S5.6. Continued in Figure S5.15.

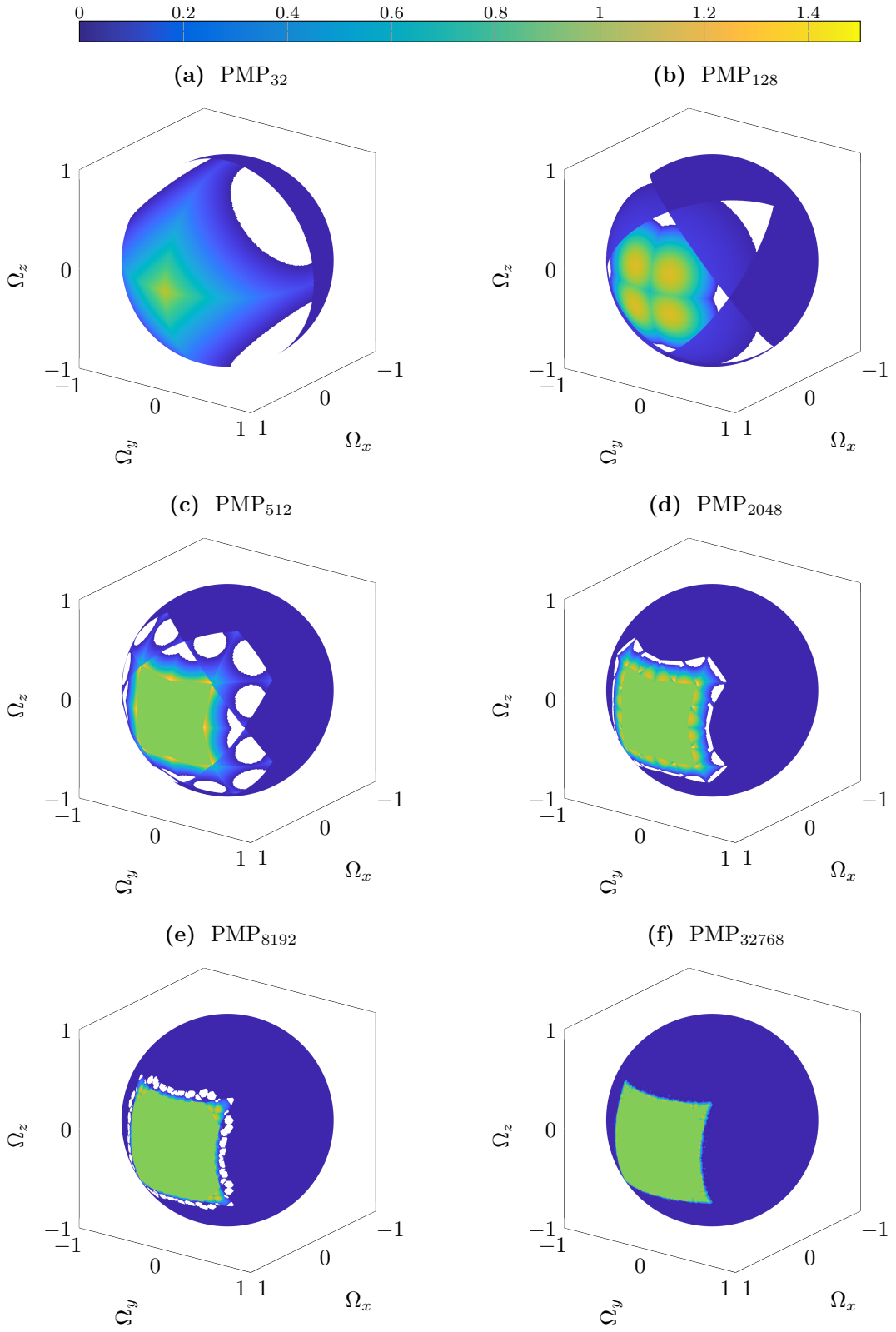

Figure S5.14: Distributions of PMP_n models for the three-dimensional Square test. Unphysical negative values are shown in white. Reference solution can be found in Figure S5.6. Continued in Figure S5.15.

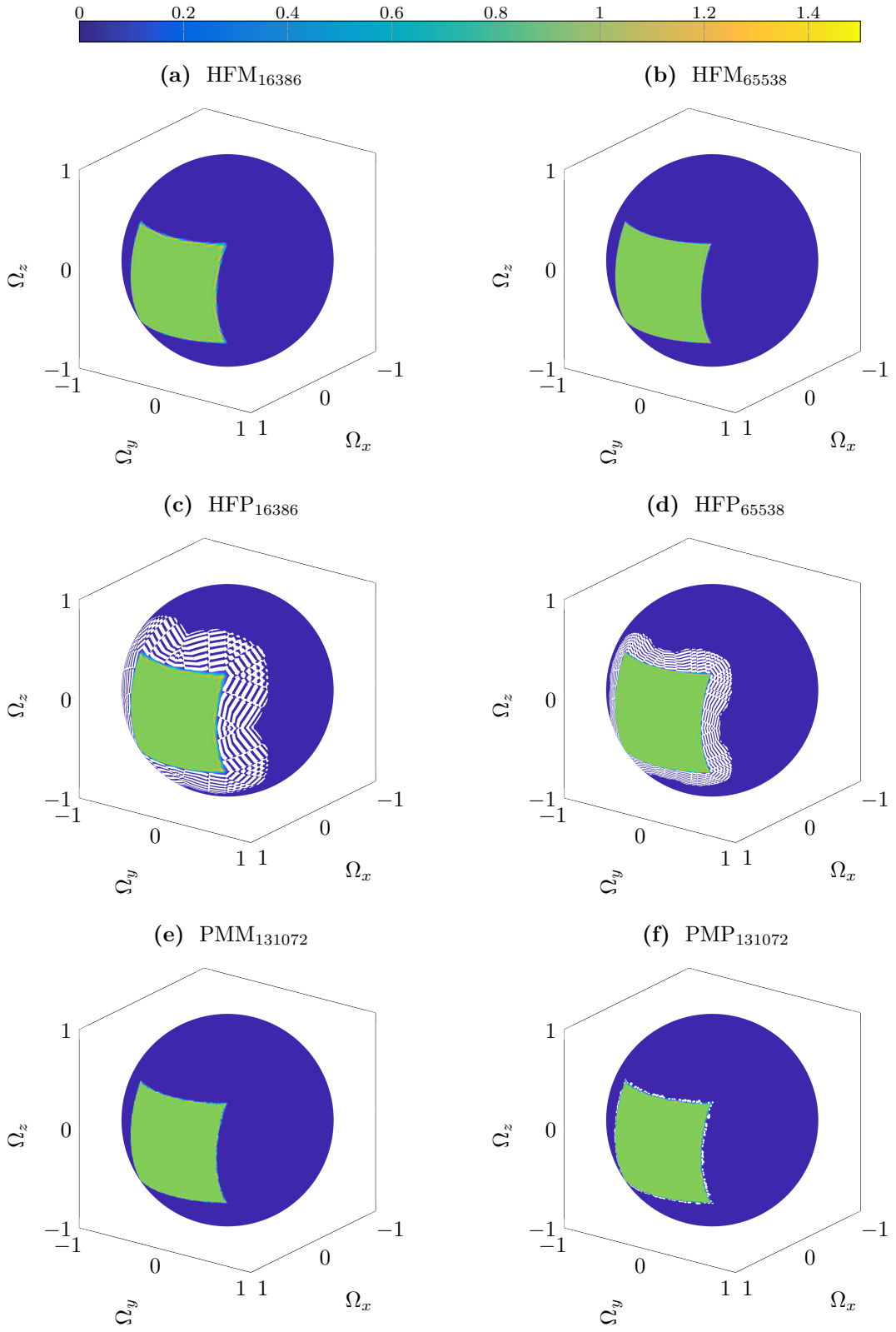

Figure S5.15: Distributions of various high-order models for the three-dimensional Square test. Unphysical negative values are shown in white. Reference solution can be found in Figure S5.6.

	HFP$_n$					PMP$_n$					P$_N$			
n	E_h^1	ν	E_h^∞	ν	n	E_h^1	ν	E_h^∞	ν	n	E_h^1	ν	E_h^∞	ν
18	9.30e-01	—	8.79e-01	—	32	1.25e+00	—	8.17e-01	—	4	2.11e+00	—	7.42e-01	—
66	6.51e-01	0.3	6.64e-01	0.2	128	4.53e-01	0.7	9.10e-01	-0.1	16	1.33e+00	0.3	6.83e-01	0.1
258	2.98e-01	0.6	7.13e-01	-0.1	512	3.33e-01	0.2	7.46e-01	0.1	121	5.37e-01	0.4	7.30e-01	-0.0
1026	2.03e-01	0.3	8.70e-01	-0.1	2048	1.71e-01	0.5	7.77e-01	-0.0	289	3.92e-01	0.4	7.00e-01	0.0
4098	9.43e-02	0.6	7.09e-01	0.1	8192	6.31e-02	0.7	9.74e-01	-0.2	529	3.03e-01	0.4	6.87e-01	0.0
16386	5.07e-02	0.4	8.44e-01	-0.1	32768	3.74e-02	0.4	9.00e-01	0.1	961	2.35e-01	0.4	6.52e-01	0.1
65538	2.50e-02	0.5	6.22e-01	0.2	131072	1.33e-02	0.7	1.01e+00	-0.1					

Table 10: L_1/L_∞ errors and observed order of convergence ν for the linear models in the Square 3D case.

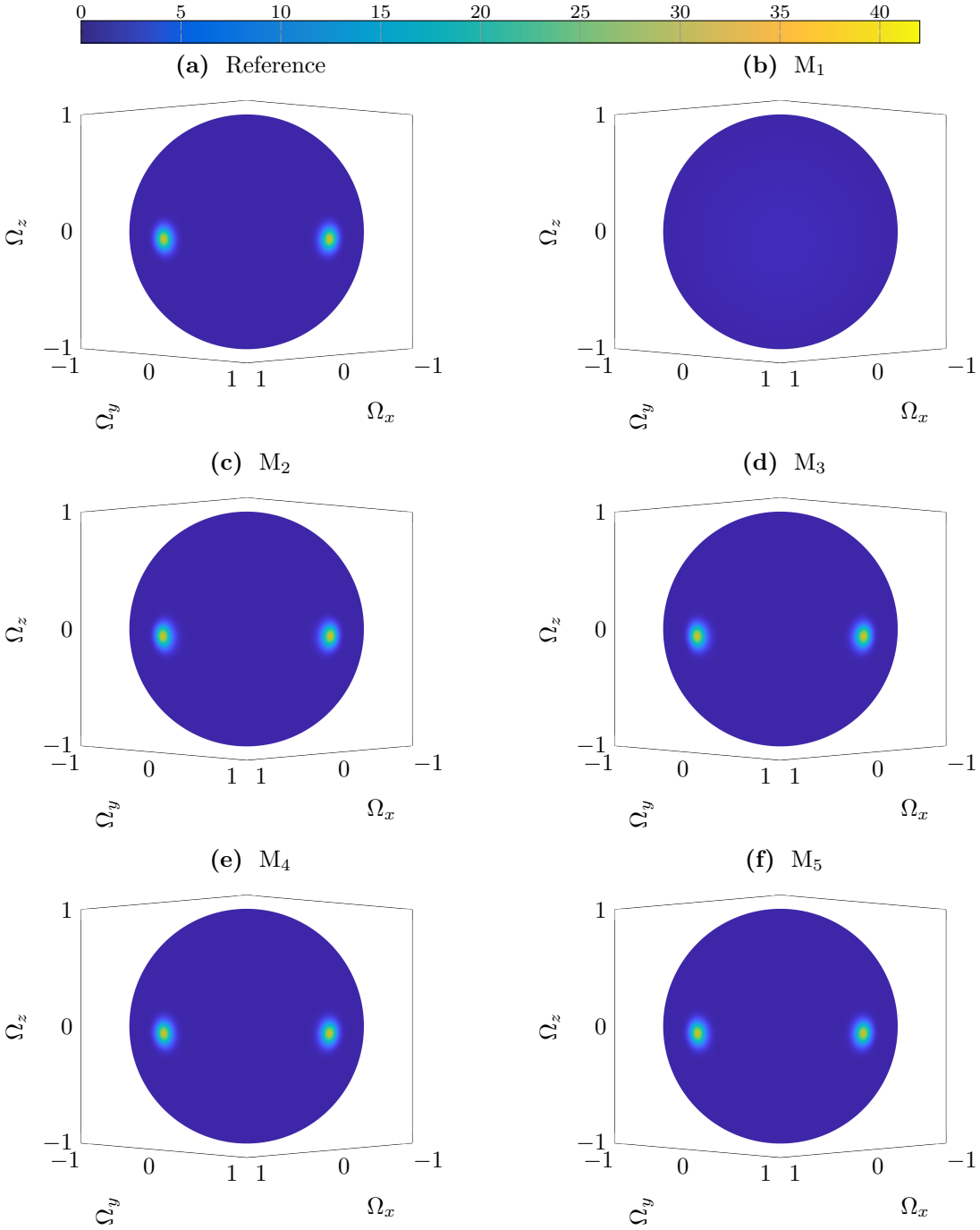

Figure S6.1: Distributions of M$_N$ models for the three-dimensional crossing beams test. Higher order models are close to the reference solution and thus omitted.

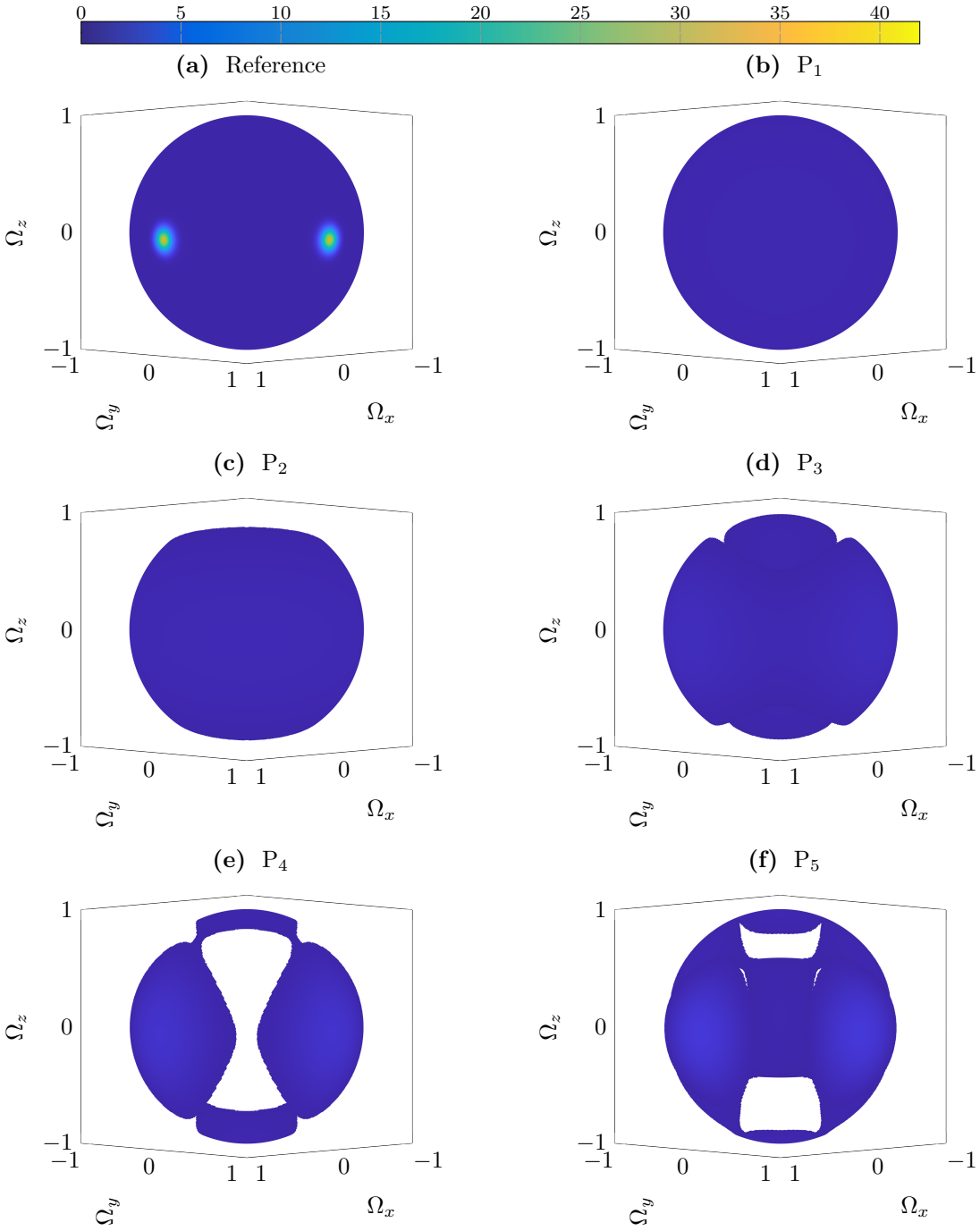

Figure S6.2: Distributions of P_N models for the three-dimensional crossing beams test. Unphysical negative values are shown in white. Continued in Figure S6.3.

	HFM$_n$					PMM$_n$					M$_N$				
n	E_h^1	ν	E_h^∞	ν	n	E_h^1	ν	E_h^∞	ν	n	E_h^1	ν	E_h^∞	ν
18	6.60e-01	—	4.88e+01	—	32	4.24e-01	—	5.76e+01	—	4	3.73e+00	—	3.14e+01	—
66	6.36e-01	0.0	4.45e+01	0.1	128	4.48e-08	11.6	1.93e-06	12.4	16	6.75e-02	2.9	1.13e+00	2.4
258	4.28e-01	0.3	2.37e+01	0.5	512	1.32e-08	0.9	1.06e-06	0.4	121	1.73e-04	2.9	3.80e-03	2.8
1026	1.54e-01	0.7	7.40e+00	0.8	2048	9.80e-10	1.9	4.18e-08	2.3	289	5.00e-05	1.4	1.51e-03	1.1
4098	4.04e-02	1.0	2.20e+00	0.9	8192	1.53e-10	1.3	5.44e-09	1.5	529	2.96e-05	0.9	9.40e-04	0.8
16386	1.46e-02	0.7	6.30e-01	0.9	32768	2.98e-11	1.2	1.03e-09	1.2	961	1.99e-05	0.7	7.01e-04	0.5
65538	3.65e-03	1.0	1.63e-01	1.0	131072	3.52e-11	-0.1	5.47e-09	-1.2					

Table 11: L_1/L_∞ errors and observed order of convergence ν for the non-linear models in the Crossing Beams 3D case.

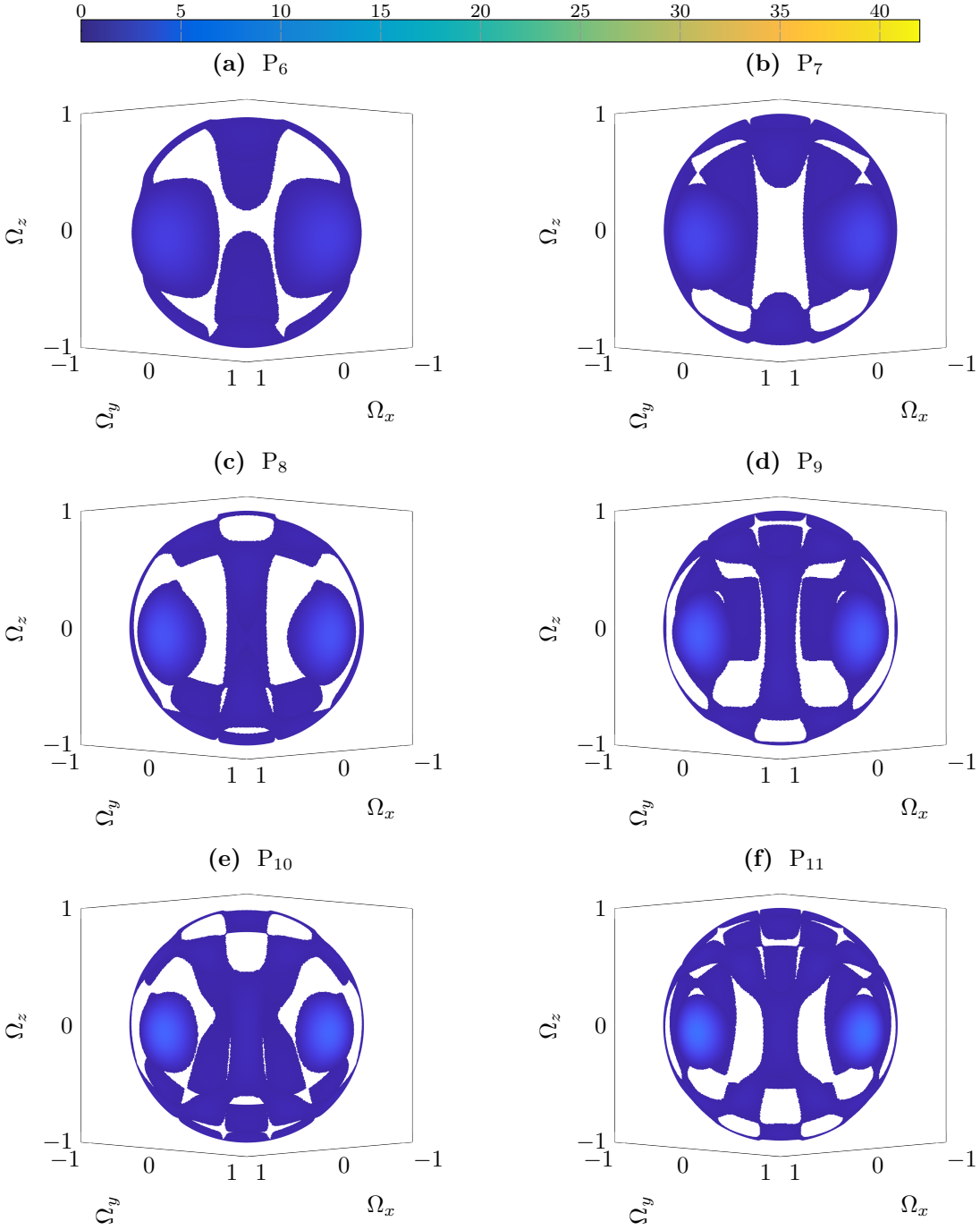

Figure S6.3: Distributions of P_N models for the three-dimensional crossing beams test. Unphysical negative values are shown in white. Reference solution can be found in Figure S6.2. Continued in Figure S6.4.

	HFP$_n$					PMP$_n$					P$_N$			
n	E_h^1	ν	E_h^∞	ν	n	E_h^1	ν	E_h^∞	ν	n	E_h^1	ν	E_h^∞	ν
18	5.39e+00	—	2.75e+01	—	32	5.96e+00	—	2.95e+01	—	4	4.32e+00	—	3.14e+01	—
66	3.22e+00	0.4	1.72e+01	0.4	128	4.33e+00	0.2	2.46e+01	0.1	16	5.32e+00	-0.2	3.07e+01	0.0
258	4.97e-01	1.4	6.12e+00	0.8	512	1.73e+00	0.7	1.25e+01	0.5	121	5.59e+00	-0.0	2.37e+01	0.1
1026	3.01e-01	0.4	5.67e+00	0.1	2048	3.18e-01	1.2	5.00e+00	0.7	289	4.33e+00	0.3	1.53e+01	0.5
4098	6.02e-02	1.2	1.99e+00	0.8	8192	8.83e-02	0.9	3.06e+00	0.4	529	2.60e+00	0.8	8.56e+00	1.0
16386	1.63e-02	0.9	6.14e-01	0.8	32768	2.11e-02	1.0	7.68e-01	1.0	961	9.74e-01	1.6	2.92e+00	1.8
65538	4.01e-03	1.0	1.62e-01	1.0	131072	6.76e-03	0.8	1.88e-01	1.0	961	9.74e-01	—	2.92e+00	—

Table 12: L_1/L_∞ errors and observed order of convergence ν for the linear models in the Crossing Beams 3D case.

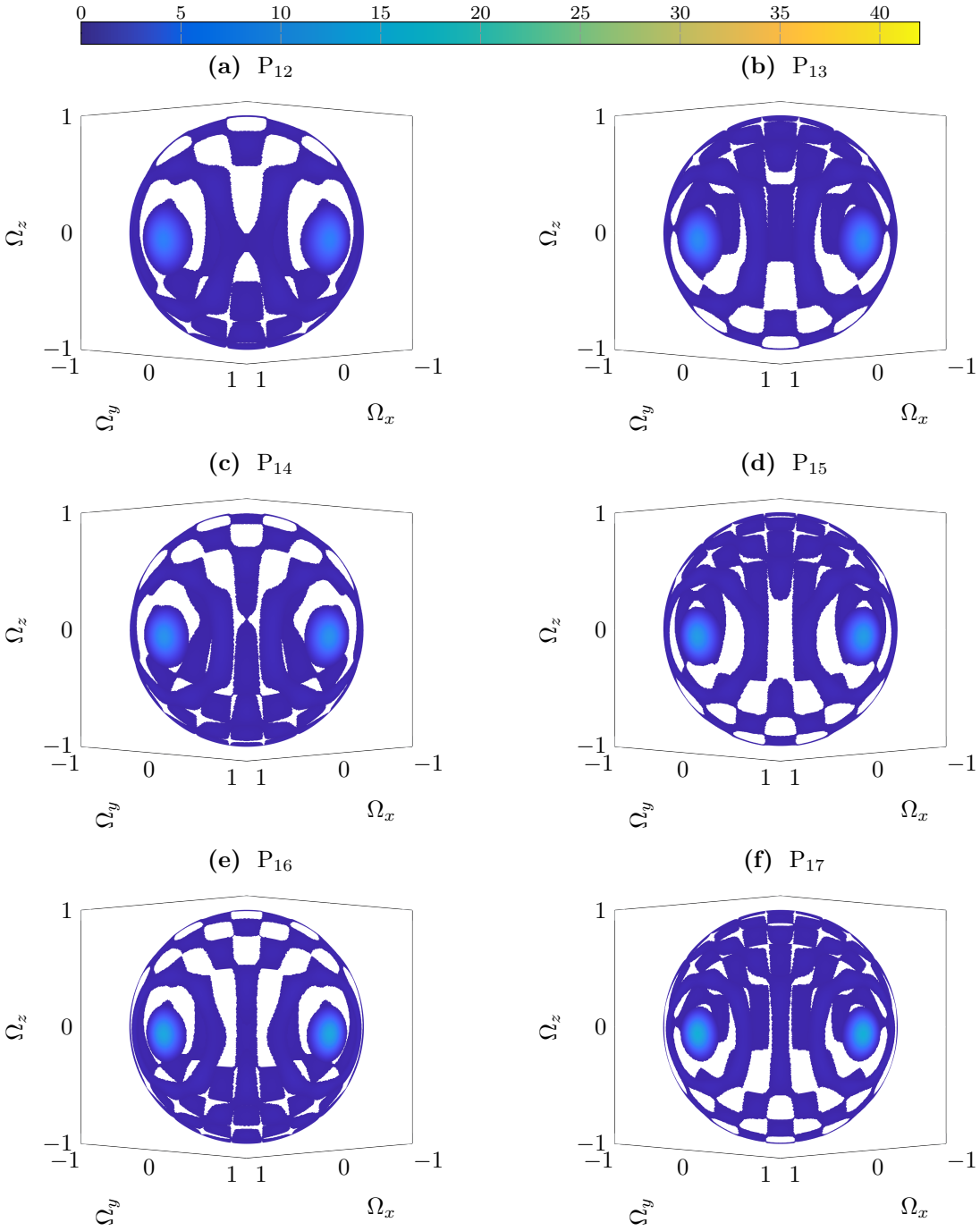

Figure S6.4: Distributions of P_N models for the three-dimensional crossing beams test. Unphysical negative values are shown in white. Reference solution can be found in Figure S6.2. Continued in Figure S6.5.

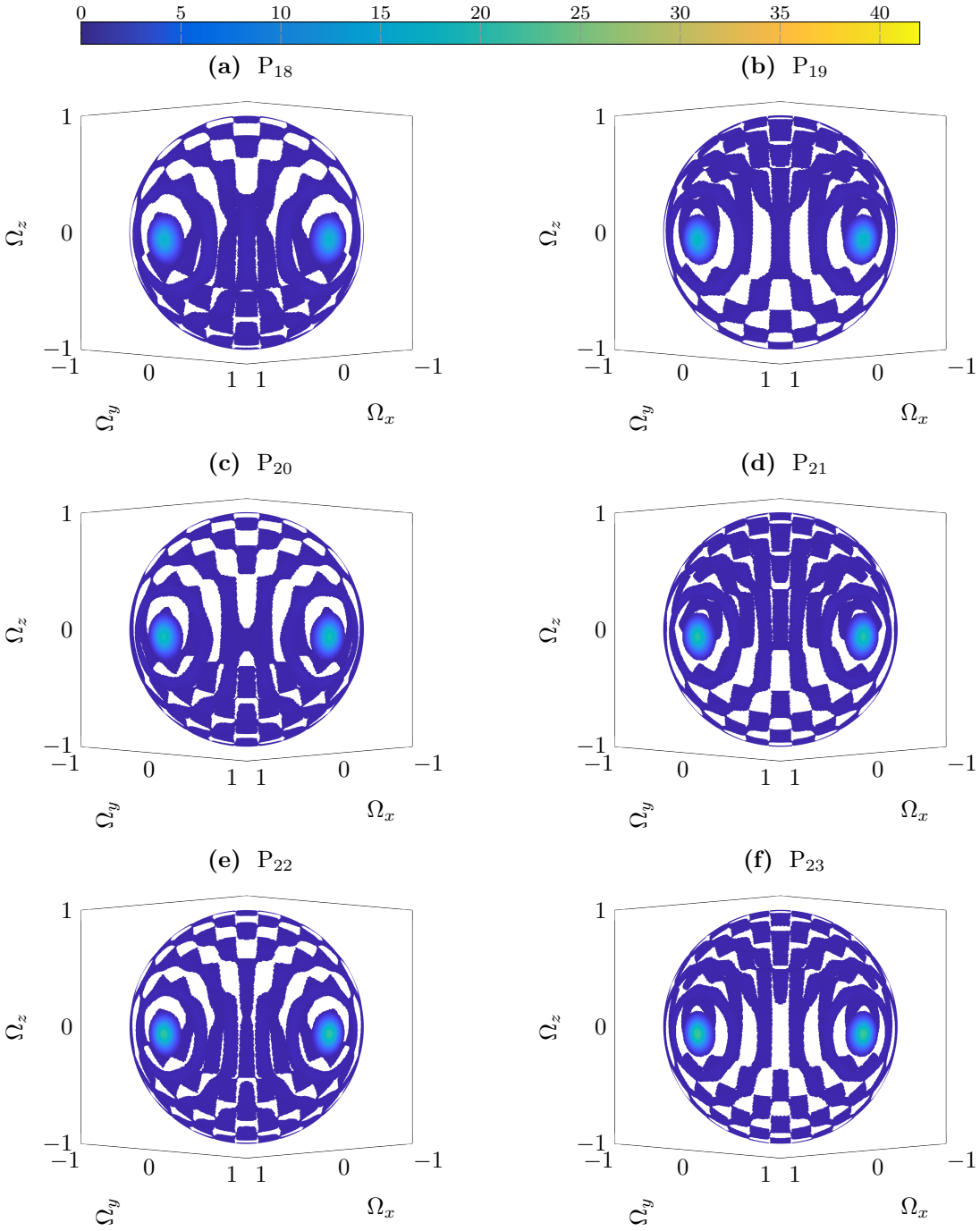

Figure S6.5: Distributions of P_N models for the three-dimensional crossing beams test. Unphysical negative values are shown in white. Reference solution can be found in Figure S6.2. Continued in Figure S6.6.

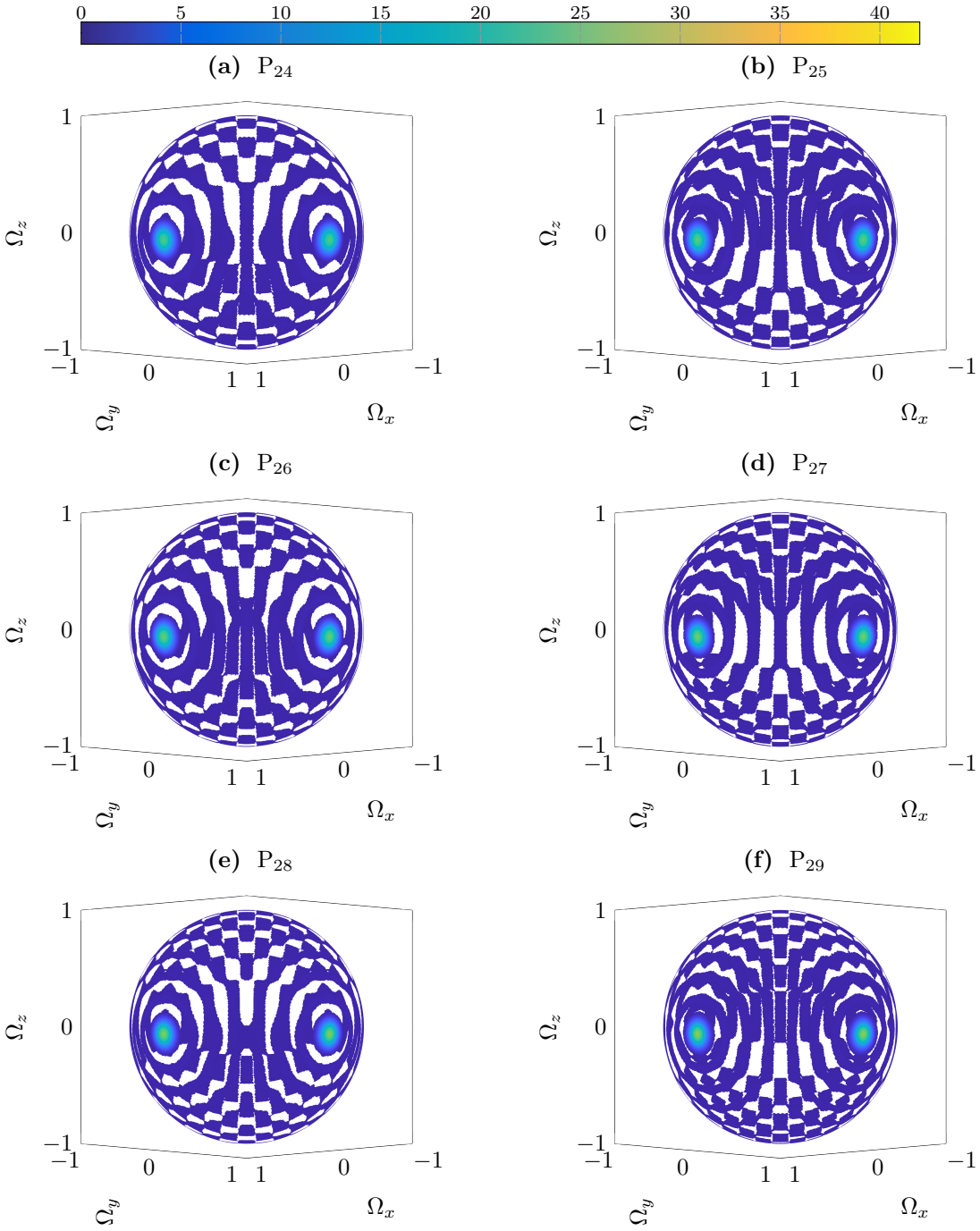

Figure S6.6: Distributions of P_N models for the three-dimensional crossing beams test. Unphysical negative values are shown in white. Reference solution can be found in Figure S6.2.

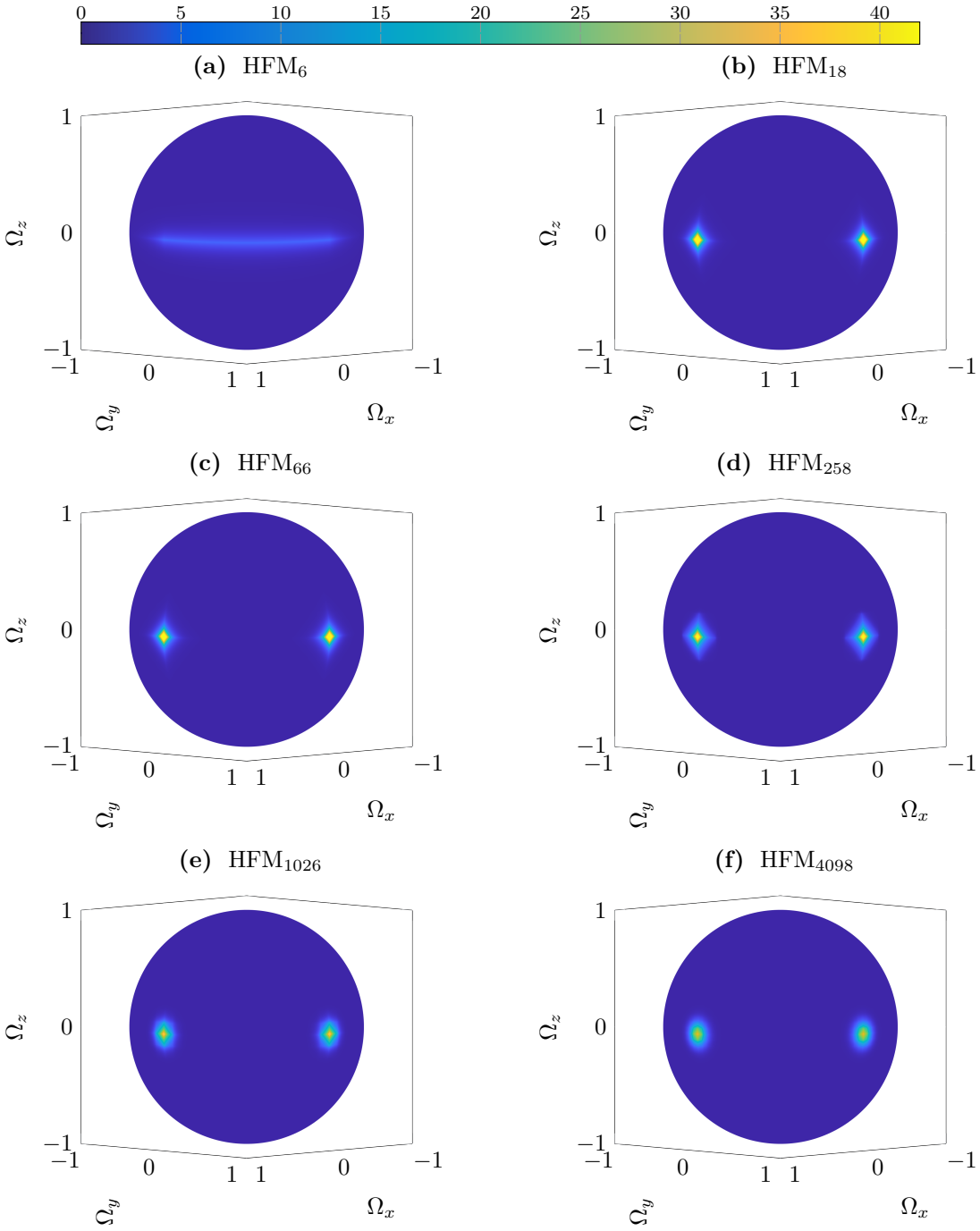

Figure S6.7: Distributions of HFM_n models for the three-dimensional crossing beams test. Reference solution can be found in Figure S6.2. Continued in Figure S6.11.

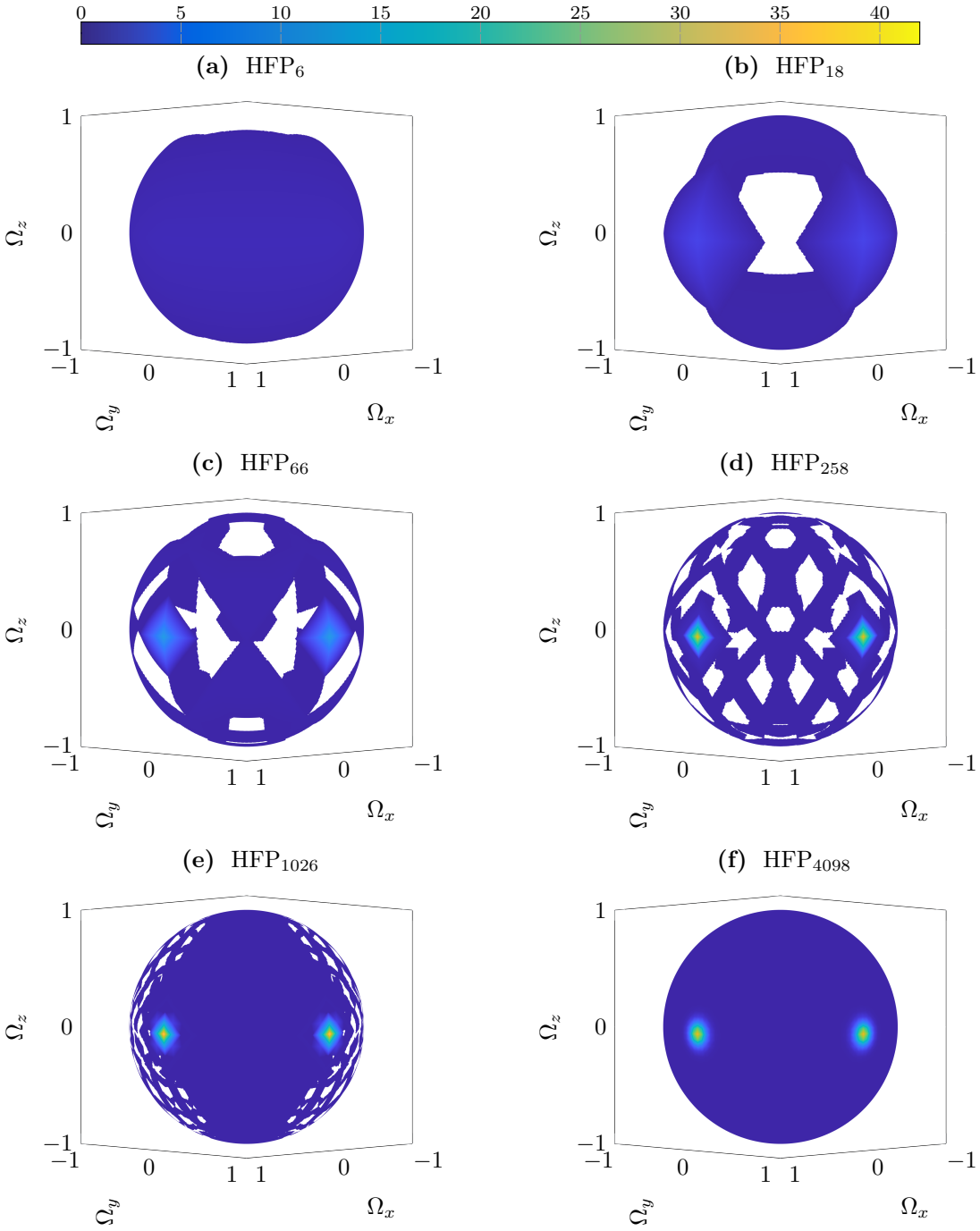

Figure S6.8: Distributions of HFP_n models for the three-dimensional crossing beams test. Unphysical negative values are shown in white. Reference solution can be found in Figure S6.2. Continued in Figure S6.11.

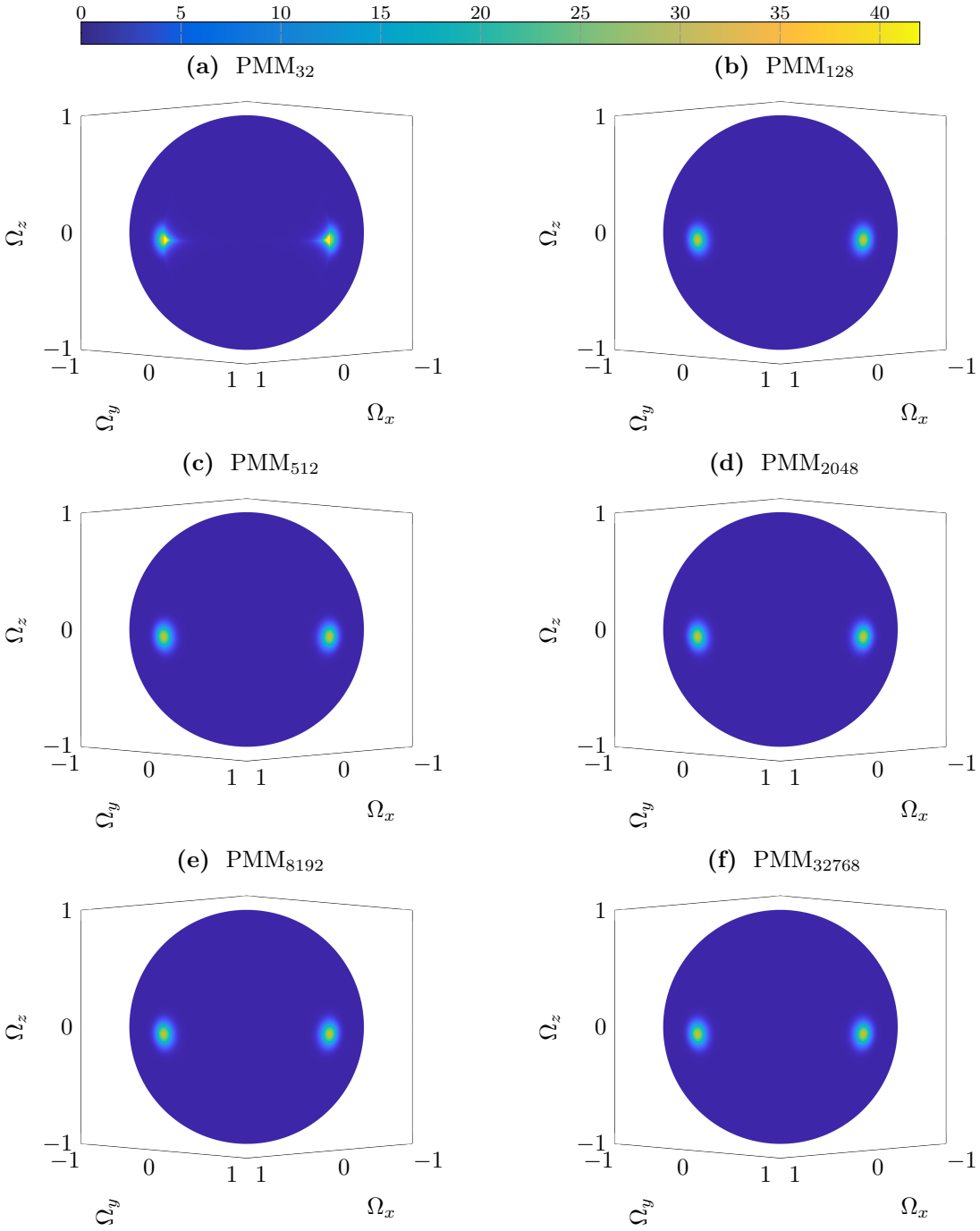

Figure S6.9: Distributions of PMM_n models for the three-dimensional crossing beams test. Reference solution can be found in Figure S6.2. Continued in Figure S6.11.

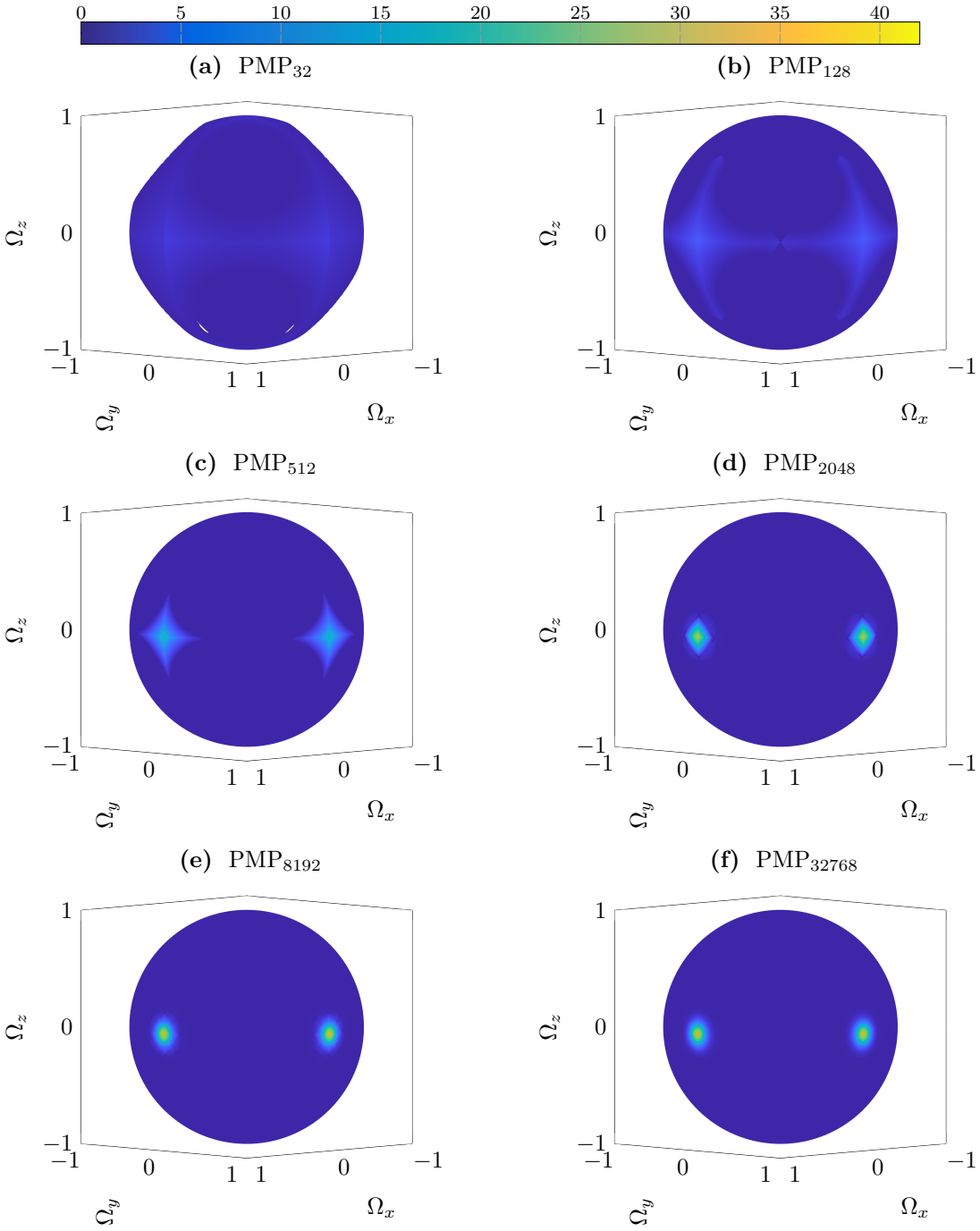

Figure S6.10: Distributions of PMP_n models for the three-dimensional crossing beams test. Unphysical negative values are shown in white. Reference solution can be found in Figure S6.2. Continued in Figure S6.11.

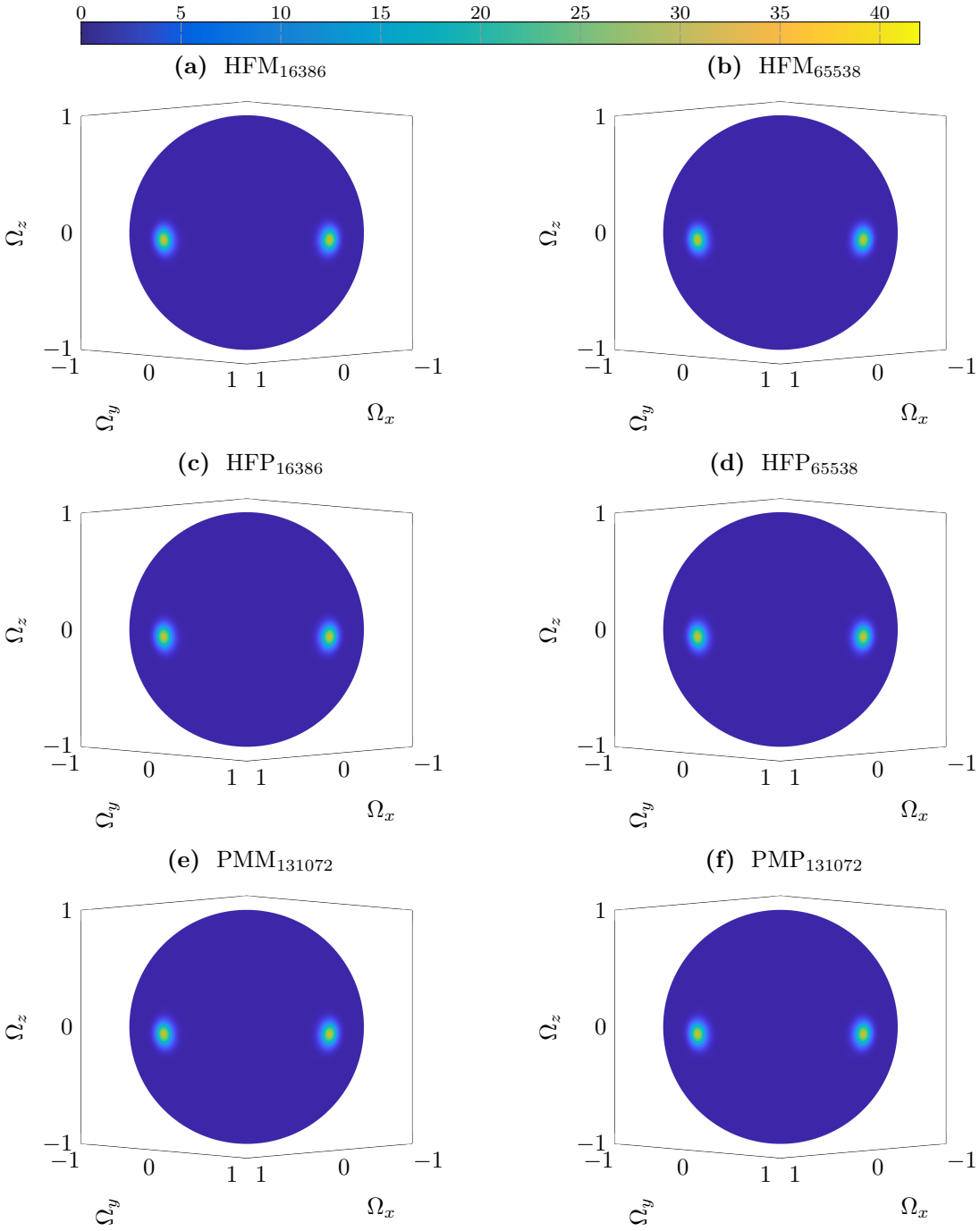

Figure S6.11: Distributions of various high-order models for the three-dimensional crossing beams test. Unphysical negative values are shown in white. Reference solution can be found in Figure S6.2.